15th Acta Oncologica Symposium
BiGART2017

Biology-Guided Adaptive Radiotherapy

Aarhus
Denmark
June 13-16, 2017

Final programme and abstracts

Contents

Welcome!

It is our great pleasure to welcome you to Aarhus, Denmark for the 2017 Acta Oncologica symposium on Biology-Guided Adaptive Radiotherapy.

Key topics for the conference will include:

- **Biology of tumours and normal tissue** to guide patient selection, target volumes and dose prescription in radiotherapy and particle therapy
- **Functional imaging of tumours and normal tissues** with functional imaging techniques based on MRI and PET, and the use of such images for dose painting and normal tissue avoidance in radiotherapy and particle therapy
- **Treatment planning and delivery challenges** in adaptation of radiotherapy and particle therapy based on changes in tumour and normal tissue biology, anatomy and/or function
- **Clinical outcome** of adaptive radiotherapy and particle therapy

The meeting has attracted 225 physicians, physicists, radiobiologists and other scientists from Denmark and internationally. With a record-breaking 135 submitted abstracts, we look forward to an active audience in exciting scientific sessions with presentations from leading scientists from several continents. This year, the meeting is organized back-to-back with ENLIGHT2017, held at Aarhus University Hospital with a visit to the emerging Danish Center for Particle Therapy.

All participants are invited to attend the social programme. Tuesday evening, we have arranged a welcome reception and dinner at the Climate Planet at Aarhus Harbour. On Wednesday, participants can use their voucher for free access to the modern art museum AROS, with the spectacular Your Rainbow Panorama. You will also have the chance to stroll through The Garden: End of Times, Beginning of Times - this year's version of the famous Sculpture by the Sea exhibition. Finally, don't miss the traditional conference dinner at the Varna Mansion, a beautifully situated restaurant in the forest next to Hotel Marselis.

We hope you will enjoy the meeting and your time in Aarhus - the European Capital of Culture 2017!

Ludvig Muren Morten Høyer Jens Overgaard Cai Grau

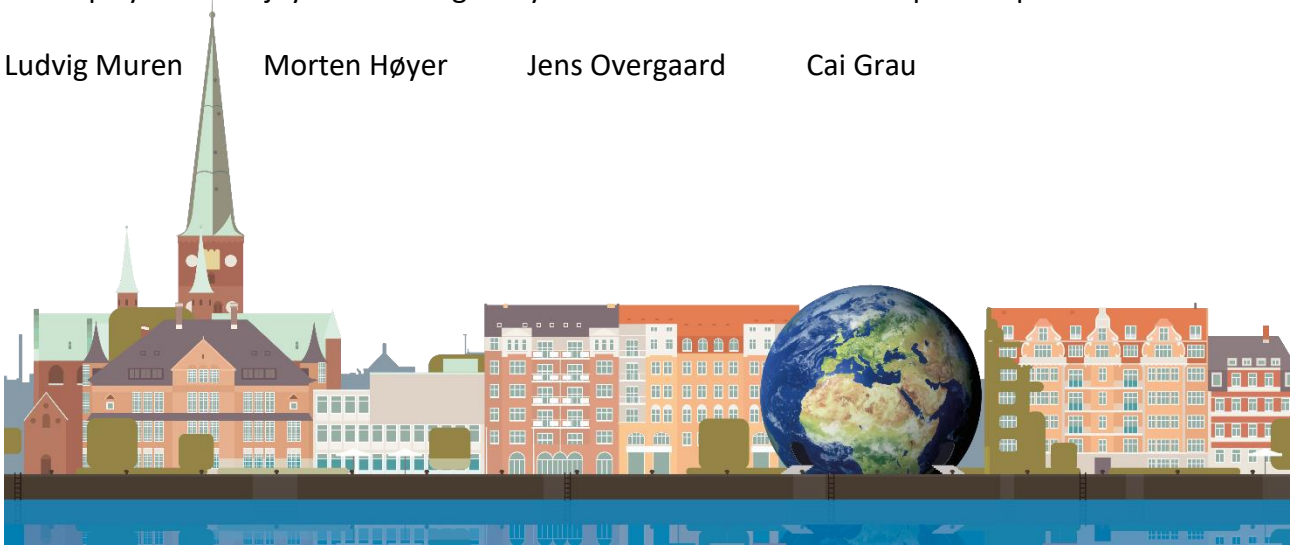

Map


Aros
Climate Planet
Hotel Marselis
Frederiksbjerg
Marselisborg
Kongsvang
Fredensvang
Banegårdsgade
Sønder Allé
Nørregade
Nørreport
Skolebakken
Dynkarken
Mindet
Sydhavnsgade
Ringgadebroen
Vestre Ringgade
Skanderborgvej
Jyllands Allé
Strandvejen
Oddervej
Tangkrogen
Skoleskoven
Havreballe Skov
Jysk Væddeløbsbane
Rømerhaven
Marselisborg Mindepark
Kirkeskov
Marselisborg Skov
Dyre-haven
Århus Bugt
Skansepark
Vennelystparken

Faculty

Invited speakers
Manjit Dosanjh, Geneva
Harald Paganetti, Boston
Bleddyn Jones, Oxford
Radhe Mohan, Houston
Niels Bassler, Stockholm
Eric Deutch, Paris
Daniel Zips, Tübingen
Albert Siegbahn, Stockholm
Mechthild Krause, Dresden
Leonhard Karsch, Dresden
Tony Lomax, Villigen
Christian Richter, Dresden
Mischa Hoogeman, Rotterdam
Antje Knopf, Villigen
Katia Parodi, München
Jan-Jakob Sonke, Amsterdam
Karin Haustermanns, Leuven
Kathrin Kirchheiner, Vienna
Joseph Deasy, New York
Dirk de Ruysscher, Maastricht
Vincenzo Valentini, Rome
Richard Pötter, Vienna
Vincent Gregoire, Brussels
Phillippe Lambin, Maastricht
Yolande Lievens, Ghent

Local faculty and organizers
Jacob Lindegaard
Jan Alsner
Jens Overgaard
Kari Tanderup
Ludvig P. Muren
Stine Korreman
Michael. R. Horsman
Birgitte Offersen
Lone Hoffmann
Ditte Møller
Morten Høyer
Per R. Poulsen
Brita Singers Sørensen
Cai Grau

Contact
Prof. Cai Grau
Department of Oncology,
Aarhus University Hospital,
Norrebrogade 44,
DK-8000 Aarhus C
Denmark
mail@bigart2017.dk

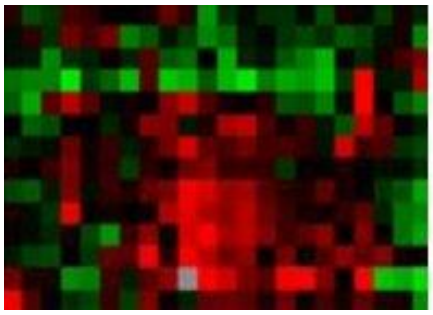
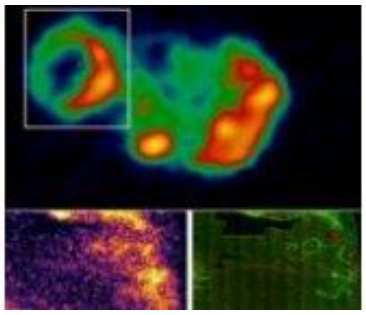


Scientific Programme

Tuesday June 13th

Climate Planet

18:30-21:30 Welcome reception at **Climate Planet, Hack Kampmanns Pl. 3,** between DOKK1 and Navitas
18:30 Drinks and snacks
19:00 Show about climate changes, from pre-industrialization to the future
19:45 Light dinner

Wednesday June 14th

Hotel Marselis

8:30 Opening session
Chair: Cai Grau

8:30 Cai Grau, Aarhus: Welcome to Rethink Radiotherapy - BiGART2017
8:45 Manjit Dosanjh, Geneva: ENLIGHT

8:50 Session 1. Radiobiology in particle therapy
Chairs: Mechthild Krause (tbc) and Brita Singers Sørensen

Invited speakers:
8:50 Harald Paganetti, Boston: The need and potential for considering a variable RBE in proton therapy
9:10 Bleddyn Jones, Oxford: Clinical radiobiology of proton therapy: Modelling of RBE
9:30 Radhe Mohan, Houston: Radiobiological Issues in proton therapy
9:50 Niels Bassler, Stockholm: LET-painting with protons

Proffered papers:
10:10 Armin Lühr, Dresden: Approach to predict the relative biological effectiveness in proton therapy for clinically relevant endpoints based on clinically accessible radiation response data.
10:20 Eivind Rørvik, Bergen: Variation in biological dose estimates among phenomenological RBE models for proton therapy.

10:30 Coffee

11:00 Session 2. Tumor biology: genomics, biomarkers and functional imaging
Chairs: Daniel Zips and Jens Overgaard

Invited speakers:
11:00 Eric Deutsch, Paris: Neutrophils as a potential biomarker for radiotherapy?
11:20 Daniel Zips, Tübingen: Preclinical and clinical exploration of multiparametric functional imaging for bio-iART
11:40 Mechthild Krause, Dresden: Biological markers for stratification of HNSCC radiochemotherapy
12:00 Phillippe Lambin, Maastricht: Imaging and targeting tumour hypoxia with Hypoxia Activated Prodrugs: learning from failures

Proffered papers:
12:20 Emanuel Bahn, Heidelberg: Non-local repair dynamics required to explain volume effect in intestinal crypt counts
12:30 Lydia Koi, Dresden: RNA-profiling of micromilieu parameters in different experimental hHNSCC mode
12:40 Michael Horsman, Aarhus: Enhancing the radiation response of tumors but not early or late responding normal tissues using vascular disrupting agents

12:50 Lunch

13:50 Session 3. Emerging technologies in ion beam therapy
Chairs: Christian Richter and Niels Bassler

Invited speakers:
13:50 Albert Siegbahn, Stockholm: Experimental grid therapy with synchrotron-generated x-ray microbeams or ion beams
14:10 Leonhard Karsch, Dresden: Status report: Ion beam therapy based on laser plasma accelerators

Proffered papers:
14:30 Martina Fuss, Darmstadt: Gold nanoparticles as radiosensitizers for ion beam therapy
14:40 Aleksandra K. Biegun, Groningen: Calibration of X-ray CT relative proton stopping power by proton radiography in proton therapy
14:50 Nigel Allinson, Lincoln: Chasing the Elusive Proton CT - Recent results from the PRaVDA consortium
15:00 Y Prezado, Orsay: Spatial fractionation of the dose in charge particle therapy
15:10 Ikechi Ozoemelam, Groningen: PET imaging of short-lived nuclides during proton beam irradiation
15:20 Johannes Müller, Dresden: Development of an experimental setup for the integration of multi-modality imaging and photon/proton irradiation for preclinical cancer research with small animals

15:30 Coffee

16:00 Session 4. Treatment planning in particle therapy
Chairs: Mischa Hoogeman and Stine Korreman

Invited speakers:
16:00 Christian Richter, Dresden: Dual-energy CT for range prediction in particle therapy: What can we gain?
16:20 Tony Lomax, Villigen: The golden triangle of outcomes guided radiotherapy
16:40 Mischa Hoogeman, Rotterdam: Challenges in treatment planning for intensity modulated proton therapy

Proffered papers:
17:00 Vicki Taasti, Aarhus: Comparison of projection- and image-based methods for proton stopping power estimation using dual energy CT
17:10 Jonathan Scharff Nielsen, Herlev/Lyngby: Patch-based CT metal artifact reduction using MRI for proton and photon radiation therapy
17:20 Per Poulsen, Aarhus: Efficient interplay effect mitigation for proton pencil beam scanning by spot-adapted layered repainting evenly spread over the full breathing cycle
17:30 Marta Peroni, Villigen PSI: Shaping proton therapy dose with DTI and DSC MRI data: functional SIB and avoidance proof of concept study
17:40 Bonny Abal, Bergen: Plan selection in proton therapy for simultaneous treatment of the prostate, seminal vesicles and pelvic lymph nodes
17:50 Leszek Grzanka, Krakow: LET-painting using multiple ions

18:00-19:10 Poster session I, at the poster stands; drinks & snacks

Evening on your own. Use your voucher for free admission to AROS Art Museum with Your Rainbow Panorama until 22:00 (voucher in conference bag).

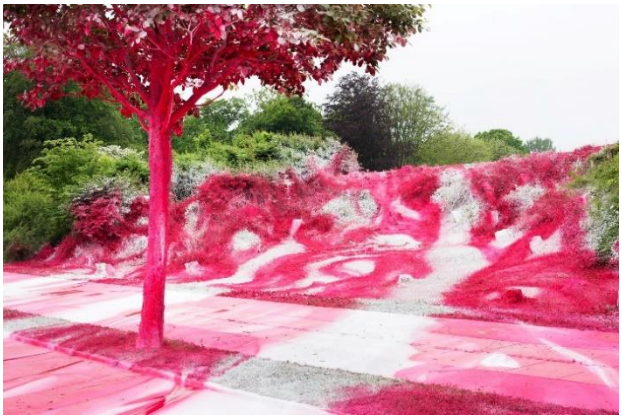

Thursday June 15th

8:30 Session 5. Image-guidance, adaptation and motion management
Chairs: Eirik Malinen and Ludvig Muren

Invited speakers:
8:30 Katia Parodi, München: Imaging for reduced range uncertainties and in-vivo verification in ion beam therapy
8:50 Antje Knopf, Villigen: Treating moving targets with scanned proton beams: vision of an Image-Guided Adaptive workflow
9:10 Jan-Jakob Sonke, Amsterdam: The MR-Linac @ NKI: research and clinical implementation

Proffered papers:
9:30 Esben Worm, Aarhus: Respiratory gated liver SBRT based on motion monitoring of implanted electromagnetic transponders
9:40 Janna van Timmeren, Maastricht: Prognostic value of longitudinal CBCT radiomics for non-small cell lung cancer patients: potential for adaptive radiotherapy
9:50 Ditte Møller, Aarhus: Robustness of photon and proton treatment of advanced lung and esophageal cancer against anatomical changes

10:00 Coffee

10:30 Session 6. Normal tissues, radiogenomics, PROM and modelling
Chairs: Joachim Widder and Jan Alsner

Invited speakers:
10:30 Joseph Deasy, New York: Normal tissue probability modeling: adding genomics and patient reported outcomes to dose-volume data
10:50 Kathrin Kirchheiner, Vienna: Late, persistent, substantial, treatment-related, patient reported symptoms (LAPERS)

Proffered papers:
11:10 Katherina Farr, Aarhus: Patient reported symptoms and quality of life analysis before and after definitive chemo-radiotherapy for non-small cell lung cancer: correlation with radiation pneumonitis
11:20 Christopher Peeler [David Grosshans], Houston: Evaluating a model to predict post-treatment imaging changes in patients treated for brain tumors with proton therapy
11:30 Line Schack, Aarhus: Published biomarkers of late radiation-induced morbidity tested in prostate cancer patients
11:40 Nina Niebuhr, Heidelberg: Application of local effect accumulation in contrast to dose accumulation
11:50 Jesper Pedersen, Aarhus C: Biological dose and complication probabilities for the rectum and bladder based on linear energy transfer distributions in spot scanning proton therapy of prostate cancer

12:00 Lunch

13:00 Session 7. Adaptive radiotherapy – clinical implementation and results
Chairs: Dirk de Ruysscher and Cai Grau

Invited speakers:
13:00 Karin Haustermans, Leuven: How to facilitate the clinical implementation of adaptive radiotherapy?
13:20 Richard Pötter, Vienna: MRI based response adaptive radiotherapy in cervix cancer - volumes, doses and clinical results

Proffered papers:
13:40 Ate Haraldsen, Aarhus: Robustness of high FDG uptake volumes during radiotherapy in Non Small Cell Lung Cancer
13:50 Patrick Berkovic, Liège: Adaptive radiotherapy for locally advanced non-small cell lung cancer: Dosimetric gain and treatment outcome prediction.
14:00 Anne Vestergaard, Aarhus: Clinical Phase II trial in adaptive radiotherapy for urinary bladder cancer reports low acute and late toxicity rates
14:10 Faisal Mahmood, Herlev: Ultra-early ADC footprint successfully detects tumor irradiation and predicts radiotherapy outcome
14:20 Christian Hvid, Aarhus: Cone beam CT based parotid sparing adaptive radiation therapy in the head and neck region

14:30 Coffee

15:00 Session 8. Radiotherapy indications, treatment volumes and fractionation (lung, rectum, anal, prostate)
Chairs: Karin Haustermans and Morten Høyer

Invited speakers:
15:00 Dirk de Ruysscher, Maastricht: Emerging trends in radiotherapy indications, treatment volumes and fractionation in high-dose radiotherapy for lung cancer
15:20 Vincenzo Valentini, Rome: Emerging trends in radiotherapy of rectal cancer

Proffered papers:
15:40 Maria Kandi, Aarhus: Local failure after radical radiotherapy of non-small cell lung cancer in relation to the planning PET/CT
15:50 Emely Lindblom, Stockholm: Non-linear conversion of HX4 uptake for automatic segmentation of hypoxic volumes and dose prescription in NSCLC
16:00 Ferenc Lakosi, Kaposvar: HDR brachytherapy boost using MR-only workflow for intermediate- and high-risk prostate cancer patients
16:10 Anna Kuisma, Turku: Follow up of biologically guided radiotherapy of prostate cancer
16:20 Vilde Skingen, Oslo: A patient-specific tumor control probability model based on total lesion glycolysis of anal cancer

16:30 Andrea Lancia, Rome: Oligometastatic cancer: stereotactic ablative radiotherapy for patients affected by isolated body metastasis

16:40-17:50 Poster session II, at the poster stands

19.00 Dinner (Varna Mansion, next to Hotel Marselis)

Friday June 16th

8:40 Session 9. Health economics and radiomics
Chairs: Bhadrasain Vikram and Kari Tanderup

Invited speakers:
8:40 Yolande Lievens, Ghent: How to guarantee the introduction and sustainability of innovative radiotherapy technologies and techniques?

Proffered papers:
9:00 Ralph Leijenaar, Maastricht: Development and validation of a radiomic signature to predict HPV status from standard CT imaging
9:10 Stefan Leger, Dresden: CT imaging during treatment improves radiomic predictions for patients with locally advanced head and neck cancer
9:20 Marta Bogowicz, Zurich: Comparison of PET and CT radiomics for prediction of local tumor recurrence in head and neck squamous cell carcinoma

9:30 Coffee

10:00 Session 10. Radiotherapy indications, treatment volumes and fractionation (breast, cervix, head and neck cancer)
Chairs: Anni Morsing and Jørgen Johansen

Invited speakers:
10:00 Jens Overgaard, Aarhus: Radiotherapy of early breast cancer: "the 2% challenge"
10:20 Vincent Gregoire, Brussels: Head and neck radiation oncology: a never-ending success story….
Proffered papers:
10:40 Kari Tanderup, Aarhus: Early clinical outcome of coverage probability based treatment planning in locally advanced cervical cancer for simultaneous integrated boost of nodes
10:50 Ruta Zukauskaite, Odense: Distribution of loco-regional recurrences after primary IMRT for head and neck squamous cell carcinomas (HNSCC). A study from three Danish head and neck cancer centres
11:00 Simon Boeke, Tübingen: Patterns of loco-regional failure (LRF) in patients with hypoxic head and neck cancers (HNSCC)
11:10 Gregers B. D. Rasmussen, Copenhagen: Immunohistochemical and molecular imaging biomarker signature for the prediction of failure site after chemoradiation for head and neck squamous cell carcinoma
11:20 Mette Saksø, Aarhus: High risk of treatment failure for patients with p16-negative, FAZA-PET positive HNSCC after primary radiotherapy - update from the DAHANCA 24 trial
11:30 Sebastian Sanduleanu, Maastricht: Non-invasive imaging for tumor hypoxia: a novel externally validated CT-based radiomics signature

11.40 Conference wrap-up
12.00 Departure. Box lunch

Posters

All posters are on display throughout the entire meeting

Poster discussion session I (Wednesday)

(walking through posters in five thematic groups)

Poster discussion group 1. Proton biology/ RBE studies

Chairs: Olav Dahl and Harald Paganetti

1. **Tordis J. Dahle, Bergen:** Sensitivity of the Microdosimetric Kinetic Model to variations in model parameters
2. **Steffen Nielsen, Aarhus:** Patient-specific Gene Expression Patterns Predictive of Radiation-induced Fibrosis Are Comparable After Proton Pencil Beam Scanning and Cobalt-60 Irradiation
3. **Jakob Ödén, Stockholm:** Will breathing motion and a variable relative biological effectiveness jeopardize the plan quality in proton radiotherapy of breast cancer?
4. **Silke Ulrich, Heidelberg:** Impact of respiratory motion on variable relative biological effectiveness in 4D dose distributions for protons
5. **Kristian Ytre-Hauge, Bergen:** Biological dose to patients receiving cranio-spinal irradiation with protons

Poster discussion group 2. Radiomics

Chairs: Joseph Deasy and David Hansen

6. **W. van Elmpt, Maastricht** [presented by **Ruben Larue**]: Influence of grey level discretization on radiomic feature stability for different CT scanners, tube currents and slice thicknesses: a phantom study
7. **Jurgen Peerlings, Maastricht:** Repeatability of Radiomics features derived from test-retest diffusion-weighted MR images
8. **Sara Carvalho, Maastricht** [presented by **Janita van Timmeren**]**:** FDG-PET-Radiomics of metastatic lymph nodes and primary tumor in NSCLC – a prospective externally validated study
9. **R.T.H.M. Larue, Maastricht:** Pre-treatment CT radiomics to predict 3-year overall survival in oesophageal cancer patients

Poster discussion group 3. Radiobiological/pre-clinical studies
Chairs: Bleddyn Jones and Michael Horsman

10. **Thomas Wittenborn, Aarhus C:** Preclinical Investigation of Hypoxia-induced Gene Expression in Prostate Cancer Cell Lines and Xenografts
11. **David Grosshans, Houston:** Radiation induces age dependent deficits in cortical synaptic plasticity
12. **Jacob Lilja-Fischer, Aarhus:** Oropharyngeal cancer patient-derived xenografts: Characterization and radiosensitivity.
13. **Morten Busk, Aarhus:** Hypoxia PET imaging: combining information on perfusion and tracer retention to improve hypoxia-specificity
14. **Pernille Elming, Aarhus:** Combination of Vascular Disrupting Agents and Checkpoint Inhibitors: a Method of Increasing Tumour Immunogenicity?

Poster discussion group 4. Clinical outcomes
Chair: Birgitte Offersen

15. **Timo Deist, Maastricht:** On the selection of classifiers for boutcome prediction in radiotherapy
16. **Jan Alsner, Aarhus:** Associations between skin toxicity, survival, and single nucleotide polymorphisms in head and neck cancer patients receiving the EGFr-inhibitor Zalutumumab: Results from the DAHANCA 19 trial
17. **Einar Dale, Oslo:** Dose painting for reirradiation of head and neck cancer
18. **Simon Lønbro, Aarhus:** Immediate loss of lean body mass in locally advanced head and neck cancer during (chemo)-radiotherapy.
19. **Arthur Jochems, Maastricht:** A random forest model to predict early death in NSCLC patients receiving chemo(radio)therapy
20. **Tinne Laurberg, Aarhus:** Intrinsic subtype classification of local recurrences and new contralateral primary tumors in patients with low risk breast cancer. Influence of age and primary surgery.
21. **Oscar Casares-Magaz, Aarhus:** The association between genitourinary toxicity and planned vs delivered bladder dose/volume metrics in radiotherapy for prostate cancer
22. **Lotte Fog, Copenhagen:** Early pain relief and toxicity after image guided volumetric modulated radiation therapy for spinal cord compression

Poster discussion group 5. Proton therapy: Dosimetry and Treatment planning
Chairs: Radhe Mohan and Christian Søndergaard

23. **Ellen Marie Høye, Aarhus:** Saturation dose and quenching in proton beams in a radiochromic 3D dosimeter
24. **Jeppe Brage Christensen, Roskilde:** On the potential of proton dosimetry using Cerenkov radiation in optical fibers
25. **Thomas Henry, Stockholm:** Proton grid therapy (PGT) with mm-wide beam elements: a Monte-Carlo simulation study

26. **Gracinda Mondlane, Stockholm:** Evaluation of TCP and NTCP after radiosurgery of liver metastases with photon- or scanned proton-beams
27. **Camilla Hanquist Stokkevåg, Bergen:** Normal tissue sparing in very young children treated with proton therapy
28. **Laura Toussaint, Aarhus:** Doses to brain structures associated with cognitive impairment following radiotherapy of paediatric CNS tumours with contemporary photon vs. proton techniques
29. **Charlotte Espensen, Copenhagen:** Ruthenium-106 brachytherapy and proton therapy for uveal melanomas: Biologically Effective Dose for tumour and organs at risk from comparative dose planning

Poster discussion session II (Thursday)

(walking through posters in five thematic groups)

Poster discussion group 6. Functional imaging: PET and SPECT

Chairs: Malene Fischer and Azza Khalil

30. **Evelyn de Jong, Maastricht:** Quality assessment of [18F]FDG PET scans of the NVALT12 imaging sub-study: Recommendations for future multicenter PET trials
31. **Marta Lazzeroni, Stockholm:** Evaluation of third treatment week as temporal window for assessing responsiveness on repeated FDG-PET scans in NSCLC patients
32. **Aniek Even, Maastricht:** Predicting hypoxia in non-small cell lung cancer: combining CT, FDG PET and dynamic-constrast enhanced CT parameters
33. **Ingvild Støen, Oslo:** Optimal threshold for PET-based autocontouring of boost volume for radiotherapy of anal carcinoma
34. **Espen Rusten, Oslo:** The prognostic value of FDG-PET uptake parameters in anal cancer
35. **Mette Marie Fode, Aarhus:** Functional treatment planning using 2[18F]fluoro-2-deoxy-D-galactose PET/CT for stereotactic body radiotherapy of liver metastases – a phase I study
36. **Azadeh Abravan, Oslo:** PET based evaluation of lung toxicity after radiotherapy- Assessment of two approaches for dose response evaluation
37. **Tine Bisballe Nyeng, Aarhus:** Comparing functional lung volumes obtained by using 2 different methods: Do perfusion SPECT and 4D-CT ventilation maps define the same voxels in lung cancer treatment?

Poster discussion group 7. Photon therapy: Inter-fractional challenges

Chair: Lise Bentzen

38. **Kristina Giske, Heidelberg:** In-silico patient models: beyond contour propagation in radiation therapy
39. **Anne Holm, Aarhus:** Carotid sparring intensity modulated radiotherapy for early laryngeal glottis cancer; What is clinically achievable?
40. **Lone Hoffmann, Aarhus:** Anatomical changes in advanced lung cancer patients occurring during RT can be predicted from pre-treatment characteristics.
41. **Karen Zegers, Maastricht** [presented by **Jose Baeza**]**:** 3D dose evaluation in breast cancer patients to define parameters for adaptive radiotherapy

42. **Karina Lindberg Gottlieb, Odense:** A new adaptive position verification protocol for breast cancer with simultaneous boost
43. **Annette Schouboe, Aarhus:** Full bladder approach sparing bowel in external radiotherapy for cervical cancer patients
44. **Akos Gulyban, Liege:** Margin of the day with ITV concept during EBRT for locally advanced cervical cancer: Evaluation of 0, 5 and 10 mm safety margins with dose accumulation uncertainty
45. **Marianne Sanggaard Assenholt, Aarhus:** Bladder filling feed back and CBCT monitoring during external beam radiotherapy with tight margins for patients with locally advanced cervical cancer.

Poster discussion group 8. Photon therapy: Intra-fractional challenges
Chairs: Antje-Christin Knopf and Per Poulsen

46. **Ander Biguri, Bath** [presented by **Steven Hancock**]**:** Improving image quality of 4D-CBCT respiratory-correlated and motion-corrected reconstruction using iterative algorithms and GPU acceleration
47. **Mai Lykkegaard Schmidt, Aarhus:** Intrafraction baseline shifts between setup CBCT and treatment delivery of involved mediastinal lymph nodes of lung cancer patients
48. **Patrik Sibolt, Roskilde:** Monte Carlo evaluation of dose-escalated lung radiotherapy in free-breathing and deep-inspiration breath-hold
49. **Marianne Knap, Aarhus:** Difference in target volume using three different methods to include respiratory uncertainty in advanced lung cancer
50. **Susanne Bekke, Herlev** [presented by **Faisal Mahmood**]**:** Non-interchangeability of respiratory gating areas using surface scanning in deep inspiration breath-hold radiotherapy
51. **Jenny Bertholet, Aarhus:** Validation of a fully automatic real-time liver motion monitoring method on a conventional linac
52. **Simon Skouboe, Aarhus:** Real-time gamma evaluations of motion induced dose errors as QA of liver SBRT tumour tracking
53. **Camilla Skinnerup Byskov, Aarhus:** Intra- vs. inter-fractional target motion in radiotherapy of rectal cancer evaluated with repeat volumetric imaging

Poster discussion group 9. Proton therapy: Inter- and intra-fractional challenges
Chairs: Marta Peroni and Katia Parodi

54. **Stine Korreman, Aarhus:** Minimum prescription concept for dose painting with protons increases robustness towards geometrical uncertainties
55. **Kia Busch, Aarhus:** On-line dose-guided proton therapy to account for inter-fractional motion: a proof of concept
56. **Maria Fuglsang Jensen, Aarhus:** Optimizing delivery speed of lung cancer treatments using single and multi field intensity-modulated proton therapy
57. **Alina Santiago, Marburg:** Beam-specific planning target volumes for scanned particle therapy of lung tumors under tumor fixation conditions
58. **Emma Colvill, Aarhus:** Validation of fast motion-including dose reconstruction for proton scanning therapy in the liver

59. **Thomas Berger, Aarhus:** Dosimetric impact of air cavities and weight loss with intensity modulated proton therapy in locally advanced cervical cancer patients.
60. **Toke Printz Ringbæk, Gießen:** Evaluation of new 2D ripple filters in scanned proton therapy.

Poster discussion group 10. Functional imaging: MRI
Chairs: Faisal Mahmood and Erik Morre Pedersen

61. **Ane Iversen, Aarhus:** Functional imaging of cancer metabolism using hyperpolarized 13C magnetic resonance spectroscopy to monitor the effect of vascular disrupting agents
62. **Jesper Kallehauge, Aarhus:** Comparison of common approaches for DCE-MRI analysis in cervical cancer
63. **René Winter, Tübingen:** Simultaneous PET/MRI in radiotherapy treatment position: Diffusion-weighted imaging in head and neck cancer
64. **Morten Bjoern Jensen, Aarhus:** Diffusion Tensor Imaging driven growth modelling for target definition in gliomas

Posters – on general display

65. **Erik Pedersen, Aarhus:** Real-time magnetic resonance imaging of the simultaneous motion of lung tumors and metastatic mediastinal lymph nodes
66. **Anders Traberg Hansen, Aarhus:** Isotoxic treatment planning strategies for stereotactic liver irradiation: The price of dose uniformity
67. **Jasmin M. Mahdavi, Herlev** [presented by **Faisal Mahmood**]: Critical dose reduction effect of unwanted air gaps under bolus in volumetric modulated arc therapy
68. **Helena Sandström, Stockholm:** Multi-institutional study of the variability in target delineation for six targets commonly treated with radiosurgery
69. **Christian Rønn Hansen, Odense:** Automatic treatment planning facilitates fast adaptive re-planning for oesophageal cancer treatments
70. **Chris Monten, Ghent:** Prone breast irradiation: Can we improve precision and accuracy of tumor bed delineation?
71. **Cecile Wolfs, Maastricht:** Dosimetric consequences of simulated anatomical changes in lung cancer patients
72. **Yvonka van Wijk, Maastricht:** Development of a virtual spacer for a multifactorial decision support system for prostate cancer radiotherapy: Comparison of dose, toxicity and cost-effectiveness
73. **Iosif Papoutsis, Oslo:** From dose prescription to dose delivery - can dose painting by numbers be accurately delivered?
74. **Paulo Magalhaes Martins, Heidelberg** [presented by **Paulo Crespo**]**:** Fast full-body reconstruction for a functional human RPC-PET imaging system using list-mode simulated data and its applicability to radiation oncology and radiology
75. **Jose A Baeza Ortega, Maastricht:** Validation and uncertainty analysis of a pretreatment prediction model for EPID dosimetry
76. **Ebbe Lorenzen, Odense** [presented by **Karina L. Gottlieb**]**:** Automatic treatment planning of FFF VMAT for breast cancer: fast planning and fast treatment
77. **Esben Svitzer Yates, Aarhus:** Total Body Irradiation – patient in vivo dosimetry.
78. **Marie Louise Milo, Aarhus:** Pectus excavatum and adjuvant radiotherapy for early breast cancer: is the heart an issue?
79. **Manjit Dosanjh, Geneva:** Collaborative strategies for meeting global needs for affordable, high quality radiation therapy (RT) treatment
80. **Virginia Greco, Geneva:** ENLIGHT (European Network for Light Ion Hadron Therapy): a network to foster collaboration and train experts in hadrotherapy
81. **Maja Sharma, Aarhus:** Simultaneous integrated prophylactic cranial irradiation in sinonasal cancer
82. **Jolanta Hansen, Aarhus:** Risk of developing radiation induced secondary malignancies in the thyroid glands after radiotherapy for a pediatric brain tumour

Sponsors

ACTA ONCOLOGICA

Kræftens Bekæmpelse

Abstracts

Wednesday June 14, 2017

Session 1. Radiobiology in particle therapy

8:50-9:10. Harald Paganetti, Boston MA, USA

The need and potential for considering a variable RBE in proton therapy

Paganetti H; Giantsoudi D; Underwood T; Unkelbach J. Department of Radiation Oncology, Masschachusetts General Hospital and Harvard Medical School, Boston, USA.

It is well known that the RBE varies among cell lines, tissues, endpoints, as well as with beam-quality. Experimental data do show a trend towards an increase in RBE as α/β of the linear-quadratic model decreases. Furthermore, one would also expect the RBE to increase as dose decreases. The RBE also increases with increasing linear energy transfer (LET). Phenomenological models are capable of predicting the RBE as a function of the parameters mentioned above. Uncertainties, especially in vivo, are preventing the clinical application. Input parameters for these models are solely based on cell survival data obtained in vitro. It is unclear if in vitro relationships can be translated to in vivo endpoints even for tumor control. Furthermore, to define normal tissue complications, the endpoint of cell survival may not be appropriate at all. Most importantly, patient specific radiosensitivity is poorly understood and clinical evidence that RBE variations indeed matter in patients is scarce. Consequently, RBE variations are currently not considered quantitatively in proton therapy. However, some qualitative consideration is given towards variable RBE values by, for instance, avoiding specific beam angles or reducing the dose to critical structure for a limited number of fractions. Thus, the current clinical focus is on mitigating potential impacts of proton RBE uncertainties. Moving forward, one potential strategy is to focus on the well-known fact that the RBE is increasing with increasing LET. One can improve a treatment plan by redistributing the LET away from critical structures without significantly changing the dose distribution. This presentation will summarize the current evidence for RBE variations in vitro and in vivo. Next, clinical examples will be presented where RBE considerations play a role in treatment planning. Lastly, concepts for biological treatment planning will be presented.

Wednesday June 14, 2017

9:10-9:30. Bleddyn Jones, Oxford, UK

Clinical Radiobiology of Proton Therapy: Modelling of RBE

Jones B. Gray Laboratory, CRUK-MRC Oxford Centre, Department of Oncology, University of Oxford, UK.

Introduction: Concerns exist about the 1.1 RBE in proton therapy, believed by some to be correct within spread out Bragg peaks (SOBP), with linear energy transfer (LET) values of 1-2 keV.µm-1, compared with 0.22 keV.µm-1 for control megavoltage photon beams. Late reacting normal tissues (with low □/β values), might be overdosed if RBE>1.1 and very radiosensitive tumours (with high □/β), might be under-dosed if RBE <1.1. Some physicists recommend ignoring RBE in favour of a LET□dose product to predict effects, but this seems radio-biologically unsound. Materials and Methods: Extensive linear quadratic based modelling is scaled between control low LET □ and β values and their values at higher LETs. Graphical methods and Random Sampling methods using Mathematica (Wolfram, USA) are used to find RBE values for ranges of □/β from 2 to 27 Gy. The concept of using a LET x Dose product is assessed by comparing it with biological effective dose (BED). Results: Low □/β values have the widest RBE ranges with dose per fraction changes and increasing LET, often above 1.1 even within the SOBP range, although have lower values at higher dose per fraction. Highly radiosensitive tumours (□/β>10 and up to 27 Gy) have the lowest RBEs, some well below 1.1, and are not fraction-sensitive. The RBE`s increase further with LET, so curtailment of LET in normal tissues is important. The LET x Dose product is shown to be insufficiently discriminating when plotted with biological effective dose (BED) for protons and ions, and should not be used over wide ranges. Conclusions: Suggestions are made as to an overall research framework. The promised advantages of proton therapy will only be fully realised if reasonably correct RBE values are used instead of 1.1. Carefully modelled RBE values, possibly with a degree of hypo-fractionation, should improve the therapeutic index.

Wednesday June 14, 2017

9:30-9:50. Radhe Mohan, Houston, TX, USA

Radiobiological Issues in Proton Therapy

Mohan, R; Peeler, C; Guan, F; Cao, W; Grosshans, D. G. Division of Radiation Oncology, MD Anderson Cancer Center, Housston, TX, USA.

The relative biological effectiveness (RBE) of a particle is a complex variable function of radiation type, radiation dose, LET, tissue or cell type, endpoint, etc. For protons, it is assumed to have a fixed value of 1.1. Recent experiments show that RBE may vary significantly along the proton beam path, especially near the end of the particle range. RBE variability, along with other uncertainties, may mean that the biologically effective dose distributions received by the patient may be significantly different from what is seen on treatment plans. This may contribute to unforeseen toxicities and/or failure to control the disease. With the passage of time there is increasing acceptance of the fact that proton RBE is variable. However, there is an ongoing debate. An argument in favour of the assumption of RBE of 1.1 and its continued use in proton therapy is that there are large uncertainties in RBE, in particular with regard to its dependence on individual patient's sensitivity. Another argument is that the higher RBE affects only a small region near the distal edge because of steep distal falloff. However, while the fall-off is steep in water, it is degraded in tissue, particularly when a beam passes through a complex heterogeneity, and may spread over a large region in low-density media such as lung. Another reason often quoted is that there is no clinical evidence to-date indicating harm of RBE of 1.1. It is plausible, however, that the evidence is masked by various physical uncertainties. A reduction in such uncertainties and their incorporation in the estimation of dose actually delivered may isolate and reveal the variability of RBE. The improvement in the knowledge of RBE thus gained could lead to better understanding of outcomes of proton therapy and the incorporation of this knowledge in the optimization of intensity-modulated proton therapy (IMPT) could, in principle, lead to improvement in therapeutic ratio of proton therapy.

Wednesday June 14, 2017

9:50-10:10. Niels Bassler, Stockholm, Sweden

LET-painting with Protons

Niels Bassler. Medical Radiation Physics, Dept. of Physics, Stockholm University, Sweden.

The relative biological effect of protons in clinical therapy have in recent years been subject to renewed discussion. As the number of proton centers is in near exponential growth, reports of unexpected toxicities found at the distal end of the spread out Bragg peak are rising. The widely adopted RBE of 1.1 is based on clinical data established in the center of the SOBP. Nonetheless, a possible increased effect at towards the distal end due to the elevated LET is acknowledged. Here we will take a closer look at several treatment options which may be employed in clinical practice which can reduce this effect, some involving various degrees of LET-painting. Investigated strategies were: 1) Field patching, 2) Dose feathering, 3) RBE-optimization, 4) Full LET-painting using dose-ramps. Other strategies will briefly be mentioned. Treatment plans were calculated using TRiP98 in conjunction with PyTRiP98, where several proton biological models were implemented. Field patching is capable of reducing exposure of high-LET parts towards the organs at risk by simple rearranging the incoming fields. Dose feathering dilutes the high-LET region over a slightly larger area at the distal SOBP range, in order to reduce the risk of toxicity. RBE-optimization is well known from heavier ions, needs to rely on available biological models. Finally, LET-painting using dose ramps effectively shifts the high-LET areas from the rim of the tumour into the center, but at the cost of an increased dose in the entry channel. Caution must be applied when reporting dose-averaged LET, as it highly depends on the underlying algorithm, thereby impacting the outcome of RBE-models. In conclusion, several strategies are available to reduce possible toxicity of proton beams at the distal end of the SOBP, and employing any of the here presented strategy will lead to a reduced toxicity at the distal edge. Quantitative assessment is in progress

Wednesday June 14, 2017

10:10-10:20. Armin Lühr, Dresden, Germany

Approach to predict the relative biological effectiveness in proton therapy for clinically relevant endpoints based on clinically accessible radiation response data

Lühr, A. 1,2,3, Helmbrecht, S. 1,2, Enghardt, W. 1,2,3, Krause, M. 1,2,3. (1) OncoRay - National Center for Radiation Research in Oncology, Faculty of Medicine and University Hospital Carl Gustav Carus, Technische Universitaet, Dresden, Germany (2) Helmholtz-Zentrum Dresden - Rossendorf (HZDR), Institute of Radiooncology - Onc.

Introduction Recently, phenomenological modeling of the relative biological effectiveness (RBE) for proton therapy as function of physical parameters, e.g. linear energy transfer (LET), received a lot of attention. However, clinical application of RBE models is primarily hampered by large uncertainties in the biological input data, especially, when derived in vitro. This study demonstrates the feasibility of using (pre-) clinical fractionation response data to estimate RBE in proton therapy. Methods Pre-clinical literature RBE data of the rat spinal cord (myelopathy, paresis grade II) for carbon ions with different LET were analyzed including data for one and two fractions. For each LET value, the linear-quadratic (LQ) parameters for particles, α_p and β_p, were obtained from the response to fractionation. Also, for each LET value the corresponding beam quality Q = Z^2/E (Z and E: ion charge and energy) was obtained by Monte Carlo simulation. A recently proposed beam quality (BQ) model, predicting α_p to increase linearly with Q and independently of ion type, was applied. Results RBE and α_p were found to increase linearly with beam quality Q for both fractionation schemes. The BP model remarkably reproduced α_p data as function of Q. The quadratic term β_p did hardly change with Q. Given α_p and β_p as well as α and β for photon irradiation (from fractionation analysis), the measured RBE could directly be calculated via the LQ model. Since the BQ model could estimate α_p and β_p as function of Q and photon α, β, also the variable RBE could be predicted for both fractionation regimens – independent of ion type. Conclusions The approach successfully estimated pre-clinical RBE. It can be directly translated to patient treatment, since it relies on clinically accessible input data (such as fractionation response) for clinically relevant endpoints. The recent finding that RBE depends on Q but not on ion type suggests applying this approach also to estimate proton RBE.

Wednesday June 14, 2017

10:20-10:30. Eivind Rørvik, Bergen, Norway

Variation in biological dose estimates among phenomenological RBE models for proton therapy

Rørvik E^1, Fjæra LF^1, Dahle TJ^1, Dale JE^2, Engeseth GM^2, Stokkevåg CH^2, Thörnqvist S^1,2 and Ytre-Hauge KS^1. 1: Department of Physics and Technology, University of Bergen, Bergen, Norway 2:Department of Oncology and Medical Physics, Haukeland University Hospital, Bergen, Norway.

Introduction Previous studies have shown that the relative biological effectiveness (RBE) of protons varies with factors such as deposited dose, tissue type and linear energy transfer (LET). Acknowledging this complexity, multiple different phenomenological RBE models have been developed in the recent years. We therefore compared all published phenomenological RBE models and a constant RBE of 1.1 for proton therapy for different tumour sites. Materials and Methods We created proton therapy plans for three patients with different types of cancer (head and neck, sarcoma, prostate) in the Eclipse Treatment Planning System. The FLUKA Monte Carlo code was used to obtain biological dose distributions and to extract the dose-averaged LET distributions. Nine phenomenological RBE models were applied, in addition to two models with a normalised mean RBE of 1.1. The impact of using different biological models for organs at risk (OARs) (heart and lungs for sarcoma, rectum for prostate, chiasm/optic nerve and brainstem for a head and neck patient) was found by comparing clinically relevant dose parameters, such as mean dose or the maximum dose found in a single dose voxel. Results For all patients, all phenomenological models calculated a higher mean dose to the PTV compared to using an RBE of 1.1. The estimated mean RBE to the PTV regions ranged from 1.11 to 1.29. The variation in maximum dose was larger than the variation in mean dose, due to the heterogeneous dose distribution of protons. The largest deviation of maximum dose was found in the left optic nerve for the head and neck patient, where the various models calculated doses in the range 56-72 Gy(RBE), while the 1.1-weighted quantity was 48 Gy(RBE). Conclusions There were considerable variations in the dose distributions calculated by the different RBE models. When choosing a specific model for dose planning studies, future users should be aware of the differences and assumptions of the phenomenological RBE models.

Wednesday June 14, 2017

Session 2. Tumor biology: genomics, biomarkers and functional imaging

11:40-12:00. Mechthild Krause, Dresden, Germany

Biological markers for stratification of HNSCC radiochemotherapy

Mechthild Krause. Department of Radiotherapy and Radiation Oncology and OncoRay – National Center for Radiation Research in Oncology, Faculty of Medicine and University Hospital Carl Gustav Carus, Technische Universität Dresden, Dresden, Germany; Helmholtz-Zentrum Dresden.

During the past decades, cancer treatment has been improved in a technically and medically manner. Nonetheless, the 5-year overall survival rate for head and neck squamous cell carcinoma (HNSCC) is still at about 50%. Currently, most patients with functionally inoperable HNSCC are treated with primary radiochemotherapy (RCTx). In contrast to radiotherapy alone, clinical trials showed that patients who received RCTx benefit in terms of increased overall survival and loco-regional control as well as freedom of distant metastases. However, concomitant chemotherapy is leading to increased toxicity. Another obstacle is the heterogeneity of tumor response to this treatment. Therefore, biomarkers are urgently needed to identify patient groups who require de-escalated or intensified treatment schedules based on their tumor biology in addition to established clinical parameters. Currently, a panel of promising biomarkers is tested in numerous clinical studies, such as human papilloma virus (HPV) status. A positive HPV infection status may be a suitable biomarker for patient stratification towards de-escalation treatment regimens. However, additional biomarkers are needed for further stratification of patients with HPV-negative tumors. This talk will give an overview about the results of biomarker studies and ongoing clinical trials.

Wednesday June 14, 2017

12:20-12:30. Emanuel Bahn, Heidelberg, Germany

Non-local repair dynamics required to explain volume effect in intestinal crypt counts

Bahn, E., van Heerden, M. Gueulette, J. Slabbert, K. Shaw, W. Alber, M.. 1: Abteilung für Radioonkologie und Strahlentherapie, Universitätsklinikum, Heidelberg, Germany; 2: Department of Medical Physics, University of the Free State, Bloemfontein, South Africa; 3: Université Catholique de Louvain, Louvain-la-Neuve, Belgium; 4:.

INTRODUCTION Rodent jejunum is a well established model for the study of dose and fractionation effects and a high precision technique for the determination of the RBE of high-LET radiation. However, studies traditionally avoided or suppressed volume effects. The roles of various stem cell populations, which constitute the hierarchical base of the intestinal epithelium, are highly controversial and require sophisticated statistical analysis for precise parameter determination. Here, we present a technique for the analysis of microcolony assays that incorporates effects of repair dynamics and of crypt selection thresholds. It allows to explain the volume effect observed by us in intestinal crypts of irradiated mouse jejunum. MATERIALS AND METHODS In a series of experiments, 5mm and 10mm jejunum of female NIH strain mice were irradiated extra-corporally and the whole bowel (WB) intra-corporally via a whole body irradiation, with single doses of 8–20 Gy of 6 MV X-Rays. Following the standard procedure of the microcolony assay, the number of regenerated crypts per H&E stained cross-section was counted 84 hours post irradiation, and the spatial distribution of crypts was quantified. RESULTS While the dose-responses of WB and of 10mm irradiated jejunum are identical, a shift of the dose-response to 3.5 Gy higher doses is observed for the 5mm irradiated jejunum. We developed a model that explains the observed volume effect by a increase of the cell doubling time from 20 to 27 hours for small and large fields, respectively. In addition, precise values for cell sensitivity and clonogenic content are obtained. The detailed spatial distribution of regenerated crypts is also predicted by our model with great accuracy. CONCLUSIONS The observed volume effect requires the existence of a non-local regeneration milieu. We can explain this effect as a volume-dependency of clonogenic cell doubling rates and propose a model for RBE determination that avoids common systematic errors.

Wednesday June 14, 2017

12:30-12:40. Lydia Koi, Dresden, Germany

RNA-profiling of micromilieu parameters in different experimental hHNSCC models

Lydia Koi1,2, Antonia Wolf1, Annett Linge1,3,4,5, Steffen Löck1,3,4, Michael Baumann1,2,4,5, Mechthild Krause1,2,3,4,5. 1) Dept. of Rad. Oncology and OncoRay – Natl. Center f. Rad. Research in Oncology, Fac. of Medicine/ University Hospital C. G. Carus, TU Dresden, Germany 2) Helmholtz-Zentrum Dresden - Rossendorf 3) DKTK, Dresden, Germany 4) DKFZ, Heidelberg, Germany 5) N.

Introduction: Previous in vivo studies demonstrated that hypoxia measured by pimonidazole staining is associated with local tumor control in human head and neck squamous cell carcinoma (hHNSCC). This project intends to identify and validate genes which are expressed differently in hypoxic and oxic cells and therefore may play an important role in radiation resistance. This might lead to the establishment of new targets and biomarkers for potential therapeutic. Materials and methods: Seven different hHNSCC in nude mice were studied. For gene expression analysis untreated tumors were excised and stained for pimonidazole hypoxic areas. Using laser-capture microdissection (LCM), material was collected separately from consecutive unstained slides. RNA was isolated and subjected to gene expression analysis using nanoString technologies. The applied gene panel included hypoxia classifier (Toustrup et al.) as well as genes that have been reported to be involved in radioresistance, such as genes which are encoding for putative cancer stem cell markers. Results: Several genes showed large differences in expression between hypoxic and well perfused areas. Differences were found in the expression level of hypoxia-associated genes within the hypoxic areas between the individual tumor models. In addition, the more radioresistant tumors do not necessarily coincide with the intensity of the expression of these genes. Besides the hypoxic gene signature, genes encoding for stem cell markers, are significantly different between these two micromilieu areas. Conclusion: LCM allows analysing RNA from different microenvironmental areas. We found significantly different expressions of genes which can play an important role with regard to radioresistance in tumors, and are involved in processes, such as DNA repair, proliferation and invasiveness. In this way, new targets and biomarkers could be established in order to obtain potential therapeutic approaches in combination with radiotherapy.

Wednesday June 14, 2017

12:40-12:50. Michael Horsman, Aarhus, Denmark

Enhancing the radiation response of tumors but not early or late responding normal tissues using vascular disrupting agents

Horsman MR. Department of Experimental Clinical Oncology, Aarhus University Hospital, Aarhus, Denmark.

Introduction: Vascular disrupting agents (VDAs) damage tumor vasculature and enhance tumor response to radiation. In this pre-clinical study we compared the effects of VDAs on tumor radiation response to those effects seen in relevant normal tissues, using the lead VDA combretastatin A-4 phosphate (CA4P) and its analogue OXi4503. Materials and methods: CDF1 mice were used for all experiments. Radiation (240 kV X-rays; 2.3 Gy/minute) was applied locally to tissues to produce full radiation dose-response curves. VDAS were i.p. injected 1-hour after irradiating at drug doses giving similar anti-tumor effects (i.e., 250 mg/kg CA4P and 50 mg/kg OXi4503). Response of 200 cubic mm foot implanted C3H mammary carcinomas was assessed using percent tumor control at 90 days. Normal tissue effects were evaluated using early responding skin (development of moist desquamation in the foot at 11-30 days), and late responding bladder (a 50% reduction in reservoir function estimated by cystometry up to 9 months after treatment), and lung (a 20% increase in ventilation rate measured by plethysmography within 9 months). Statistical comparisons were made using a Chi-squared test (significance level of $p<0.05$). Results: The radiation dose (with 95% confidence intervals) controlling 50% of irradiated tumors was 54 Gy (52-57). This significantly decreased to 46 Gy (42-49) and 41 Gy (38-45) with CA4P and OXi4503, respectively. The radiation dose inducing moist desquamation in 50% of mice was 32 Gy (30-34). No significant change was induced by CA4P or OXi4503; the respective values being 33 Gy (32-34) and 31 Gy (30-33). In bladder and lung the radiation dose inducing a 50% change was 14 Gy (11-18) and 13 Gy (12-13), respectively. These were unchanged by CA4P; the values being 12 Gy (8-16) in bladder and 12 Gy (11-13) in lung. Conclusions: VDAs significantly enhance tumor radiation response, but have absolutely no effect on the radiation response of early or late responding normal tissues.

Wednesday June 14, 2017

Session 3. Emerging technologies in ion beam therapy

13:50-14:10. Albert Siegbahn, Stockholm, Sweden

Experimental grid therapy with synchrotron-generated x-ray microbeams or ion beams

Albert Siegbahn. Department of Physics, Stockholm University, Department of Oncology and Pathology, Karolinska Institutet.

Introduction The doses produced in tissue with grid therapy are alternating in a periodic pattern. Biological experiments performed with grids containing narrow (µm- to cm-wide) beam elements have demonstrated that the tolerance doses for certain biological endpoints are rising with reduced beam widths. Materials and methods A single grid, containing cm-wide beam elements, has normally been used for the grid therapy carried out clinically. During the past decades, pre-clinical research projects related to grid therapy with µm- or mm-wide beam elements have been initiated. Animals (sometimes tumor-bearing), such as fruit flies, zebra fish, rodents and pigs have been irradiated. Developments in accelerator technology have made extremely intense and parallel x-ray beams available for therapy, with which a large dose (~100s of Gy) can be delivered within a few milliseconds. Results Large cohorts of patients have been treated with grid therapy using conventional photon-beam radiotherapy systems. A reduction in the size of large tumors, combined with a low toxicity in the neighboring organs, has been demonstrated. Patient treatments with more than one beam grid have not been carried out frequently, due to the use of divergent beams which may result in overlapping dose distributions outside of the target volume. Experimental in vivo studies, carried out at research labs with grids containing µm- or mm-wide beam elements, have shown that it is possible to produce focal damage in a selected tissue volume by crossfiring the beam grids. Conclusions The main therapeutic advantage of grid therapy, compared to conventional radiotherapy with wide uniform beams, is related to a reduction of the early and late side effects produced by the treatment. The potential issues related to organ motion during the grid irradiation can be reduced by using beams of higher flux and motion-control methods, e.g. total anesthesia.

Wednesday June 14, 2017

14:10-14:30. Leonhard Karsch, Dresden, Germany

Status report: Ion Beam Therapy based on Laser Plasma Accelerators

Karsch L, Beyreuther E, Enghardt W, Gotz M, Masood U, Schramm U, Zeil K, Pawelke J. OncoRay – National Center for Radiation Research in Oncology, Faculty of Medicine and University Hospital Carl Gustav Carus, Technische Universität Dresden, Helmholtz-Zentrum Dresden - Rossendorf, Dresden, Germany.

Background: Only few ten radiotherapy facilities worldwide provide ion beams, in spite of their physical advantage of better achievable tumour conformity of the dose compared to conventional photon beams. Since, mainly the large size and high costs hinder their wider spread, great efforts are ongoing to develop more compact ion therapy facilities. Methods: One promising approach for smaller facilities is the acceleration of ions on micrometre scale by high intensity lasers. Laser accelerators deliver pulsed beams with low pulse repetition rate but high number of ions per pulse, broad energy spectra and high divergences. A clinical use of a laser based ion therapy requires not only a laser accelerator which delivers beams of therapeutic quality, but also new approaches for beam transport and delivery, dosimetric control, tumour conform dose delivery procedure together with the knowledge of the radiobiological effectiveness of laser-driven beams. Results: Over the last decade research was mainly focused on protons and progress was achieved in all of the necessary tasks. Although currently the maximum proton energy is not yet high enough for patient irradiation, suggestions and solutions have been reported for compact beam transport and dose delivery procedure, respectively, as well as precise dosimetric control. Radiobiological in vitro and in vivo studies performed so far show no indications of an altered biological effectiveness by laser-driven beams. Conclusion: Laser based facilities will hardly improve the availability of ion beams for patient treatment in next decade. Nevertheless, there are possibilities for a need of laser based therapy facilities in future.

Wednesday June 14, 2017

14:30-14:40. Martina Fuss, Darmstadt, Germany

Gold nanoparticles as radiosensitizers for ion beam therapy

Fuss, M.C.,1 Boscolo, D.,1 Bolsa-Ferruz, M.,2 Porcel, E.,2 Sokol, O.,1 Wiedemann, J.,1 Tinganelli, W.,1,3 Friedrich, Th.,1 Scholz, M.,1 Jakob, B.,1 Lacombe, S.,2 Scifoni, E.,3 Kraemer, M.1. 1) Biophysics Department, GSI Helmholtzzentrum für Schwerionenforschung GmbH, Planckstr. 1, 64291 Darmstadt, Germany. 2) Institut des Sciences Moléculaires d'Orsay (UMR8214), Bât 351, Université Paris Sud, CNRS, 91405 Orsay, France. 3) Trento Institute fo.

Introduction: The enhanced permeability and retention effect [1] makes nanoparticles a promising candidate for delivering or improving cancer therapies. In particular, gold nanoparticles (AuNPs) are biocompatible, easy to functionalize, and their high atomic number (Z) can locally increase dose deposition under irradiation in biological tissues, producing effective radiosensitization in photon beams [2]. Here we present our recent results on the combined action of ion beams and AuNPs. Materials and Methods: HeLa cells were irradiated with carbon and oxygen ion beams at varying dose-averaged linear energy transfer (<LET>) values corresponding to different depths in an extended target. Cell survival after irradiation with different doses in presence/absence of DTDTPA-coated AuNPs was assessed by means of colony formation assays. For the different experimental conditions, the dose distribution patterns on the micro-scale were modelled using the Monte Carlo track structure code TRAX [3]. For a realistic comparison of the physical dose deposited in presence/absence of the NPs, secondary electrons were fully simulated down to energies of ~eV. Next, the biological implications of the different local doses were approached in analogy to the local effect model (LEM). In agreement with the reported extra-nuclear localization of AuNPs and the marginal importance of nuclear DNA damage related to the NPs, different possible origins of radiosensitization were taken into account. Results: We present radial dose distributions as simulated with TRAX and discuss the dose increase and clustering effects induced by AuNPs. The biological damage thus expected in subcellular sensitive targets is analyzed and is compared to the enhancement observed in cell killing for cells incubated with AuNPs as compared to controls. References: [1] Peer et al., Nat. Nanotechnol. 2, 751 (2007) [2] Hainfeld et al., Phys. Med. Biol. 49, N309 (2004) [3] Wälzlein et al., Phys. Med. Biol. 59, 1441 (2014)

Wednesday June 14, 2017

14:40-14:50. Aleksandra K. Biegun, Groningen, The Netherlands

Calibration of X-ray CT relative proton stopping power by proton radiography in proton therapy

K.J. Ortega Marin, S. Brandenburg, A.K. Biegun (presenting author). KVI-Center for Advanced Radiation Technology, University of Groningen, Groningen, The Netherlands.

Introduction An accurate determination of relative proton stopping powers (PSP) is crucial to prepare the most optimum proton treatment plan for the patient. The novel proton radiography (pRG) imaging technique has a big potential to be used in determining PSP directly (without any model) in various tissues of the patient. The pRG technique can be used to calibrate PSP from X-ray CT, which can increase their accuracy and can optimize a "patient-specific" clinical calibration curve in proton therapy treatment. Materials and methods The optimization of the calibration curve has been performed on a phantom built of PMMA, filled with 6 inserts of different diameters and contents, comprising 11 materials, including 5 tissue surrogates, of known composition and density. A CT scan of the phantom was done at 120 kV X-ray tube voltage. An initial 9-segments calibration curve of relative PSP vs. CT number was constructed based on Schneider method to obtain a Water Equivalent Path Length (WEPL) map, WEPL_DRR. A proton energy loss radiography of the same phantom was simulated with Geant4. Only protons traveling along almost straight lines were considered to build the radiography image, giving a high resolution WEPL_pRG map. Protons with larger scattering angles, causing the image blurring, were discarded. The difference between WEPL_DRR and WEPL_pRG was evaluated by means of $\chi 2$ statistic, used to iteratively modify the calibration curve. Results Small differences between these two maps, caused by its imperfect alignment in the CT scanner, were observed. The iterative optimization on WEPL decreased the $\chi 2$ statistic significantly, by 55%, and the calibration curve has been optimized. Conclusion The iterative optimization of the "patient-specific" CT calibration curve has been performed with the use of proton radiography imaging technique, resulting in more homogeneous WEPL_DRR. Further development includes real patients CT data in the proton radiography simulations.

Wednesday June 14, 2017

14:50-15:00. Nigel Allinson, Lincoln, United Kingdom

Chasing the Elusive Proton CT - Recent Results from the PRaVDA Consortium

Allinson N M and the PRaVDA team. Computer Science, University of Lincoln, Lincoln, United Kingdom.

Prior to treatment, x-ray CT scans are acquired for treatment planning. Translation of electron density to proton stopping power is appreciable source of uncertainty. Paganetti's detailed analysis (Phys Med Biol. 57, 99-117: 2012) suggests total uncertainty in proton range including range degradation due to inhomogeneities of ±4.6% +1.2 mm. If effects due to this are excluded (use of Monte Carlo calculations) reduces to ±2.7% +1.2 mm. Largest single uncertainty component relates to tissue I-values at ±1.5% and second is related to CT conversion to tissue at ±0.5%. Proton CT should remove these components to yield overall uncertainty of ±1%. However, acquiring clinical-quantity proton CT imagery has proved challenging. The PRaVDA consortium has designed, built, commissioned and exploited a fully solid-state integrated imaging and dosimetry system. It employs custom sensors, both silicon strips and radiation-hard CMOS imagers, and is capable of recording the individual trajectories and residual energies of up to 25M protons/s. Tracking efficiency through four sets of trackers is >85%. Novel CT reconstruction algorithms have been developed that are fully analytical and account in a principled manner for non-linear paths and the finite extent of the beam. Furthermore, several proton CT modes have been explored based not only on stopping power but scattering, attenuation, and straggling powers. High quality proton CTs of custom phantoms and biological samples have been produced and measured relative stopping power for a range of tissue substitute test materials with uncertainties <1.6%, at diagnostic dose levels. This paper introduces operational requirements for proton CT instrumentation, outline design and operation of our current system, show proton imagery examples, and discuss potential for different proton CT modalities. Overall we show how proton CT cannot only improve planning and treatment monitoring but how it can fit into clinical workflows.

Wednesday June 14, 2017

15:00-15:10. Y Prezado, Orsay, France

Spatial fractionation of the dose in charge particle therapy

Prezado Y (1), Gonzalez W (1), Guardiola C (1), Heinrich S (2), Jouvion G (3), Jourdain L (4), , Juchaux M (1), Labiod D (2), Martinez-Rovira I (1), Nauraye C (2), Patriarca A (2), Peucelle C (1), Pouzoulet F (2), Sebrie C (4). 1. IMNC-CNRS, Orsay, France; 2. Institut Curie, Orsay, France; 3. Insitut Pasteur, Paris, France; 4. IR4M University Paris Sud, Orsay, France.

Introduction The dose tolerances of normal tissues continue being the main limitation in radiotherapy. As a strategy to overcome it we propose to ally inherent physical advantages of protons and heavy ions (up to Fe) with the normal tissue preservation observed when irradiated with submillimetric spatially fractionated beams (minibeam radiation therapy) [1, 2]. Materials and methods Monte Carlo simulations, gafchromic films and a PTW microdiamond detector (60019) were used for dosimetric evaluation from protons up to Fe ions. Concerning proton MBRT, a first implementation was performed by means of a mechanical collimation [4]. The whole brain of 7 weeks old Fischer 344 rats was irradiated. Half of the animals received conventional seamless proton irradiation (25 Gy in one fraction). The other half were irradiated with pMBRT (58 Gy peak dose in one fraction). Results The first complete set of dosimetric data in such small proton field sizes was obtained [3]. Rats treated with conventional proton irradiation exhibited moist desquamation, and important brain damage. In contrast, the pMBRT group presented no damage. Concerning heavy ions MBRT, our work shows very favourable dose distributions, even for very heavy ions (from Ne to Fe) despite fragmentation, supporting a potential renewed use of those ions for therapy Conclusions Our results show that the use of the spatial fractionation of the dose in charge particle therapy could lead to a widening of the therapeutic widow for radioresistant tumors. The promising results obtained support further explorations of this novel avenue. [1] Prezado et al., Rad. Research. 184, 314-21 (2015). [2] Deman et al., IJROBP 82, 693-700 (2012). [3] Peucelle et al., Med. Phys. 42 7108-13 (2015).

Wednesday June 14, 2017

15:10-15:20. Ikechi Ozoemelam, Groningen, Netherlands

PET imaging of short-lived nuclides during proton beam irradiation

Ozoemelam I S, Buitenhuis H J T, Diblen F, Brzezinski K W, Brandenburg S and Dendooven P. KVI-Center for Advanced Radiation Technology, University of Groningen, Zernikelaan 25, 9747AA Groningen, The Netherlands.

Introduction In-vivo dose delivery verification in proton therapy can be performed by positron emission tomography (PET) of the positron-emitting nuclei produced by the proton beam in the patient. A PET scanner installed in the treatment position of a proton therapy room that takes data with the beam on will see very short-lived nuclides as well as longer-lived ones. The most important short-lived nuclide for proton therapy is 12N (T1/2 = 11 ms). Other important short-lived nuclides, including 38mK (T1/2 = 925 ms) and 29P (T1/2 = 4.1 s), are produced during the irradiation of bone. The results of a proof-of-principle experiment of beam-on PET imaging of short-lived nuclides are presented. Materials and methods A 90 MeV proton beam from the cyclotron at KVI-CART was used with the PDPC ModuleTEK PET-system to investigate the energy and time spectra of PET coincidences during beam on. An anti-coincidence filter with the cyclotron RF enabled the removal of prompt gamma signals ensuring a good identification of the 511 keV PET counts during beam-on. A method was developed to subtract the long-lived background from the short-lived nuclide image by introducing a beam-off period into the cyclotron beam time structure. Results A range shift of 5 mm in a graphite target was measured as 6 ± 3 mm using 12N PET. A 5 mm shift of a calcium phosphate target in the proton path was measured as 4.5 ±2.2 mm via PET imaging of 38mK and 29P. A simulation of 12N imaging shows that a large dual-panel scanner that images a single spot directly after it is delivered can measure a 5 mm range shift with millimeter accuracy: 5.5 ± 1.1 mm for 1×108 protons and 5.2 ± 0.5 mm for 5 × 108 protons. Conclusions The combination of proof-of-principle experiments and simulations shows that 12N PET imaging of single spots in the distal layer of an irradiation allows proton range verification with millimetric precision. This makes fast and accurate feedback on the dose delivery during treatment possible.

Wednesday June 14, 2017

15:20-15:30. Johannes Müller, Dresden, Germany

Development of an experimental setup for the integration of multi-modality imaging and photon/proton irradiation for preclinical cancer research with small animals

Müller J. (1,2), Neubert, C. (1,6) , Lühr, A. (1,3, 4), von Neubeck, C. (1,3,4), Schürer, M. (5), Beyreuther, E. (1,2), Tillner, F. (1), Krause, M. (1,2,3,4,5), Bütof, R. (1), Dietrich, A. (1,3,4). 1Dept. of Rad. Oncology and OncoRay – Natl. Center f. Rad. Research in Oncology, Fac. of Medicine/ University Hospital C. G. Carus, TU Dresden, Germany 2Helmholtz-Zentrum Dresden - Rossendorf 3DKTK, Dresden, Germany 4DKFZ, Heidelberg, Germany 5NCT, Partne.

In this abstract, we present an experimental setup that allows for multi-modal, cross-platform imaging of small animals as well as image-guided proton- and photon irradiation under laboratory conditions. The setup consists of two units: A primary bedding unit which holds the animal and which is equipped with a breathing mask for inhalation anesthesia, an inlet for warm air and a breathing sensor. The primary unit was designed to meet the demands of the various imaging (magnetic resonance imaging, positron emission tomography, computed tomography, proton radiography,) and treatment modalities (photon- and proton irradiation). The bedding unit can be mounted inside a container, which is designed to maintain pathogen-free conditions outside designated animal laboratory facilities. The second, peripheral unit comprises a heating module, several sensors and read-out electronics to control and monitor temperature as well as vital signs. Moreover, it allows for remote emergency intervention (e.g. oxygen flush) during the animal's anesthesia. The setup has currently been tested for proton irradiation in an experimental area. A method was implemented to perform on-line position verification by proton radiography. The presented setup features multiple advantages for combined, multi-modal treatment which is of special importance for the monitoring and treatment planning of experimental tumor models. In particular, orthotopic tumors which require accurate imaging – the modality of which can be chosen based upon tissue and treatment – and treatment planning. It satisfies the various modalities' requirements, hence allowing for one combined workflow. Moreover, image analysis is strongly simplified as multi-modal images can be co-registered without sophisticated techniques.

Wednesday June 14, 2017

Session 4. Treatment planning in particle therapy

16:40-17:00. Mischa Hoogeman, Rotterdam, The Netherlands

Challenges in treatment planning for intensity modulated proton therapy

Hoogeman M.S. Radiation Oncology, Erasmus MC Cancer Institute, Rotterdam, The Netherlands.

Treatment planning for intensity-modulated proton therapy (IMPT) has it specific challenges compared to photon radiotherapy. These are related to the physical properties of the proton beams as well as the method of delivery. For example, the large number of degrees of freedom makes the optimization of an IMPT treatment plan a large-scale and lengthy process. A solution to this problem will be presented and also how this solution can be used to reduce the time for dose delivery by energy-layer reduction. Another challenge is related to robust optimization. Although in literature this technique has been well established, the clinical introduction is lagging behind. One of the reasons is the lack of recipes for the robustness settings that have to be applied given random and systematic patient-setup and range error distributions in order to yield an adequate treatment for a patient population. The first derived so-called “robustness-recipe” will be discussed. Finally, two different methods will be presented to minimize the impact of anatomical changes on the proton therapy dose distribution. The first one includes model-predicted anatomies in the robust optimization and the second one uses an automated dose restoration method to mitigate range deviations induced by daily density changes in the patient. References 1. Jagt T et al. Near real time automated dose restoration in IMPT to compensate for daily tissue density variations in prostate cancer. PMB 62:4254-4272. 2. van de Water S et al. Shortening delivery times of intensity modulated proton therapy by reducing proton energy layers during treatment plan optimization. IJROBP 92:460-8. 3. van der Voort S et al. Robustness Recipes for Minimax Robust Optimization in Intensity Modulated Proton Therapy for Oropharyngeal Cancer Patients. IJROBP 95:163-70. 4. van de Water S et al. Improved efficiency of multi-criteria IMPT treatment planning using iterative resampling of randomly placed pencil beams. PMB 58:6969-83.

Wednesday June 14, 2017

17:00-17:10. Vicki Taasti, Aarhus, Denmark

Comparison of projection- and image-based methods for proton stopping power estimation using dual energy CT

Vilches-Freixas G (1), Taasti VT (2), Muren LP (2), Petersen JBB (2), Létang JM (1), Hansen DC (1), Rit S (2). (1) CREATIS, Université de Lyon, Lyon, France. (2) Dept. of Medical Physics, Aarhus University Hospital, Aarhus, Denmark.

Introduction Several strategies for estimating stopping power ratio (SPR) from dual-energy CT (DECT) have been proposed to improve accuracy of proton dose calculations. DECT methods can mainly be categorized into projection-based methods, where material decomposition is performed prior to image reconstruction, and image-based methods, where decomposition takes place after image reconstruction. With the advent of photon-counting and dual-layer technology, projection-based methods could be considered for SPR estimation. In this simulation-based study we compared the SPR accuracy of one projection- and two image-based DECT methods. Materials and Methods X-ray CT projections of the female ICRP phantom were simulated using two different X-ray spectra with a realistic detector response and noise levels. ICRP slices at four locations were selected: head, sternum, breast and pelvis. Reference SPR-maps were computed at 200 MeV. The SPR comparison was based on percentage deviation inside ROIs and relative range errors calculated with Radon transform of difference maps. Results SPR root-mean-square errors (RMSE) over the selected ROIs were 0.54% for the projection-based method and 0.68% and 0.61% for the two image-based methods. The RMSE for the relative range errors were slightly smaller for the projection-based approach, but close to zero for all decomposition domains as positive and negative errors averaged out over the slice. Conclusions SPR estimations with the projection-based method produced slightly better results than the two image-based methods used in this simulation-based study, therefore, with the advent of technological developments, projection-based methods could be considered for SPR estimation if projection data is available.

Wednesday June 14, 2017

17:10-17:20. Jonathan Scharff Nielsen, Herlev/Lyngby, Denmark

Patch-based CT metal artifact reduction using MRI for proton and photon radiation therapy

Nielsen JS(1,2), Van Leemput K(2,3), Edmund JM(1). 1 Copenhagen University Hospital, Department of Oncology, Herlev, Denmark. 2 Technical University of Denmark, DTU Compute, Lyngby, Denmark. 3 Harvard Medical School, Department of Radiology, Boston, USA.

Introduction CT streak artifacts from dental implants in the head-and-neck (H&N) may compromise the CT numbers and act as an exclusion criterion for proton therapy. Commercial CT scanners offer metal artifact reduction (MAR) corrections but are often insufficient. An MRI acquired for tumor delineation can provide useful anatomical information for MAR. We preliminarily evaluate a novel patch-based method for MAR that incorporates the MRI. Materials & methods One H&N patient with a unilateral parotid tumor was investigated. The clinically used MAR CT (oMAR), sinogram and T1w MRI were extracted. 4 MAR approaches were studied: 1) oMAR, 2) oMAR corrected with the patch-based MAR (MR-oMAR), 3) sinogram iterative reconstruction with the patch-based MAR as prior (MR-prior) and 4) oMAR, manual replacement with water (water test). The latter is often clinical practice and acts as the reference. We re-calculated the clinical oMAR photon plan (RapidArc) on the 3 other CTs. Two oMAR optimized proton plans (IMPT) with respectively 1 of 3 and 2 of 2 fields (F) intentionally directed through the artifact contaminated oral cavity were similarly re-calculated. Percentage difference in dose volume histogram (DVH) points of the PTV (D98, Dmean, D2) and oral cavity (Dmean) as compared to water test are reported. Results Qualitatively, MR-prior produced the least bright streaks near the implants but with more dark areas as compared to oMAR. Compared to water test, photon DVH point differences were ~0% for all MARs. For the 3F and 2F proton plan PTV, D98=1.0/1.0/-0.2% and -0.5/-0.4/0.8%, Dmean=0.0/0.0/0.0% and -2.3/-2.2/-0.4%, D2=-2.3/-2.3/-0.6% and -6.0/-6.0/-4.2% (oMAR/MR-oMAR/MR-prior). For the oral cavity, Dmean=1.0/1.0/1.3% and 1.4/1.4/0.6%. Conclusion As expected, the protons were more sensitive to differences in MAR corrections than the photons. The MR-prior MAR visually produced the best result and yielded the smallest dosimetric difference relative to the clinically used oMAR.

Wednesday June 14, 2017

17:20-17:30. Per Poulsen, Aarhus, Denmark

Efficient interplay effect mitigation for proton pencil beam scanning by spot-adapted layered repainting evenly spread over the full breathing cycle

Poulsen PR (1), Eley J (2), Langner U (2), Langen K (2). (1) Department of Oncology, Aarhus University Hospital, Aarhus, Denmark; (2) Maryland Proton Treatment Center, Baltimore, USA.

Introduction: Proton pencil beam scanning (PBS) allows accurate 3D dose shaping to radiotherapy targets, but interplay effects caused by simultaneous beam and target motion may considerably deteriorate the target dose. The aim of this study was to develop and implement a practical repainting method for efficient interplay effect mitigation in proton PBS. Methods: A new flexible repainting scheme with spot-specific numbers of repaintings evenly spread over the whole breathing cycle (here assumed to be 4s) was developed. Twelve fields from five thoracic/abdominal PBS plans were delivered three times with the new repainting scheme to an ion chamber array on a motion stage: Once static and twice with 4s, 3cm peak-to-peak sinusoidal motion (with different starting phases). For comparison, all dose measurements were repeated with no repainting and 8 repaintings. For each motion experiment, the 3%/3mm gamma pass rate was calculated using the motion-convolved static dose as reference. Simulations were first validated with the experiments and then used to extend the study to 0-5cm motion amplitudes, 2-6s motion periods, patient-measured liver tumor motion, and 1-6 fraction treatments. Results: The mean (SD) gamma pass rates in the experiments were 59.6% (9.7%) (no repainting), 76.5%□(10.8%) (8 repaintings), and 92.4% (3.8%) (new repainting scheme). Simulations reproduced the experimental gamma pass rates with 1.3% root-mean-square error and demonstrated largely improved gamma pass rates with the new repainting scheme for all investigated motions. One- and two-fraction deliveries with the new repainting scheme had similar gamma pass rates as 3-4 and 6-fraction deliveries with 8 repaintings. Conclusions: A novel repainting strategy for efficient interplay effect mitigation was proposed, implemented, and shown to outperform conventional repainting in experiments, simulations and dose reconstructions. It may be used for safe thoracic and abdominal SBRT with proton PBS.

Wednesday June 14, 2017

17:30-17:40. Marta Peroni, Villigen PSI, Switzerland

Shaping proton therapy dose with DTI and DSC MRI data: functional SIB and avoidance proof of concept study

Peroni M.1, Bolsi A. 1, Poel R. 1,4, Ahlhelm F. 2, Kubik-Huch R. 2, Weber D.C. 1,3,4, Lomax A.1. 1Center for Proton Therapy, Paul Scherrer Institute, Villigen, CH, 2Department of Radiology, Cantonal Hospital Baden, Baden, CH, 3Radiation Oncology Inselspital, Bern, CH, 4Radiation Oncology, University Hospital of Zurich, CH.

Radiotherapy of brain lesions can result in neurocognitive toxicities. Nonetheless, treatment planning typically ignores functional structures, such as white matter neural networks or hypoxic/aggressive sub-areas of tumours, despite modern MRI techniques that can visualize these. Here, we investigate the potential of incorporating cortico-spinal tract structures (DTI_CST), using deterministic tractography, and relative Cerebral Blood Volume (rCBV), thought to correlate with aggressiveness and identified using T2* perfusion imaging, into treatment planning for PBS proton therapy. For an oligoastrocytoma (WHO II) patient, four treatment plans have been calculated. i) A uniform (to the target) plan, ii) a SIB plan based on rCBV, iii) a uniform plan with DTI_CST sparing and iv) both SIB and DTI_CST sparing. Dose constraints for DTI_CST were defined on the whole volume and by splitting into upper, middle and lower portions, the middle portion of which overlapped with the PTV. For the rCBV-SIB plan (ii), mean and max doses in the cochlea were reduced by 3% and 5% respectively c.f. the uniform plan, max dose to the brainstem by 3% and dose to the central and lower DTI_CST by 2%. Using an alternative field arrangement, the CST-centre could be better spared (mean dose -5%), but at the cost of increased mean/max dose to the cochlea (3% and 5% respectively). For the DTI_CST sparing plan (iii), CST_centre mean (61% vs 103%) and maximum (70% vs 103%) doses were substantially reduced c.f. the uniform plan (i), and max dose was reduced by 5% and 2% in the brainstem and cochlea respectively, but at the cost of a reduced V90 to the CTV (91.3% vs 100%). With different constraints for the different DTI_CST portions, mean and max dose to CST_centre could be reduced to 52 and 56% respectively. Similar results were found for the SIB_DTI plan (iv). In conclusion, it has been shown that IMPT plans can be generated to account for constraints on MRI defined functional volumes.

Wednesday June 14, 2017

17:40-17:50. Bonny Abal, Bergen, Norway

Plan selection in proton therapy for simultaneous treatment of the prostate, seminal vesicles and pelvic lymph nodes

Bonny Abal1, Liv Bolstad Hysing1,2, Grete May Engeseth2, Kristian Ytre-Hauge1, Sara Thörnqvist1,2. 1Faculty of Mathematics and Natural Sciences, University of Bergen, Norway, 2Department of Oncology and Medical Physics, Haukeland University Hospital, Bergen, Norway.

Introduction: Proton therapy to the prostate and the pelvic lymph nodes are challenging due to the different motion patterns of the targets affecting the proton range. The aim of the current study was to evaluate if a plan library with different positions of the prostate/seminal vesicle PTV (p/sv-PTV) in relation to the BA can improve proton therapy for locally advanced prostate cancer. Methods: Target motion were analysed from rigid shifts of the GM relative to BA in 18 patients, each with a planCT and 7-10 repeat CTs. The shifts were used to define p/sv-PTVs in the plan library as well as a conventional PTV using a standard margin recipe. The p/sv-PTVs in the library used both shifts of the p/sv-CTV position in relation to the BA and reduction of the PTV margins. The PTV for the lymph nodes target was identical in all plans. IMPT plans were optimised for all PTVs. The dose delivered using plan selection from the library as compared the conventional plan was simulated for a patient having 9 repeat CTs, excluded from the target motion analysis. Plan selection used visual inspection of the library PTVs to choose the PTV that best fit the delineated CTVs in the repeat CTs. Results: Due to correlation in the anterior-posterior (AP) and superior-inferior (SI) direction, the library consisted of 3 p/sv-PTVs: 2 p/sv-CTVs shifted +/- 1.5 SD of the systematic error in AP (+/- 5.0mm) and SI (+/-4.6mm) direction and 1 p/sv-PTV without shift. These CTVs used 5mm isotropic PTV margins. The conventional plan used p/sv-PTV margins of 5, 10, 10mm in left-right, AP and SI directions. The median D98 delivered with plan selection and the conventional plan was>95% of the prescribed dose for all targets. A reduction of 6.6 and 2.6 Gy gEUD was obtained for the rectum (k=12) and bladder (k=8), respectively using plan selection. Conclusions: Plan selection was feasible for the new patient and reduced doses to the rectum and bladder as compared to the conventional plan.

Wednesday June 14, 2017

17:50-18:00. Leszek Grzanka, Krakow, Poland

LET-Painting using Multiple Ions

Grzanka L1, Ureba A2, Lindblom E2, Toma-Dasu I2, Krämer M3, Petersen JBB4, Bassler N2. 1IFJ-PAN, Polish Academy of Sciences, Krakow, Poland 2Medical Radiation Physics, Dept. of Physics, Stockholm University, Sweden 3GSI, Darmstadt, Germany 4Dept. of Medical Physics, Aarhus University Hospital, Aarhus Denmark.

Background LET-painting using multiple ion species has earlier been suggested as an approach to mitigate radioresistance in tumours. Based on pre-treatment imaging, the target can be segmented with respect to hypoxia-related radioresistance. Thus, hypoxic regions within the tumours can be identified and targeted with high-LET radiation from carbon or heavier ions, while the normoxic regions are irradiated with low-LET radiation. Anticipated benefits are: 1) reducing the volume of tissue exposed to high-LET radiation could potentially reduce the toxicity, and 2) the dose-averaged LET in the target is increased, effectively reducing the oxygen enhancement ratio (OER). Furthermore, 3) healthy tissue exposed to low-LET radiation in the vicinity of the tumour tissue will retain the therapeutic advantage from fractionation. In this study we present various multi-ion LET-painting strategies and discuss their feasibility. Materials and Methods LET-painting was achieved using the PyTRiP98 package and the treatment planning system TRiP98, mixing protons with carbon or oxygen ions. Among the strategies investigated were: a) LET-painting as a heavy ion boost on top of a low-LET dose distribution in the hypoxic target, or b) to substitute the low-LET entirely with a high-LET component. TCP was calculated using the LET-parametrized repairable-conditionally repairable (RCR) model. Results Method a) turned out to substantially dilute the LET in the hypoxic target, whereas method b) could achieve a significantly higher LET and lower OER. In either case, dose ramps seemed to be essential for proper high-LET coverage over the hypoxic target. Conclusion Multi-ion LET-painting may represent a promising way of mitigating radioresistance given prior biological assessment and verification of the underlying physical parameters. Multi-ion LET-painting is already possible in at least one facility where fast switching dual-ion sources are available, but may also require a heavy-ion gantry.

Thursday June 15, 2017

Session 5. Image-guidance, adaptation and motion management

8:30-8:50. Katia Parodi, Munich, Germany

Imaging for reduced range uncertainties and in-vivo verification in ion beam therapy

Parodi, K. Department of Medical Physics, Ludwig-Maximilians-Universität München, Munich, Germany.

Ion beams are increasingly used in external beam radiotherapy as a promising treatment modality offering superior tumour-dose conformality and better sparing of critical organs and healthy tissue in comparison to established photon radiation. However, full clinical exploitation of the advantages of ion beams is still hampered by several sources of uncertainties, particularly related to the in-vivo beam range. Therefore, several techniques are being explored to reduce range uncertainties at the stage of treatment planning or treatment delivery. Here, special emphasis will be given to methods based on the detection of acoustic and nuclear-based emissions induced by ion interaction in tissue during treatment. In particular, this contribution will review available clinical experience and ongoing developments of advanced imaging for in-vivo verification in ion beam therapy.

Thursday June 15, 2017

8:50-9:10. Antje Knopf, Groningen, Netherlands

Treating moving targets with scanned proton beams: vision of an Image-Guided Adaptive workflow

Antje-Christin Knopf. Radiotherapy department, UMCG.

For many indications proton therapy (PT) permits dose distributions with less integral dose than conventional radiotherapy which results in a reduction of toxicity. Furthermore, due to its conformity, PT allows for higher target doses improving the local control. However, range uncertainties and interplay effects compromise the conformity of the high does region and the local control. To safely treat moving targets at the future Groningen Proton Therapy Center (GPTC) we envision the following Image-Guided Adaptive (IGA) workflow: - Based on 4D image information we will establish a robustly optimized treatment plan. - We will perform a 4D evaluation of the robust plan to confirms that it passes a set of clinical uncertainty scenarios. - For plans that fail or patient cases that are considered to have a high probability to change their motion characteristics during the course of treatment we will employ additional motion mitigation techniques (breath hold). - Before delivering each fraction of the treatment we will validate the motion assumptions with 4DCBCT. - During delivery of each fraction we will monitor the motion and acquire machine log-files to perform a subsequent dose accumulation. - After each fraction we will check if the accumulated dose stays within pre-defined thresholds. If not plan adaptation is initialized.

Thursday June 15, 2017

9:30-9:40. Esben Worm, Aarhus, Denmark

Respiratory gated liver SBRT based on motion monitoring of implanted electromagnetic transponders

Worm ES (1), Høyer M (2,3), Hansen R (1), Larsen LP (4), Weber B (1), Grau C (1,3), and Poulsen PR (1,3). (1) Department of Oncology, (2) The Danish Centre for Particle Therapy, (3) Institute of Clinical Medicine, and (4) Department of Radiology, Aarhus University Hospital, Aarhus, Denmark.

Introduction Intra-fraction motion may compromise the target dose in SBRT of liver tumors. Respiratory gating can improve treatment delivery, but gating based on external surrogates is inaccurate. This study presents our results with gated liver SBRT guided by internal electromagnetic motion monitoring with the Calypso system. Methods Fifteen patients were included in a study of three-fraction respiratory gated liver SBRT guided by three implanted electromagnetic transponders at a TrueBeam Linac. The PTV was created by a 5mm axial and 7mm (n=12) or 10mm (n=3) cranio-caudal expansion of the CTV and covered with 67% of the prescribed CTV mean dose. Free-breathing treatment was gated to the end-exhale phase with beam-on when the target deviated less than 3mm (LR/AP) and 4mm (CC) from the planned position, according to the continuously monitored (25Hz) transponder centroid position. The couch was adjusted remotely if baseline drifts above 1-2mm occurred. Log files of transponder motion were used to determine the geometrical error and to reconstruct the delivered CTV dose distribution during beam-on in the actual gated treatments and in simulated non-gated treatments. Results In all 15 patients, the transponders were implanted with no severe side effects. All 45 treatment fractions were guided by the internal transponder motion as planned. Without gating the mean (range) 3D geometrical error during a fraction would be 5.4 (2.7-12.1)mm. As treated with gating the error was reduced to 2.0 (1.2-3.0)mm. The mean number of couch corrections during each gated fraction to counteract baseline drifts was 2.8 (0-7). The mean duty cycle during gated treatment was 62.5 (29.1-84.9)%. The mean reduction in CTV D95 relative to the planned dose was 6.2 (0.4—29.8) %-points without gating and 0.9 (0.1-2.4) %-points with gating. Conclusion Gating based on internal motion monitoring markedly reduced geometric and dosimetric errors in liver SBRT compared to non-gated standard treatment.

Thursday June 15, 2017

9:40-9:50. Janna van Timmeren, Maastricht, the Netherlands

Prognostic value of longitudinal CBCT radiomics for non-small cell lung cancer patients: potential for adaptive radiotherapy

van Timmeren, J.E., Leijenaar, R.T.H., van Elmpt, W., Lambin, P.. Department of Radiation Oncology (MAASTRO), GROW – School for Oncology and Developmental Biology, Maastricht University Medical Centre (MUMC), Maastricht, the Netherlands.

Introduction: Cone-beam CT (CBCT) scans are typically acquired daily for positioning verification of non-small cell lung cancer (NSCLC) patients. Quantitative information, derived using radiomics, can potentially contribute to (early) treatment adaptation. The aim of this study was to 1) select stable features and 2) show prognostic value of longitudinal CBCT radiomics. Materials and methods: For 63 NSCLC patients 4 scans were analyzed: CBCT of first (CBCT1) and second (CBCT2) treatment fraction, three weeks after start of treatment (CBCT3) and one day before or after CBCT3 (CBCT4). 133 radiomic features were extracted from GTV of all scans. Test-retest scans (CBCT1/CBCT2 and CBCT3/CBCT4) were used to calculate coefficient of variability (CoV) and concordance correlation coefficient (CCC) for feature selection: features having CCC below 0.85 and delta features (percentage differences (pD) between CBCT3 and CBCT1) not changing more than the CoV for at least 25% of patients were excluded. A model was developed on a training set of 80% of the data using 200-times repeated 10-fold CV LASSO with overall survival as endpoint. Prognostic value of features described in literature was also examined. Model performance was assessed using c-index. Results: Radiomic feature selection resulted in 80/133 stable features for CBCT1 and CBCT3 and 61/133 delta features which were used in a survival prediction model. LASSO resulted in a 7-feature model, including baseline and pD features, with c-index 0.69 (95%C.I. [0.60–0.78]) for training and 0.60 (95%C.I. [0.41–0.78]) for validation. A model of literature features (First order statistics–Energy, Shape–Compactness and GLRLM–GrayLevel Nonuniformity) achieved a c-index of 0.64, adding pD of one of these features did not improve the model. Conclusions: This study shows that longitudinal combined with baseline CBCT radiomics has prognostic value. This information could potentially be used for treatment adaptation to optimized outcome.

Thursday June 15, 2017

9:50-10:00. Ditte Møller, Aarhus, Denmark

Robustness of photon and proton treatment of advanced lung and esophageal cancer against anatomical changes

Møller DS1, Alber M2, Nyeng TB1, Jensen MF3, Holt MI3, Nordsmark M3 and Hoffmann L1. 1 Department of Medical Physics, Aarhus University Hospital, 2 Department of Radiation Oncology, Heidelberg University Hospital, 3 Department of Oncology, Aarhus University Hospital.

Introduction: Large anatomical changes during radiotherapy are often seen for lung cancer(LC) and esophageal cancer(EC). Precise delivery of proton therapy is highly sensitive to these changes which may result in under dosage of target. Material/methods: Twenty-three LC patients and 26 EC patients treated with IMRT (5-8 fields) were retrospectively planned with robust IMPT using three fields (LC) or one posterior field (EC). One or two surveillance CTs(sCT) were acquired during the treatment course. The consequences of anatomical changes were evaluated by recalculation of the plans on the sCTs. The CTV receiving 95% of the prescribed dose was analyzed. Results: For both patient groups IMPT showed a significant decrease in normal tissue dose compared to IMRT with a 5 Gy and 6 Gy median reductions in mean dose to lungs and heart. The sCTs reveal that for IMRT 26% (LC) and 27% (EC) of the patients showed a CTV coverage < 99% during treatment. Using IMPT, the CTV coverage decreased for LC (43% with coverage < 99% on sCT), while the CTV coverage improved for EC (15% with coverage < 99% on sCT). The median decrease in CTV coverage was for LC-IMRT 100% [95-100%], LC-IMPT 94% [66-100%], EC-IMRT 99% [87-100%] and EC-IMPT 100% [92-100%]. For LC the under dosage was due to atelectasis, target deformations and non-rigid positioning, while for EC target deformations and diaphragm positions were the cause. Due to the central position of the target EC-IMPT can be made robust with respect to the diaphragm using one posterior beam, while the decrease in CTV coverage for LC-IMPT is seen independently of field angle selection. Conclusion: Anatomical changes occur for both LC and EC, but the different target locations and types of changes make EC more robust with IMPT while LC is more robust with IMRT. Robust optimization does not eliminate the need for adaptation. Thus frequent imaging and adaptive strategies are recommended for both patient groups regardless of treatment modality.

Thursday June 15, 2017

Session 6. Normal tissues, radiogenomics, PROM, and modelling

10:50-11:10. Kathrin Kirchheiner, Vienna, Austria

A novel approach to identify patients with late, persistent, substantial and treatment-related symptoms in longitudinal studies including patient reported outcomes

Kirchheiner K (1). Pötter R (1). Nout RA (2). Lindegaard J (3). Kirisits C (1). Tanderup K (3).. (1) Department of Radiation Oncology, Medical University Vienna, Vienna, Austria. (2) Department of Radiation Oncology, Leiden University Medical Center, The Netherlands. (3) Department of Oncology, Aarhus University Hospital, Aarhus, Denmark..

Introduction: In the longitudinal analysis of patient reported symptoms within the EORTC quality of life questionnaires (QLQ), different statistical methods can be applied to comprehensively summarize the outcome. Beside the scoring method recommended by the EORTC QOL study group, other methods may be applied on patient reported symptoms in parallel to physician assessed morbidity, such as crude incidence rates, actuarial estimates and prevalence rates. These methods give all different impressions about the symptom burden of patients, resulting in considerable different outcome numbers and have specific advantages and shortcomings. Material & methods: A novel approach of a stepwise selection of patients with late, persistent, substantial and likely treatment-related symptoms (LAPERS concept) is introduced. The LAPERS concept is highlighted with an example of the EORTC QLQ CX24 item 32 “difficulties controlling bowel” within the prospective, observational, longitudinal and multi-institutional study on MRI image-guided, adaptive brachytherapy in locally advanced cervical cancer (EMBRACE study) and jointly discussed with other statistical methods, emphasizing the pros and cons. Results: Patient-reported quite a bit / very much difficulties controlling bowel reveals a crude incidence rate of 22%, 5 year actuarial estimates of 27.2%, prevalence rates ranging from 5-14% over time and a LAPERS proportion of 4.6% in the EMBRACE cohort with a median follow-up of 27 months (range 1-85). Preliminary results of testing the robustness of the LAPERS concept and validation approaches are presented. Conclusion: The novel methodological approach in analyzing of longitudinal patient reported symptoms shows promising preliminary results and will be further tested within the EMBRACE study and beyond.

Thursday June 15, 2017

11:10-11:20. Katherina Farr, Aarhus, Denmark

Patient reported symptoms and quality of life analysis before and after definitive chemo-radiotherapy for non-small cell lung cancer: correlation with radiation pneumonitis

Farr KP, Khalil AA, Grau C. Department of Oncology, Aarhus University Hospital.

Introduction The objective of the study was to investigate quality of life (QOL) before and after chemo-radiotherapy (RT) in the patients with non-small-cell lung cancer (NSCLC). Correlation of QOL measures with radiation pneumonitis (RP) was investigated, together with predictive value of dose-volume parameters on the lung symptoms and QOL outcomes. Materials and methods The patient cohort consisted of 71 NSCLC patients treated with curative radiotherapy of minimum 60 Gy. QOL was prospectively assessed via EORTC QLQ-C30 and LC13 questionnaires at baseline and after 3 months. Functional and symptoms scales, as well as global health and QOL status were analysed in patients who developed RP (CTCAE grades 2-5) and compared to those without RP (grades 0-1). Functional dose-volume parameters were derived from single photon emission computed tomography (SPECT/CT) images, performed on all patients before RT, and compared with conventional parameters from CT scan. Results Of the 71 eligible patients included in the study, 65 (92%) completed baseline QOL assessment, 57 (80%) completed the 3-month assessment. In all, 47% of patients had overall QOL improved or unchanged, while 53% experienced decline in QOL. Patients with RP had significantly higher lung symptoms scores for cough, dyspnoea and pain compared with patients without RP ($p<0.01$). QOL decline in the RP group was also significantly larger than in non-RP group. Linear regression analysis revealed that functional dose-volume parameters (functional mean lung dose and volume of functional lung receiving 20 and 30 Gy) were predictive of lung symptoms scores increase after RT ($p=0.02$ $R2=0.09$). Conclusions Large number of patients experienced decline in QOL and significant worsening of lung symptoms after curative chemo-radiotherapy for NSCLC, which correlated with radiation pneumonitis development. Increase in lung symptoms scores after RT could be predicted by dose-volume parameters to the functional lung.

Thursday June 15, 2017

11:20-11:30. Christopher Peeler, Houston, USA

Evaluating a model to predict post-treatment imaging changes in patients treated for brain tumors with proton therapy

Peeler CR, Grosshans DR, Mohan R, Mirkovic D. Department of Radiation Physics, UT MD Anderson Cancer Center, Houston, TX, USA; Department of Radiation Oncology, UT MD Anderson Cancer Center, Houston, TX, USA.

Introduction: The purpose of this study is to investigate the evaluative properties of a recently published model which describes the probability of the induction of post-treatment magnetic resonance (MR) image changes in pediatric patients treated for brain tumors as a function of dose and linear energy transfer (LET). Materials and Methods: The model was tested for other patients treated for brain tumors at our institution that were not included in the original study. For each patient, areas of post-treatment image change were identified on magnetic resonance imaging. Dose and LET distributions were calculated with Monte Carlo. The model was used to calculate a receiver operating characteristic curve and corresponding area under the curve (AUC) based on its predictions of image change compared to the identified areas of post-treatment image changes. A volume-based histogram of the probability of image change values predicted by the model was also calculated for the region of image change, brain, and brain stem for each of the patients. Results: The AUC values produced from testing the model on the new patients were high (in many cases > 0.9), which indicated that the model predictions agreed well with the identified regions of image change. The probability of image change volume-histograms provided a reasonable method of evaluating the model predictions in the image change regions as compared to the brain or brain stem volumes. Conclusions: A model which predicts the probability of post-treatment MR image change according to delivered proton dose and LET has thus far been applicable to patients outside of the cohort used to develop the model. Future work will aim to implement the model into the optimization of intensity modulated proton therapy plans so that it may eventually be used in the evaluation of treatment plans.

Thursday June 15, 2017

11:30-11:40. Line Schack, Aarhus, Denmark

Published biomarkers of late radiation-induced morbidity tested in prostate cancer patients.

Schack LMH1, Petersen SE2, Nielsen S1, Lundby L3, Høyer M4, Bentzen L2, Overgaard J1, Andreassen CN1,2, Alsner J1. 1Department of Experimental Clinical Oncology, Aarhus University Hospital, Denmark 2Department of Oncology, Aarhus University Hospital, Denmark 3Department of Surgery, Aarhus University Hospital, Denmark 4Danish Centre for Particle Therapy, Aarhus Univers.

Introduction Normal tissue morbidity sets the dose limit for radiotherapy (RT) in cancer treatment and has importance for quality of life for cancer survivors. A previous study of prostate cancer patients generated clinical data for radiation-induced morbidity measured by anal physiological methods and validated questionnaires. Other studies have identified biomarkers associated with late radiation-induced morbidity outcome. We have expanded biobank material and repeated questionnaires aiming to validate single nucleotide polymorphisms (SNPs) and a gene expression profile with endpoints from our cohort matching originally published endpoints. Materials and methods A cohort of prostate cancer patients was treated with RT curative intent in 1999-2007. A validated gene expression profile predictive of resistance to radiation-induced skin fibrosis was tested in 42 patients. A radiotherapy-induced anorectal dysfunction score (RT-ARD) served as a fibrosis-surrogate and a measure of over-all radiation-induced morbidity. Seven SNPs associated with late radiation-induced morbidity were tested in 96 patients (rs1800629, rs2682585, rs2268363, rs1801516, rs13035033, rs7120482 and rs17779457). Results Preliminary results showed an association between rs2682585 minor allele(A) and the RT-ARD score with an OR=2.0; 95%CI (1.1 - 3.7) p=0.02, out of concordance with original data showing a protective effect of the minor allele. The gene expression profile in patients classified as fibrosis-resistant was associated with higher RT-ARD scores OR=9.2; 95%CI (2.1 - 40.5) p=0.004. Conclusion We aimed to validate seven SNPs and a gene expression profile in a cohort of prostate cancer patients with unique scoring of radiation-induced morbidity. Two significant associations were found, both showed effects pointing to the opposite direction of originally published data. We conclude that the material was not able to validate previously published biomarkers of radiation-induced morbidity.

Thursday June 15, 2017

11:40-11:50. Nina Niebuhr, Heidelberg, Germany

Application of local effect accumulation in contrast to dose accumulation

Niebuhr, N I (1,2,3); Hentschke, C M (1,2,3); Floca, R O (1,2,3); Alber, M (2,3,4); Kraus, K M (1,4); Pfaffenberger, A (1,2,3). (1) German Cancer Research Center (DKFZ), Heidelberg, Germany; (2) Heidelberg Institute for Radiation Oncology (HIRO), Heidelberg, Germany; (3) National Center for Radiation Research in Oncology (NCRO), Heidelberg, Germany; (4) Heidelberg University Hospi.

Introduction: Organ motion introduces fractional dose variations that are neglected by averaging when accumulating dose. We investigate the impact on the prediction of the biological effect. Methods: A fraction-by-fraction application of the linear-quadratic model followed by effect accumulation is compared with calculation of the local survival fractions from accumulated dose in a standard fractionation scheme (30x2Gy). AVID and RTToolbox are used to implement an automated workflow for 3D data. An anthropomorphic deformable multimodality phantom of the pelvis with controllable interfractional motion of bladder, rectum and prostate (PTV) is used for isolated analysis of the influence of the respective organ motion types, and two patient cases are studied. Results: Using Jensen's inequality for a theoretical comparison of both approaches reveals that the dose accumulation based effect prediction systematically overestimates survival in all voxels. Hypofractionation is prone to larger differences. In accordance to theory, the results in 3D data showed that the difference increases over the course of therapy and is higher for lower α/β. Both phantom and patient cases showed only moderate motion amplitudes. For the phantom, bladder motion showed the highest impact on the model-difference in the gradient region outside the PTV with a relative overestimation of 7% at mid treatment. Peak values in patient data after 13 fractions reached 10% (absolute survival: 0.5) in the dose entrance region in the bowel. Conclusion: Overestimation of the survival fraction might lead to critical errors in the prediction of the biological outcome of treatment in normal tissue. Adjustment of tissue response models could be vital on the basis of fractional effect accumulation. Results in phantom and patient data indicate the importance of investigating the model-difference for cases with stronger motion patterns and different fractionation schemes (i.e. hypofractionation).

Thursday June 15, 2017

11:50-12:00. Jesper Pedersen, Aarhus C, Denmark

Biological dose and complication probabilities for the rec-tum and bladder based on linear energy transfer distribu-tions in spot scanning proton therapy of prostate cancer

Pedersen J [1], Petersen JBB [1], Stokkevåg CH [2], Ytre-Hauge KS [3], Flampouri S [4], Li Z [4], Mendenhall N [4], Muren LP [1]. [1] Department of Medical Physics, Aarhus University Hospital/Aarhus University, Aarhus, Denmark; [2] Dept. of Oncology and Medical Physics, Haukeland University Hospital, Bergen, Norway; [3] Dept. of Physics and Technology, University of Bergen, Bergen,.

Introduction The increased linear energy transfer (LET) at the end of the Bragg peak causes concern for an elevated and spatially varying relative biological effectiveness (RBE) of proton therapy (PT), often in or close to dose-limiting normal tissues. In this study, we investigated dose-averaged LET (LETd) distributions for spot scanning of prostate cancer patients using different beam angle configurations. In addition, we derived RBE weighted (RBEw) dose distributions and related normal tissue complication probabilities (NTCPs) for the rectum and bladder. Materials and methods Spot scanning plans (5mm spots/2mm spacing) were created in the treatment planning system TRiP for six patients (without rectal balloons/spacers). The CTV-to-PTV margins were 4mm axially and 6mm superior/inferior. The prescribed PTV dose was 78 Gy(RBE1.1) in 39 fractions. Physical dose and LETd distributions were calculated for all patients with two 'mirrored' beams (going from 110°/250° to 70°/290° in steps of 2°). RBEw dose distributions were calculated using RBE=1.1 and three different RBE models (McNamara (MN), Carabe (CB), and Wedenberg (WB); α/β: 1.93 prostate, 3.0 rectum, 4.0 bladder). The resulting biological dose distributions were used as input to Lyman-Kutcher-Burman NTCP models for the rectum and bladder. Results For the 80°/280° configuration, the median RBEw mean dose (MD) of the rectum increased from 3.6 Gy(RBE1.1) to 4.5 Gy (WB) while the median rectum NTCP increased from 1% to 7% (WB). The median prostate MD increased to 87.3 Gy (MN) compared to the prescribed dose of 78 Gy(RBE1.1). For the 100°/260° configuration, the MD of the bladder increased from 22.7 Gy(RBE1.1) to 24.8 Gy (WD/MN) while the bladder NTCP increased from 34% (RBE1.1) to 58% (CB). Conclusion Compared to using the standard RBE1.1, the three RBE models resulted in increased biological doses to the rectum, bladder and prostate, which in turn lead to substantially higher estimated rectum and bladder NTCPs.

Thursday June 15, 2017

Session 7. Adaptive radiotherapy – clinical implementation and results

13:00-13:20. Karin Haustermans, Leuven, Belgium

How to facilitate the clinical implementation of adaptive radiotherapy?

Haustermans K, Isebaert S. Department of radiation oncology, University hospitals Leuven.

Although the principle of adaptive radiotherapy (ART) is well known, i.e. adapting radiation delivery throughout treatment based on treatment variations observed between the planning CT/MR/PET and the during treatment images, its clinical implementation is less straightforward. ART can be as simple as the mere correction of treatment position but also as complex as 4D adaptive inverse re-planning, depending on the cause of the variation and the clinical goals of ART. Different tools that can be used for ART, including cone-beam CT, laser surface scanning systems and biological imaging, will be discussed. Despite the wide range of ART solutions, the optimal strategy for ART is still to be defined as it requires significant time and resources. To reduce this extra burden for the staff and the associated costs related to the application of ART, strategies need to be defined in order to facilitate its clinical implementation. Such strategies include the automation of the different steps of the treatment planning process (e.g. automatic contouring), faster treatment plan optimization and dose calculations, and strategies to reduce the frequency of plan adaptation.

Thursday June 15, 2017

13:20-13:40. Richard Poetter, Vienna, Austria

MRI based response adaptive radiotherapy in cervix cancer – concept, volumes, doses and clinical results

Richard Poetter. Department of Radiation Oncology, Medical University of Vienna.

Introduction: The concept of MRI-based response-adaptive radiotherapy implies adaptation of target during treatment according to tumour response. In cervix cancer this tumour response-adaptive concept has been implemented in clinical practice by using T2 weighted MRI and repetitive gynaecologic examination to carry out one major adaptation towards the end of radiochemotherapy (45 Gy/cis-Platin 5x40 mg/m2) and tested in a prospective study (EMBRACE). Materials and Methods: Various tumour related volumes were defined: initial and residual GTV-T (GTV-Tinit, GTV-Tres), initial and adaptive high risk CTV-THR, an adaptive intermediate risk volume CTV-TIR, related to GTVinit, and low risk CTV-TLR (ICRU 89/GEC ESTRO Rec). Initial volumes are targeted through dose from EBRT and adaptive volumes in addition through image guided brachytherapy (IGABT). Different doses were prescribed in EQD2 for these volumes, both for EBRT and IGABT and total. Results: Mean volumes and (median) doses achieved in the EMBRACE studies (EMBRACE 1 (1416 pats.), EMBRACE 2 (50 pats.) were the following: GTV-Tinit 55 cm3, 45 Gy; initial CTV-THR 90 cm3, 45 Gy; initial CTV-TLR 230 cm3, 45 Gy; GTV-Tres 9 cm3, 102 Gy (D98); adaptive CTV-THR 33cm3, 89 Gy (D90); CTV-TIR 78 cm3, 70 Gy (D90). Out of 80 local failures in 1230 patients one was not related to these volumes (Schmid 2017). Mature RetroEMBRACE data (n=731) (Sturdza 2016) show act.local/pelvic control at 3 y 91/87%; 98/96% in IB, 93/89% in IIB, 79/73% in IIIB. Overall survival was 74%. Conclusions: Within EMBRACE 2 these adaptive strategies are further elaborated and tested with focus on image guided EBRT and IGABT with multiple endpoints for clinical research. This tumor response-adaptive approach using one step of adaptation at 45 Gy based on repetitive T2 MRI may serve as research template at other tumor sites using photon, electron, particle or brachytherapy boost modalities and repetitive morphologic and/or functional imaging.

Thursday June 15, 2017

13:40-13:50. Ate Haraldsen, Aarhus, Denmark

Robustness of high FDG uptake volumes during Radiotherapy in Non Small Cell Lung Cancer.

Haraldsen A., Lutz C.M., Khalil A., Hoffmann L., Møller D. Nuklearmedicine Department & PET Center, Aarhus Universityhospital, Aarhus, Denmark. Department of Oncology, Aarhus Universityhospital, Aarhus, Denmark.

INTRODUCTION: The Danish NARLAL 2 Trial (NCT02354274) compares 18F-FDG-guided dose escalation to standard RT treatment. The dose is escalated heterogeneously, delivering mean doses up to 95Gy/33fx to high FDG uptake volumes to improve local control for patients with locally advanced NSCLC. We investigated the robustness of high FDG uptake regions within GTV-Tumour during RT and calculated changes in mean dose. MATERIALS/METHODS: 16 patients with three FDG-PET/CT scans were evaluated. Baseline scan (PET0) was dated 14 days prior to RT. The first and second scan during RT were performed at day 7 (PET1) and 14 (PET2). The most FDG avid part of the tumor (50% of SUVpeak) was delineated within the GTV-T on each scan (V050, V150 and V250). Overlap of the volumes was evaluated with overlap fraction (OF) and OF-boost (fraction of V150 or V250 included in the initial escalation volume, V050). Escalated dose plans were recalculated on CT2 and dose to V250 compared to the planned dose to estimate changes in dose coverage. RESULTS: Median values for OF0-1 and OF0-2 were 0.79 [0.43;0.91] and 0.83 [0.39;0.95]. OF-boost0-1 and OF-boost0-2 yielded slightly lower median values of 0,75 [0,43-0,91] and 0.78 [0,39-0,92], respectively. For 70% of patients, we found an OF-boost >70% and no dose decrements to V250. This indicates that a 70% OF-boost suffices to maintain planned dose. In 30% of patients, the OF-boost was <70% and the mean dose to high FDG uptake volumes decreased with up to 4 Gy. These patients either had necrotic tumours with a high FDG-uptake rim or a SUVpeak ~2 times background activity, rendering the definition of V150 and V250 questionable. CONCLUSION: For the majority of the patients, high FDG uptake sub-volume and escalated dose level were maintained during RT. For 30% of patients, the OF-boost decreased below 70% and a decrease in mean dose to the high FDG uptake volumes was observed due to low SUV peak values or large necrotic areas in the tumour.

Thursday June 15, 2017

13:50-14:00. Patrick Berkovic, Liège, Belgium

Adaptive radiotherapy for locally advanced non-small cell lung cancer: Dosimetric gain and treatment outcome prediction.

Berkovic P.1,2, Paelinck L.1, Gulyban A.2, Van Eijkeren M.1, Surmont V.1, Lievens Y.1, Vandecasteele K.1. [1] Department of Radiation Oncology, Ghent University Hospital, Ghent, Belgium, [2] Department of Radiation Oncology, Liège University Hospital, Liège, Belgium.

Introduction Adaptation of the treatment plan to the shrinking tumor volume during chemoradiation (CRT) in stage III non-small cell lung cancer patients could reduce organs at risk (OAR) dose burden, especially when performed at fraction (fr) 15/20 for concomitant/sequential (c-/s-)CRT. We aimed to 1) quantify tumor shrinkage, 2) determine gains on OAR doses, 3) evaluate dose coverage of the primary clinical target volume (CTV-T_init) after plan adaptation and 4) correlate tumor shrinkage gradient with treatment outcome. Materials and methods: Changes in primary tumor volume (GTV-T_init) of 41 (cCRT = 21) patients treated to a median dose of 70 Gy, 2 Gy/fr were analyzed using cone-beam CT. GTV-T_init was adapted and used to generate target volumes for re-optimization. OAR and CTV-T_init dosimetric parameters of the initial versus the fraction-based summation of initial and adapted plans were compared using a paired t-test. The GTV-T shrinkage was analysed at the time of adaptation (separated at median) and its impact on outcome was evaluated using Kaplan-Meier survival comparison (log-rank test). P values of <0.05 were considered significant. Results: Median shrinkage of GTV-T_init was 26.1% (Range [-25%, 75%]) for the entire cohort at the optimal time of adaptation (fr15 for cCRT, fr20 for sCRT). Mean doses of OARs were statistically significantly ($p<0.01$) lowered by adaptation: 3.6% (Standard deviation [SD] 3.7%) for lungs minus GTV-T_init, 6.7% (SD:8.9%) for heart and 2.9% (SD:4.3%) for esophagus. Initial CTV-T coverage (D95) declined from 66.1 (SD:2.1) to 65.1Gy (SD:3.1) ($p=0.02$). After a mean follow-up of 16.5 months, the higher gradient shrinkage statistically significantly affected lung progression free- and disease-specific survivals ($p=0.039$ and 0.024, respectively). Conclusions: Significant OAR dose reduction is feasible without compromising initial CTV coverage. Higher tumor shrinkage gradient leads to improved outcome.

Thursday June 15, 2017

14:00-14:10. Anne Vestergaard, Aarhus, Denmark

Clinical Phase II trial in adaptive radiotherapy for urinary bladder cancer reports low acute and late toxicity rates

Vestergaard A1, Muren LP1, Lindberg H2,Dysager L3, Jakobsen KL2, Jensen HR3, Petersen JBB1, Elstrøm UV1, Als AB4, Høyer M4. 1Department of Medical Physics, Aarhus University Hospital, Aarhus, Denmark 2Department of Oncology, Copenhagen University Hospital, Herlev, Denmark 3Department of Oncology, Odense University Hospital, Odense, Denmark 4Department of Oncology, Aarhus Unive.

Introduction: Large changes in bladder shape and size during a course of radiotherapy (RT) make adaptive RT (ART) appealing in the treatment of this tumour site. Patients with muscle-invasive bladder cancer were included in a Danish multicentre phase II trial of daily plan selection with the primary aim of reducing gastro-intestinal (GI) morbidity. Acute and late morbidity is reported. Materials and Methods: All 54 patients (median age 80 years) received 60 Gy in 30 fractions to the bladder; in 41 of the patients the pelvic lymph nodes were simultaneously treated to 48 Gy. Cone-beam CT (CBCT) was used for daily set-up. The first five fractions were delivered using large, population-based margins. CBCTs from the first four fractions were used to create a library of three plans corresponding to a small, medium and large size bladder. From fraction six all patients were treated using daily online plan selection. Morbidity scoring was performed at baseline, every second week during RT and two weeks as well as 3, 12 and 24 month after RT using CTCAE v. 4.0. The frequency of any grade 2 or higher GI morbidity was evaluated at treatment completion. Peak acute morbidity was assessed using the scorings until 3 months after RT and peak late morbidity was evaluated after 12 months after RT. Acute and late genito-urinary (GU) morbidity was also recorded. Median follow-up was 12 months. Results: The median volume ratio of PTV-ART vs. non-ART across the treatment course was 0.68 (range: 0.46-0.93). At treatment completion any GI morbidity grade 2 or higher morbidity was reported by 11 patients (20%). Peak acute grade 2 or higher diarrhoea was reported by 12 patients (22%). Only one patient had late GI grade 2 or more. GU morbidity increased during RT, but it was most often grade 1. Late GU morbidity was comparable to baseline. Conclusions: This phase II trial indicates that daily adaptive RT of bladder cancer can be delivered with low risk of morbidity.

Thursday June 15, 2017

14:10-14:20. Faisal Mahmood, Herlev, Denmark

Ultra-early ADC footprint successfully detects tumor irradiation and predicts radiotherapy outcome

Mahmood F.(1), Johannesen H.H.(2), Geertsen P.(1), Hansen R.H.(2). (1) Radiotherapy Research Unit, Department of Oncology, Herlev and Gentofte Hospital, Herlev, Denmark. (2) Department of Radiology, Herlev og Gentofte Hospital, Herlev, Denmark.

INTRODUCTION The temporal evolution of the apparent diffusion coefficient (ADC) was investigated using repeated diffusion weighted magnetic resonance imaging (DW-MRI) in brain metastases patients treated with fractionated radiotherapy (RT). The aim was to see if inter-fraction ADC changes have the potential for identification of irradiated tissue and stratification of treatment response. METHODS In this prospective study twenty-nine metastases (N=29) from twenty-one patients were analyzed. Patients were scheduled for a total dose of 30 Gy in ten fractions. A 1 T MRI system was used to acquire DW-, T2*W-, T2W- and contrast enhanced T1W scan, before start of RT and at follow-up two to three months after RT. Additionally, DW-, T2*W-, T2W- scans were acquired within 1 hour before or 1 hour after each RT fraction. Tumors were outlined using b=800 s/mm2 images and the ADC were estimated using high b-values. Treatment response was evaluated by volume criteria using T1W scans. Paired t-test with Bonferroni correction was used to test for inter-fraction ADC change. Prognostic values were evaluated using receiver operatic characteristics. RESULTS ADC decrease is observed between fraction 1 and 2 when patients are pooled ($p<0.00036$), and when grouped as responders ($p<0.0066$) and non-responders ($p<0.03$). This is followed by a significant ADC increase between fraction 2 and 3 in responders ($p<0.0011$) whereas no change is seen in non-responders ($p<0.7$). Beyond fraction 3, no significant inter-fraction change in ADC is observed. Overall, a monotonous increase in ADC in responding patients, and decrease in non-responding patients is seen. The very early stratification of treatment response corresponds with significant AUC increase. CONCLUSION Results indicate that the decrease in ADC measured after the first fraction of RT is an effective biomarker for irradiated metastases. Further, the ADC response was shown to have significant prognostic capacity for treatment outcome.

Thursday June 15, 2017

14:20-14:30. Christian Hvid, Aarhus, Denmark

Cone beam CT based parotid sparing adaptive radiation therapy in the head and neck region

Hvid CA, Elstrøm UV, Jensen K, Grau C. Departments of Oncology and Medical Physics, Aarhus University Hospital, Aarhus, Denmark.

Background The purpose of this study was to study daily image guidance and a novel adaptive workflow, using cone-beam CT (CBCT) surveillance of dose to OAR to trigger adaptive replanning, as an alternative to mid-course CT scan in head and neck cancer radiotherapy. Materials and methods Impact of daily IGRT with RTT managed match protocol and mid-course CT was assessed in both a retrospective cohort of 93 previously treated patients as well as a prospective cohort of 60 consecutive patients receiving RT to the head and neck region. In the prospective cohort, patients in high risk of xerostomia would receive weekly offline CBCT surveillance in addition to daily image guidance, while patients in low risk would receive a single mid-course CBCT review. For weekly surveillance, doses to parotid glands, spinal cord and brainstem were recalculated as well as predicted total dose without adaptation. If predicted mean dose to parotid glands increased by >2 Gy compared to planned dose, or the constraints to brainstem or spinal cord were exceeded, adaptive replanning was performed. Results Respectively, 17% and 28% of patients had adaptive replanning in the retrospective and prospective cohort. No patients had adaptive replanning triggered due to mid-course imaging. In the prospective cohort, addition of weekly CBCT surveillance to a group of 40 patients only yielded a minimal reduction in estimated accumulated mean dose to the parotid glands of 0.65 Gy (range 0.4 – 1.0 Gy) for three patients. Time consumption per CBCT/week was median 22 minutes (range 17-38 minutes). Number of patients needed to see to achieve any dose reduction to parotid glands was 13 requiring 22 working hours. Conclusion The tested dose surveillance algorithm resulted in a minimal reduction of dose (<1 Gy) to the parotid glands for only 3 of 40 patients. Mid-course CT imaging did not provide any added benefit and can be safely omitted in the presence of closely monitored daily IGRT.

Thursday June 15, 2017

Session 8. Radiotherapy indications, treatment volumes and fractionation I (lung, rectum, anal, prostate)

15:00-15:20. Dirk De Ruysscher, Maastricht, The Netherlands

Emerging trends in radiotherapy indications, treatment volumes and fractionation in high-dose radiotherapy for lung cancer

De Ruysscher D, van Baardwijk A, Peeters S, Reymen B, Lambrecht M, Verhoeven K, Wanders R, Öllers M, van Elmpt W, van Loon J. Maastricht University Medical Center+, Department of Radiation Oncology (Maastro clinic), GROW Research Institute, The Netherlands; KU Leuven, Radiation Oncology, Belgium; University Hospitals Leuven, Department of Radiation Oncology, Leuven, Belgium.

In the last years, several new studies gave more insight in the optimal dose, fractionation and treated volume for early and locally advanced stage non-small cell lung cancer (NSCLC) and localized small cell lung cancer (SCLC). Stereotactic radiotherapy or stereotactic ablative radiotherapy (SABR) is used very successfully for medically inoperable patients with early stage NSCLC or for patients who refuse surgery. The optimal dose and fractionation for tumours that are close to “central” structures such as the large blood vessels, the main bronchi and the oesophagus. Recent studies show a high rate of lethal bleeding in these circumstances and therefore the wide-spread use of SBRT for central tumours should preferentially only be done in studies. The SPACE trial and other studies will shet light on the optimal dose and fractionation. The standard of care is for most fit patients with stage III NSCLC concurrent chemotherapy and radiotherapy. It is clear that all established platinum-based combinations are similar for survival. The selection may depend on local policy, cost and tolerability. In contrast to non-concurrent chemotherapy and radiotherapy, where phase III trials showed that accelerated schedules lead to higher long-term overall survival (OS) rates, dose-escalation by adding 2 Gy fractions was associated with lower OS. The exact reason remains unclear, but the studies pointed to the influence of the heart dose on early mortality. The CONVERT trial demonstrated that early, accelerated radiotherapy delivered concurrently with chemotherapy remains the standard of care for localized SCLC and that the omission of elective nodal irradiation is indeed safe and may explain the lower incidence of severe oesophagitis. We discuss which strategies may improve the outcome of patients with non-metastatic lung cancer.

Thursday June 15, 2017

15:20-15:40. Vincenzo Valentini, Rome, Italy

Emerging trends in radiotherapy of rectal cancer

Valentini V. Department of Oncology and Haematology,

During the past few decades there have been many advances in the management of rectal cancer. Building on a more comprehensive understanding of anatomy and patterns of local recurrence, new surgical techniques such as total mesorectal resection and sphincter sparing coloanal anastomosis have become standards. The move towards preoperative adjuvant therapy has been facilitated by more effective chemoradiation programs. Advances in radiation planning, delivery, and fractionation techniques coupled with new cytotoxic and targeted chemotherapeutic agents hold the promise of reduced toxicity and increased tumor response and control rates. New diagnostic modalities such as high resolution MRI have helped identify which therapeutic approaches and modalities are best suited to an individual tumor allowing a more selective approach. Lastly, a renewed focus on expert pathologic analysis coupled with the evolving field of prognostic and predictive molecular markers have facilitated the development of surrogate endpoints of response. Emerging interested in organ preservation and prediction models to tailor treatment intensity, based also on radiomcs features are polarizing the on going research.

Thursday June 15, 2017

15:40-15:50. Maria Kandi, Aarhus, Denmark

Local failure after radical radiotherapy of non-small cell lung cancer in relation to the planning PET/CT

Kandi1 M, Hoffmann2 L, Moeller2 D.S., Schmidt1 H.J., Knap1 M.M., Khalil1 A.A. 1Aarhus University Hospital, Department of Oncology, Aarhus C, Denmark 2Aarhus University Hospital, Department of Medical Physics, Aarhus C, Denmark.

Purpose: Local recurrence (rec) in lung cancer is associated with poor survival. This study tested whether the pattern of failure is associated with the most PET avid volume in the planning FDG PET/CT scan (p-CT). Methods: 164 consecutive inoperable stage III NSCLC patients (pts) receiving radiotherapy (RT) between Jan. 2012- April 2014 were reviewed. RT was delivered in 2 Gy/fraction (5f/week) to a total dose of 60-66 Gy. Pts were followed by CT scans every 3rd month. 83 of the pts developed local rec as first event. For lymph nodes (N) the correlation between location of treated N and location of N rec was evaluated. For the primary tumour (T), the overlap fraction between 50% of SUVpeak on p-CT and the volume of T recurrence (T-rec) was calculated: OF=(SUVp50∩T-rec)/min(SUVp50, T-rec). OF was calculated based on a rigid registration between p-CT and rec-CT (delineation on rec-CT was guided by PET when available). Results: Planning target volumes (PTV) ranged from 58 to 1140 (mean = 412 cm3). Median follow up time was 45 mo (CI 42-48). Median progression free survival was 10 mo (CI 8-11) and overall survival at 2 years was 48% (SD 3.8). 56 pts had rec in T-site, 39 pts in N-site and 29 pts had rec in both T- and N-sites. Biopsies were obtained in all cases where PET or CT based rec were suspected. N-site rec frequently occurred in the station 4R (54%) and 7 (44%) regardless of primary N-stage and position. Due to anatomical changes (atelectasis, fibrosis, lung volume), reliable registration between p-CT and rec-CT was only obtained in 26 pts with T-site rec. All rec in T-site appeared within the PTV, and in 25 pts overlap between SUVp50 and T-rec was seen with mean OF 52% (SD 24%). Conclusion: This study shows that the T-site rec in majority of pts correlates with SUVp50% on p-CT. LN recurrences mainly appear in station7 and 4R irrespective of the p-PET/CT and the primary N-stage volumes and position.

Thursday June 15, 2017

15:50-16:00. Emely Lindblom, Stockholm, Sweden

Non-linear conversion of HX4 uptake for automatic segmentation of hypoxic volumes and dose prescription in NSCLC

Ureba A(1), Lindblom E(1), Dasu A(2,3), Uhrdin J(4), Even AJG(5), van Elmpt W(5), Lambin P(5), Wersäll P(6), Toma-Dasu I(1,7). 1) Stockholm University, Stockholm, Sweden; 2) The Skandion Clinic, Uppsala, Sweden 3) Linköping University, Linköping, Sweden 4) RaySearch Laboratories AB, Stockholm, Sweden 5) Maastricht University Medical Center, Maastricht, The Netherlands; 6) Karolinska.

Introduction: Non-small-cell lung cancer (NSCLC) tumours are often hypoxic. Patients with these tumours have a rather poor prognosis, which may be attributed to hypoxia-induced resistance. Pre-treatment assessment of oxygenation in these tumours could therefore give the possibility to tailor the treatment by calculating the required boost dose needed to overcome the increased radioresistance due to hypoxia. This study concerned the derivation of a non-linear dose relationship for dose painting purposes with a new hypoxia-PET tracer, HX4. Materials & Methods: A model for the inhibition of a chemical reaction was used to describe the binding of hypoxia tracers. Building on the experience with FMISO binding, tracer-specific parameters were derived for converting the normalized uptake of HX4 to partial oxygen pressure (pO2). The conversion function was implemented in a scripting module in RayStation to determine pO2 values in 8 NSCLC patients imaged with HX4-PET before the start of radiotherapy. Next, automatic segmentation of hypoxic target volumes (HTVs) was performed using suitable hypoxic thresholds. The HTVs were compared to sub-volumes segmented based on a tumour-to-blood ratio (TBR) of 1.4 using the aortic arch as the reference oxygenated region. The boost dose required to achieve 95% local control was then calculated based on the calibrated levels of hypoxia, assuming inter-fraction reoxygenation due to changes in acute hypoxia but no overall improvement of the oxygenation status. Results: Using the developed conversion tool, hypoxic target volumes could be obtained using pO2 thresholds of 8-12 mmHg which were in agreement with the TBR segmentation. The dose levels required to the HTVs to achieve local control were feasible, being around 70-80 Gy in 30 fractions.Conclusions: Non-linear conversion of tracer uptake to pO2 values in NSCLC images with HX4-PET allows a quantitative determination of the dose-boost needed to achieve a high probability of local control.

Thursday June 15, 2017

16:00-16:10. Ferenc Lakosi, Kaposvar, Hungary

HDR brachytherapy boost using MR-only workflow for intermediate- and high-risk prostate cancer patients

G. Toller1, G. Antal1, J. Pall1,2, D. Nagy3,T. Jenei3, M. Csima4, A. Gulyban5, I. Repa1, J. Hadjiev1, F. Lakosi1. 1Institute of Imaging and Radiation Oncology, Kaposvar University, Kaposvar, Hungary, 2Department of Radiation Oncology,Cholnoky Ferenc Hospital, Veszprem, Hungary, 3Department of Urology, Kaposvar University, Kaposvar, Hungary, 4Faculty of Pedagogy, Kaposvar University, Kaposvar, Hungary.

Introduction: To report our experiences and clinical results with high-dose-rate brachytherapy (HDR-BT) boost using MRI-only workflow for intermediate (IR) and high-risk (HR) prostate cancer patients. Materials and Methods: Fifty-two patients were treated with 46-60 Gy of 3D EBRT preceded and/or followed by a single dose of 8-10 Gy MRI-guided HDR-BT. Navigation, contouring, planning and prediction of in vivo rectal dosimetry (MR compatible model for a fivefold probe) were exclusively based on MRI images. During implantation and planning extra effort was made to cover tumor containing region(s). Biochemical relapse–free- (bRFS), local relapse-free- (LRFS), distant metastasis-free-(DMFS), cancer-specific-(CCS) and overall survival (OS) were analyzed. Morbidity was scored using CTCAEv4.0, while urinary and bowel quality of life (QoL) was measured with the Expanded Prostate Cancer Index Composite (EPIC) at baseline and at regular intervals up to 5 years. Results: Median times for MRI unit-work and total procedure were 3 hours (r:1.5-5) and 6 hours (r:4-8.5). Image quality was found to be good to excellent in almost all cases. There were no intervention related urethra or rectal wall injury. The mean per detector measured dose was +12 % compared to MRI based prediction (SD:21). After a median follow-up of 73 (r:13-103) months the 5-year actuarial rates of bRFS, LRFS, DMFS, CSS and OS were 97.4%, 100%, 97%, 100 % and 91%, respectively. Only one Gr.3 late toxicity (GU stricture) was observed. EPIC urinary scores recovered within 6 months, followed by a slight decline and stabilized from 4th-years follow up. Bowel functions returned to baseline after 3 month and remained stable over time. Conclusions: MRI-only HDR-BT boost provides excellent disease control and QoL after 5 years follow up for IR and HR prostate cancer patients. MRI provides flexible alternative to existing procedures within prostate BT workflow.

Thursday June 15, 2017

16:10-16:20. Anna Kuisma, Turku, Finland

Follow up of biologically guided radiotherapy of prostate cancer

Anna Kuisma1; Pauliina Wright1,2; Sami Suilamo1,2; Jan Seppälä3; Paula Lindholm1; Heikki Minn1, 4. 1) Dept. of Oncology and Radiotherapy, Turku University Hospital; 2) Dept. of Medical Physics, Turku University Hospital; 4) Turku PET Centre, Turku University Hospital and University of Turku.

Introduction: Biologically modified subvolumes enable non-uniform dose distributions in prostate cancer radiotherapy (RT) thus potentially improving therapeutic ratio and reducing toxicity. We present 6-year outcome of men receiving focal boosting of carbon-11 acetate (ACE) PET-CT metabolically active areas in prostate carcinoma. Material and methods: Thirty men with localized prostate carcinoma underwent ACE PET/CT for RT planning. Tresholding based on the standardized uptake values (SUVs) metabolic target volumes (MTV) corresponding to intraprostatic lesions (IPLs) were contoured. Two planning target volumes (PTVs) were applied i.e. PTVlow risk for the prostate with 7-10 mm margin and PTVhigh risk for the MTV with 4 mm margin. Median doses to the PTVlow risk, PTVhigh risk, prostate and MTV were 72.9 Gy, 79.4, 76.6 Gy to and 80.4 Gy, respectively, in 38 fractions. At median follow-up of 72 (range 57 - 84) months dose painting parameters as well as toxicity, local control and survival data were reviewed. Results: The 5-year cancer specific survival was 90% and the biochemical failure-free ratio 70 %,. The mean progression free survival (PFS) time vas 58.0 months in the high risk group (p=0.001). The mean PFS was not reached in the lower risk groups, because there were not enough relapses so far. Two patients (8%) presented with locoregional and 3 (11%) with distant relapses. Five patients (20%) reported G2 and one patient (4%) G3 urinary toxicity. One patient (4%) reported G3 gastrointestinal toxicity, while no G2 gastrointestinal toxicity was observed. No significant differences in the dose painting parameters were observed between recurrence free and recurring patients. Conclusions: Biological guidance for de-escalated whole prostate RT is feasible with ACE. Mild toxicity seen by us encourages protocols prescribing higher doses to metabolic subvolumes to optimize focal approach in treatment planning.

Thursday June 15, 2017

16:20-16:30. Vilde Skingen, Oslo, Norway

A patient-specific tumor control probability model based on total lesion glycolysis of anal cancer

Skingen VE, Rusten E, Rekstad B, Undseth C, Guren MG, Malinen E. University of Oslo / Oslo University Hospital, Oslo, Norway.

Introduction Anal cancers (AC) show high uptake of 18F-fluorodexoyglucose (FDG) in positron emission tomography (PET). The purpose was to develop a patient-specific tumor control probability (TCP) model employing the PET-based total lesion glycolysis (TLG), to assess the prognostic role of the model and to use the model to estimate the gain in local control from dose escalation (DE). Materials and methods Eighty-eight patients with AC receiving conventional radiotherapy (RT) were prospectively included. Patients were regularly followed up at 3-6 months intervals after therapy, and only local recurrences were scored as events. FDG-PET was done prior to therapy. A TCP model was developed based on 1) published intrinsic radiosensitivity and fractionation sensitivity for AC and 2) TLG reflecting the number of clonogenic cells within the gross tumor volume (GTV). Furthermore, a scaling factor was used for the model to provide a global population-based control level of 80%. The model was thus developed without use of outcome data for the given cohort. The impact of DE from 58 Gy (conventional dose) to 65 Gy was assessed by the TCP model. Results Fourteen patients had local recurrence. The median and range of the patient-specific TCPs was 0.73 (0.08, 1.00). Dividing patients into two groups with low and high TCPs, the local control level was 56 % and 91 %, respectively. This difference in recurrence-free survival was highly significant (P=0.001; Cox regression). A comparable TCP model based on GTV did not show any association with recurrence rates. The median increase in estimated TCP from DE was 0.52 and 0.23 for the group with low and high TCPs from conventional RT, respectively. Conclusions The patient-specific TCP model incorporating TLG was prognostic for local recurrence, and was superior to a comparable model incorporating GTV only. The model estimated a clear benefit of DE for patients with high-pretreatment TLG and thus low TCP from conventional RT dosage.

Thursday June 15, 2017

16:30-16:40. Andrea Lancia, Rome, Italy

Oligometastatic cancer: stereotactic ablative radiotherapy for patients affected by isolated body metastasis

Lancia A, Ingrosso G, Carosi A, Di Murro L, Giudice E, Cicchetti S, Morelli P, di Cristino D, Bruni C, Murgia A, Cancelli A, Turturici I, Iadevaia A, Ponti E, Santoni R. Department of Diagnostic Imaging, Molecular Imaging, Interventional Radiology and Radiotherapy, Tor Vergata University Hospital, Rome, Italy.

Aim: to evaluate the outcome of patients affected by a single isolated body metastasis treated with stereotactic body radiotherapy (SBRT). Materials and methods: 78 patients were treated with SBRT for isolated body metastasis. The most frequent primary tumor was prostate cancer (28.2%), followed by colorectal cancer (23.1%), and lung cancer (20.5%). Median age at diagnosis of oligometastatic disease was 70 years (range 47-88). Median Karnofsky Performance Status (KPS) was 90 (range 70-100). The most common SBRT fractionation scheme was 5x7 Gy (total dose 35 Gy). Response to radiotherapy was determined according to RECIST criteria v1.1. Toxicity was registered according to Common Terminology Criteria for Adverse Events (CTCAE) v4.0. The survival analysis was performed with the Kaplan-Meier method. The correlation between time actuarial incidence and clinical parameters was studied, and the Kaplan-Meier method of log-rank test was applied. Results: with a median follow-up of 22.68 months, local control was achieved in 89.7% of the cases. The 2-year overall survival (OS) and progression-free survival (PFS) were 82% and 72%, respectively. 2-year cancer-specific survival (CSS) was 85%. On univariate analysis, KPS ≥ 80 is predictive for improved OS (p=0.001) and PFS (p=0.001). Acute toxicity of grade ≥ 2 occurred in 8 (10.2%) patients, and late grade ≥ 2 toxicity in 5 (6.4%) patients. Conclusions: Ablative radiotherapy in early "oligometastatic state" is a safe, effective, and minimally invasive treatment modality. A good performance status (KPS ≥ 80) seems to influence the clinical outcome.

Friday June 16, 2017

Session 9. Health economics and radiomics

8:40-9:00. Yolande Lievens, Ghent, Belgium

How to guarantee the introduction and sustainability of innovative radiotherapy technologies and techniques?

Lievens Y. Radiation Oncology Department, Ghent University Hospital and Ghent University, Ghent, Belgium.

As health care budgets are tightening, the introduction of new treatment strategies requires a careful selection of interventions with evidence-based clinical outcomes, while minimizing the costs to payers, patients, and society. Economic evaluation has become the mainstay to prove the value for money of new treatments, but represents only part of the entire health technology assessment (HTA). HTA builds on evidence from clinical efficacy and effectiveness, yet encompasses a broad multidisciplinary evaluation of the social, economic, organizational and ethical issues of a health intervention or technology. This approach has been widely adopted for drugs, but has turned out more complex to undertake for technologies. In radiotherapy, for instance, the introduction of new techniques and technologies is often incremental in nature. The uncertainty related to this gradual process, along with high upfront investment costs and a positive impact on outcome - decreased toxicity or better local control, survival or quality of life - often delayed in time, make the application of HTA more difficult to accomplish. Hence, approaches to evidence generation and data capture that better align to the specific nature of technology innovation in radiotherapy need to be leveraged, for instance by blending input from clinical trials with modelling studies and real-life evidence. Such a broad vision to the collection of clinical and economic outcome data unfortunately does not belong to routine practice (yet), but could be fostered by the introduction of novel reimbursement strategies. In coverage with evidence development, provisional access to new medical interventions is granted in exchange for generating the evidence needed. It is expected that the judicious implementation of such financing strategies would not only guarantee the necessary data collection, but in term also stimulate practitioners to provide their patients with evidence-based technologies and treatment strategies.

Friday June 16, 2017

9:00-9:10. Ralph Leijenaar, Maastricht, The Netherlands

Development and validation of a radiomic signature to predict HPV status from standard CT imaging

Leijenaar R.T.H. (1), Bogowicz M. (2), Jochems A. (1), Hoebers F.J.P. (1), Huang S.H. (4), Chan B. (4), Waldron J.N. (4), O'sullivan B. (4), Rietveld D. (5), Leemans C.R. (6), Riesterer O. (2), Ikenberg K. (3), Lambin P. (1). (1) Radiation Oncology (MAASTRO clinic), GROW-School for Oncology and Developmental Biology, Maastricht University Medical Centre, The Netherlands (2) Radiation Oncology (3) Pathology and Molecular Pathology, University Hospital Zurich and University of Z.

Introduction: For oropharyngeal cancer (OPSCC) patients, HPV positive cancers have been shown to have better tumor control with radiotherapy and increased survival. Radiomics has already been shown to be of prognostic value for head and neck cancer and radio-genomic studies have reported associations between radiomic features and underlying gene expression patterns. Here, we evaluate the use of a radiomic approach to identify the HPV status of OPSCC patients. Methods: Three independent cohorts, with a total of 802 OPSCC patients were collected: C1 (N=543), C2 (N=159) and C3 (N=100). HPV was determined by p16 for 686 patients. Patients underwent pre-treatment CT imaging and the gross tumor volume (GTV) was manually delineated for treatment planning purposes. Images with CT artifacts (e.g. streak artifacts due to dental fillings) within the GTV were excluded from further analysis. In total, 1378 radiomic features were extracted, comprising: a) first-order statistics, b) shape, and c) (multiscale) texture. Redundant features were removed by hierarchical cluster analysis ($\rho>0.9$). A random forest (RF) model was trained on the C1 cohort with the maximum number of terminal node trees set to 5 to avoid overfitting, and validated on cohorts C2 and C3. The area under the receiver operator curve (AUC) was used to assess model performance in predicting HPV status. Results: We identified 337 patients with known HPV scoring and no CT artifacts: C1 (N=206), C2 (N=88), C3 (N=43). In the C1 cohort, the model had an AUC of 0.97. External validation in the C2 and C3 cohorts showed an AUC of 0.71 and 0.75, respectively. Conclusion: We independently validated a radiomic signature to distinguish between HPV+ and HPV- OPSCC patients, using only pre-treatment CT imaging. These results indicate that molecular information can be derived from standard medical images and show the potential for radiomics to serve as an alternative, cheap, imaging biomarker of HPV status.

Friday June 16, 2017

9:10-9:20. Stefan Leger, Dresden, Germany

CT imaging during treatment improves radiomic predictions for patients with locally advanced head and neck cancer

Leger S.1; Zwanenburg A.1,3; Pilz K.1,2; Baumann M.1-5; Troost E.G.C1-3,5; Richter C.1,2,5,*; Löck S.1,*. 1. OncoRay - National Center for Radiation Research in Oncology, Faculty of Medicine and University Hospital C. G. Carus, TU Dresden, HZDR, Dresden, Germany; 2. Department of Radiation Oncology, Faculty of Medicine and University Hospital C. G. Carus, TU.

Introduction: Radiomics applies machine learning algorithms to characterize the tumor phenotype and to predict clinical outcome based on quantitative imaging data. It has been applied using pre-treatment computed tomography (CT) scans but only few studies have assessed radiomics on imaging acquired during radiotherapy. Therefore, we compared the performance of radiomic models based on the pre-treatment CT with that based on CT imaging during treatment. Material/Methods: Two datasets of patients with advanced stage head and neck squamous cell carcinoma (HNSCC) were used as an exploratory and a validation cohort (47 and 30 patients, respectively). All patients received primary radio-chemotherapy (RCT) and underwent a non-contrast-enhanced CT scan pre-treatment and in week 2 (W2) of treatment. 1610 image features were extracted from the gross tumour volume, delineated on the baseline CT and the W2 CT. Radiomic models were built to predict loco-regional tumour control (LRC). Different feature selection methods (mutual information maximization (MIM), random forest variable importance (RFVI)) and learning algorithms (Cox regression (COX), random forest (RF)) were evaluated using the concordance index (CI) as performance measure. Results: On the W2 CT both FS methods combined with the RF algorithm achieved a higher performance (CI=0.71) than on the baseline CT (CI<0.65), which was also observed using the Cox regression model (W2 CT: CI=0.66, baseline CT:CI=0.51). Conclusions: CT scans from the second week of RCT for patients with locally advanced HNSCC improved the performance of radiomic prediction models compared to baseline CT scans. The incorporation of during-treatment imaging is a promising way to improve radiomic models for clinical treatment adaption.

Friday June 16, 2017

9:20-9:30. Marta Bogowicz, Zurich, Switzerland

Comparison of PET and CT radiomics for prediction of local tumor recurrence in head and neck squamous cell carcinoma

1Marta Bogowicz, 1Oliver Riesterer, 1Luisa Sabrina Stark, 1Gabriela Studer, 1Jan Unkelbach, 1Matthias Guckenberger, 1Stephanie Tanadini-Lang. 1 Department of Radiation Oncology, University Hospital Zurich, University of Zurich, Switzerland.

Introduction Radiomics studies have shown a link between quantitative image features extracted from CT and patient overall survival. This study investigated a potential benefit of functional imaging (18F-FDG PET) radiomics over the anatomical imaging (CT) in the context of local tumor recurrence prediction in head and neck squamous cell carcinoma (HNSCC). Material and methods Data from HNSCC patients (n=135) treated with definitive radiochemotherapy were used for model training. In total, 569 radiomic features were extracted from the contrast enhanced CT and 18F-FDG PET images in the primary tumor region. CT, PET and combined PET/CT radiomic models to assess local tumor recurrence were trained separately. Principal component analysis combined with univariable Cox modelling was used to preselect relevant and uncorrelated radiomic features. Multivariable Cox regression with backward selection of variables was used to define radiomic signatures. The performance of the final models was quantified using concordance index (CI) and compared between image modalities using bootstrapping. Obtained models were verified in the independent validation cohort (n=57). Results Principal component analysis resulted in selection of 12 and 5 radiomic features in CT and PET, respectively. Final CT and PET models consisted of 2 radiomic features (CT: GLSZM_size_entropy, HLH histogram_energy; PET: spherical disproportion, GLSZM_SZLGE), whereas combined model contained 4 features (CT HLH histogram_energy, CT LHL GLCM_MCC, PET spherical disproportion, PET GLSZM_SZLGE). All models showed a similar performance in training and validation cohorts (training: CI_CT=0.72, CI_PET=0.72, CI_PET/CT=0.77; validation: CI_CT=0.75, CI_PET=0.73, CI_PET/CT=0.72). No significant difference was observed between models. Conclusion The PET radiomic local tumor control model did not add benefit to CT radiomic model. However, it achieved equally good CI and could be used for patients with metal artifacts in CT.

Friday June 16, 2017

Session 10. Radiotherapy indications, treatment volumes and fractionation II (breast, cervix, head and neck cancer)

10:40-10:50. Kari Tanderup, Aarhus, Denmark

Early clinical outcome of coverage probability based treatment planning in locally advanced cervical cancer for simultaneous integrated boost of nodes

Lindegaard JC, Assenholt MS, Ramlov A, Fokdal L, Alber M, Tanderup K. Department of Oncology, Aarhus University Hospital, Denmark; Department of Medical Physics, Heidelberg and Institute for Radiation Oncology (HIRO), Germany.

Introduction: More than 50% of patients with locally advanced cervical cancer (LACC) have pathological nodes requiring boost. Coverage probability (CovP) is a new planning technique allowing for relaxed dose at the boost periphery minimising collateral irradiation of OAR. CovP is now being used in the multicentre Embrace II study. The aim of our study was to report the first early clinical outcome data for CovP based simultaneous integrated boost (SIB) in LACC. Materials & methods: 22 consecutive node positive pts were analysed. FIGO stage IB2/IIB/IIIB/IVA/IVB was 1/13/3/1/4. Treatment was chemo-radiation (RT) delivering 45 Gy/25 fx whole pelvis +/- para-aortic region (PAN) using IMRT/VMAT followed by MRI guided adaptive brachytherapy. PAN RT (12 pts) was given if > 2 nodes were boosted or if node(s) were present at the common iliacs (CI) or higher. Pathological nodes (GTV-N) were contoured on both planning PET-CT and MRI. CTV-N was formed by fusion of GTV-N_CT and GTV-N_MRI. A 5 mm isotropic margin was used for PTV-N. Pathological nodes in the small pelvis were boosted to 55.0 Gy/25 fx. Nodes at the CI or PAN received 57.5 Gy/25 fx. Planning aims for CovP were D98PTV-N >90%, D98CTV-N > 100% and D50CTV-N > 101.5% of prescribed dose. Results: In total 71 nodes were boosted. By use of CovP we obtained a consistent 5.0 ± 0.8 Gy dose gradient from D98CTV-N to D98PTV-N. In total 71/71 nodes were controlled at 3 month on PET-CT and MRI. Pelvic control was obtained in 21/22 patients. One patient (IB2, clear cell adenocarcinoma) had persistent but salvageable local disease with regional/systemic control. Two patients failed in un-irradiated PAN. One was age 88 (IIIB) and did not receive PAN RT despite a CI node. The other (IIB) recurred above L1. A fourth patient (IVB) failed systemically. Conclusion: Since complete remission on PET-CT and MRI at 3 month is highly predictive for a favourable long term outcome our study indicates that the Embrace II strategy is promising.

Friday June 16, 2017

11:00-11:10. Ruta Zukauskaite, Odense, Denmark

Distribution of loco-regional recurrences after primary IMRT for head and neck squamous cell carcinomas (HNSCC). A study from three Danish head and neck cancer centres

Zukauskaite R, Hansen CR, Brink C, Grau C, Samsøe E, Johansen J, Andersen E, Petersen J, Overgaard J, Eriksen JG. Department of oncology, Odense University Hospital, Odense, Denmark.

Introduction: Planning process for curative radiotherapy for HNSCC includes, among other, additional margin around gross tumour volume (GTV) to cover microscopic disease (CTV1). This margin can vary from 0 to up to 10 mm. The objective of this study was to analyse loco-regional recurrence pattern in a cohort of Danish patients with HNSCC treated with definitive IMRT, and to evaluate how the location of CT verified loco-regional recurrences (LRR) were influenced by different CTV1 margins. MATERIAL/METHODS: Patients with HNSCC treated with primary IMRT during 2006–2012 from three different centres were retrospectively identified. Treatment was primary radiotherapy 66-68 Gy, 6 fr/wk with concomitant nimorazole, and weekly cisplatin in loco-regionally advanced cases. The GTV-CTV1 margin was calculated as median surface distance from GTV to CTV1. The possible points of LRR origin (PO) were identified on diagnostic scans by two independent observers, calculated as centre of mass (COM) and a point with maximal surface distance (MSD), and were moved from recurrence-CT to planning-CT using deformable image registration. The distance from the PO to the surface of the GTV was averaged across the four POs, and the difference between LRR distribution in groups with small and large CTV margins was estimated. RESULTS: In total 1,580 patients were identified and 172 patients had LRR within at least 3 years of follow-up. Among them, 50% had GTV-CTV1 margin less than 5 mm and 50% larger than 5 mm. There was no difference in patient and tumour characteristics between these two groups. After successful DIR, in total 192 recurrences were further analysed in the two margin groups; no significant difference in LRR distribution was found (p=0.6). Of the POs in the first and the second groups, 58% and 64% received the 95% prescription dose, respectively. CONCLUSION: The presented data do not suggest any difference in distribution of loco-regional recurrence in relation to CTV margins.

Friday June 16, 2017

11:10-11:20. Simon Boeke, Tübingen, Germany

Patterns of loco-regional failure (LRF) in patients with hypoxic head and neck cancers (HNSCC)

Boeke S1,2, Thorwarth D1,2, Pfannenberg C3, Reischl G4, Pichler B4, la Fougère C5, Nikolaou K3, Mauz PS6, Mönnich D1,2, Zips D1, Welz S1. University Hospital Tübingen, Tübingen, Germany, 1 Department of Radiation Oncology, 2 Section for Biomedical Physics, Department of Radiation Oncology, 3 Diagnostic and Interventional Radiology, Department of Radiology, 4 Preclinical Imaging and Radiopha.

Introduction A previous pattern of failure study by others has suggested that up to 50% of the loco-regional recurrences (LRF) in HNSCC occur outside the initial hypoxic volume determined by [18F]-Misonidazole-PET ([18F]-FMISO-PET). The aim of the present analysis was to correlate spatial patterns of failure related to the pretherapeutic dynamic [18F]-FMISO-PET/CT in HNSCC. Materials and methods Within a running prospective randomised phase 2 trial using [18F]-FMISO-PET imaging prior to radiochemotherapy (RCT) in patients with locally advanced HNSCC (NCT 02352792) we have observed so far 11 LRF with a minimum follow-up of 12 months. For 9 patients with LRF imaging (CT or [18F]-FDG-PET/CT) for pattern-of-failure analysis was available. Results A total of five local, two regional and two loco-regional recurrences were detected. In all nine patients the recurrences occurred within the initial gross tumour volume (GTV) containing significant [18F]-FMISO-positive subvolumes after visual comparison of the initial [18F]-FMISO-PET/CT, the planning CT with the treatment ROIs and the CT or [18F]-FDG-PET/CT of the recurrent, progressive tumour. Conclusion Our data suggest that the loco-regional recurrences after RCT occur within the initial GTV (primary tumour and node metastases) containing hypoxic subvolumes supporting the concept of hypoxia-imaging based dose escalation. However, due to the therapy-induced anatomical changes and asymmetric growth pattern of recurrences we cannot exclude that recurrences originate from non-hypoxic subvolumes of the initial GTV.

Friday June 16, 2017

11:20-11:30. Gregers B. D. Rasmussen, Copenhagen, Denmark

Immunohistochemical and molecular imaging biomarker signature for the prediction of failure site after chemoradiation for head and neck squamous cell carcinoma

* Rasmussen, GBD 1,2; Håkansson, KE 1; Vogelius, IR 1; Rasmussen, JH 3; Friborg, JT 1; Fischer, BM 2; Schumaker,L 4; Cullen, KJ 4; Therkildsen, MH 5; Bentzen, SM 1,4,6; Specht, L 1. Departments of: 1) Oncology, 2) Clinical Physiology, 3) Otorhinolaryngology, 5) Pathology, Rigshospitalet, Copenhagen, Denmark, and 4) Greenebaum Cancer Center, 6) Epidemiology and Public Health, University of Maryland, Baltimore, Maryland.

Objective: To identify a failure site specific prognostic model by combining immunohistochemistry (IHC) and molecular imaging information to predict long term failure type in squamous cell carcinoma of the head and neck. Materials and Methods: Tissue microarray blocks of 196 head and neck squamous cell carcinoma cases were stained for a panel of biomarkers using IHC. Gross tumor volume (GTV) from the PET/CT radiation treatment planning CT-scan, maximal Standard Uptake Value (SUVmax) of fludeoxyglucose (FDG) and clinical information were included in the model building using Cox proportional hazards models, stratified for p16 status in oropharyngeal carcinomas. Separate models were built for time to locoregional failure, and time to distant metastasis. Results: Higher than median p53 expression on IHC tended towards a risk factor for locoregional failure but was protective for distant metastasis, $\chi 2$ for difference p=0.003. The final model for locoregional failure included p53 (HR:1.9; p:0.055), concomitant cisplatin (HR:0.41; p:0.008), β-tubulin-1 (HR: 1.8; p:0.08), β-tubulin-2 (HR:0.49; p:0.057) and SUVmax (HR:2.1; p:0.046). The final model for distant metastasis included p53 (HR:0.23; p:0.025), Bcl-2 (HR:2.6; p:0.08), SUVmax (HR:3.5; p:0.095), and GTV (HR:1.7; p:0.063). Conclusion: The models successfully distinguished between risk of locoregional failure and risk of distant metastasis, which, if confirmed, is important information for clinical decision making. Of special interest is the finding that high p53 expression has opposite prognostic effects for the two endpoints; increasing risk of locoregional failure, but decreasing the risk of metastatic failure.

Friday June 16, 2017

11:30-11:40. Mette Saksø, Aarhus, Denmark

High risk of treatment failure for patients with p16-negative, FAZA-PET positive HNSCC after primary radiotherapy - update from the DAHANCA 24 trial

Saksø M, Mortensen LS, Johansen J, Primdahl H, Overgaard J. Dept. of Experimental Clinical Oncology, Aarhus University Hospital (AUH), Aarhus, Denmark. Dept. of Oncology, Aarhus University Hospital (AUH), Aarhus, Denmark. Dept. of Oncology, Odense University Hospital (OUH), Odense, Denmark.

Introduction: In the DAHANCA 24 trial, pretreatment PET/CT scans with hypoxia-specific tracer fluoroazomycin arabinoside (FAZA) was evaluated as a prognostic marker in HNSCC patients planned for primary chemo-radiation along with hypoxic modification with Nimorazole. However, patient outcome was not stratified for HPV-status, and data suggested that both HPV-positive and –negative tumors were equally hypoxic, when assessed on FAZA. Materials and methods: Retrospective analysis of the DAHANCA 24 patient cohort with a complete revision of FAZA scans and outcome data (loco-regional failure and disease-specific survival). Results: Data from 39 out of 40 patients with were revised. Loco-regional control rates were 100% for patients with p16-positive, FAZA-negative tumors (4 patients), 88% for p16-positive, FAZA-positive tumors (12 patients), 84% for p16-negative, FAZA-negative tumors (11 patients) and 40% among p16-negative, FAZA-positive tumors (13 patients). Results on disease-specific survival are pending. Conclusions: Patients with p16-positive tumors responded well to treatment, regardless of hypoxic status as determined by FAZA. Patients with p16-negative tumors had tumor control rates similar of p16-positive patients, if deemed non-hypoxic as imaged by FAZA. Patients with tumors characterized as p16-negative and FAZA-hypoxic had poor loco-regional control rate, as compared to the rest of patients treated with curative intent according to national guidelines. It seems from this, that the issue of treatment resistance due to hypoxia is not properly being addressed, even with Nimorazole added daily prior to radiation.

Friday June 16, 2017

11:40-11:50. Sebastian Sanduleanu, Maastricht, The Netherlands

Non-invasive imaging for tumor hypoxia: a novel externally validated CT-based radiomics signature

Sanduleanu S1, Upadhaya T2,3, Even A.J.G1, Jochems A1, Leijenaar R(1), Dankers F(1,4), Hatt M(2), Kaanders J.H.A.M(4), Lambin P(1). (1) Department of Radiation Oncology (MAASTRO), GROW – School for Oncology and Developmental Biology, Maastricht University Medical Center (MUMC +), Maastricht, The Netherlands (2) Laboratory of Medical information processing (LaTIM – INSERM UMR 1101), U.

Introduction: Tumor hypoxia increases resistance to radiotherapy and systemic therapy and promotes tumor metastasis. In this multicenter study we developed and validated a CT-based radiomics prediction model for tumor hypoxia. Materials and methods: In total 130 patients (69 HNSCC and 61 NSCLC) from 3 centers were included. On CT images primary gross tumor volumes (GTV) were manually defined by an experienced radiation oncologist and radiomics features were extracted from the CT-delineations. [18F]HX4 hypoxia tracer PET-images for 90 patients and biopsies stained with pimonidazole (ARCON-trial) for 40 patients were used as ground truth for hypoxia. A cutoff value of 2.6% for hypoxic fractions (HF) was used to dichotomize between well-oxygenized and hypoxic tumors. HX4-patients HF were defined as the ratio of hypoxic (tumor-to-background ratio > 1.4 on 4h post-injection images) to GTV and for pimonidazole as positive staining area. A machine-learning classifier, support vector machines (SVM) with recursive feature elimination and leave one out cross-validation (LOOCV) was used to classify patients as hypoxia-positive/ negative based on the optimal combination of radiomics features. Results: The best SVM model in the training set (n=70) with LOOCV reached an accuracy 98% (AUC 1) by combining 23 radiomics features. Accuracy in the validation dataset (n=60) was 71% (AUC 0.67), with positive and negative predictive values of 80% and 63% respectively. Conclusion: Our study is the first to validate a CT-based radiomics signature to identify hypoxic HNSCC and NSCLC patients. More efficient trial inclusion, training on a larger patient population, learning on additional PET images and integrating different machine learning algorithms may form the basis for a future integrative hypoxia signature.

Poster discussion groups

Group 1 Proton biology/RBE studies
Chairs: Olav Dahl and Harald Paganetti
Tordis J. Dahle, Bergen
Steffen Nielsen, Aarhus
Jakob Ödén, Stockholm
Silke Ulrich, Heidelberg
Kristian Ytre-Hauge, Bergen

Group 2 Radiomics
Chairs : Joseph Deasy and David Hansen
W. van Elmpt [Ruben Larue], Maastricht
Jurgen Peerlings, Maastricht
Sara Carvalho, Maastricht
R.T.H.M. Larue, Maastricht

Group 3 Radiobiological/pre-clinical studies
Chairs: Bleddyn Jones and Michael Horsman
Thomas Wittenborn, Aarhus
David Grosshans, Houston
Jacob Lilja-Fischer, Aarhus
Morten Busk, Aarhus
Pernille Elming, Aarhus

Group 4 Clinical outcomes
Chair: Birgitte Offersen
Timo Deist, Maastricht
Jan Alsner, Aarhus
Einar Dale, Oslo
Simon Lønbro, Aarhus
Arthur Jochems, Maastricht
Tinne Laurberg, Aarhus
Oscar Casares-Magaz, Aarhus
Lotte Fog, Copenhagen

Group 5 Proton therapy: Dosimetry and treatment planning
Chairs: Radhe Mohan and Christian Søndergaard
Ellen Marie Høye, Aarhus
Jeppe Brage Christensen, Roskilde
Thomas Henry, Stockholm
Gracinda Mondlane, Stockholm
Camilla Hanquist Stokkevåg, Bergen
Laura Toussaint, Aarhus
Charlotte Espensen, Copenhagen

Group 6 Functional imaging: PET and SPECT
Chairs: Malene Fischer and Azza Khalil
Evelyn de Jong, Maastricht
Marta Lazzeroni, Stockholm
Aniek Even, Maastricht
Ingvild Støen, Oslo
Espen Rusten, Oslo
Mette Marie Fode, Aarhus
Azadeh Abravan, Oslo
Tine Bisballe Nyeng, Aarhus

Group 7 Photon therapy: Inter-fractional Challenges
Chair: Lise Bentzen
Kristina Giske, Heidelberg
Anne Holm, Aarhus
Lone Hoffmann, Aarhus
Karen Zegers [Jose Baeza], Maastricht
Karina Lindberg Gottlieb, Odense
Annette Schouboe, Aarhus
Akos Gulyban, Liege
Marianne Sanggaard Assenholt, Aarhus

Group 8 Photon therapy: Intra-fractional challenges
Chairs: Antje-Christin Knopf and Per Poulsen
Ander Biguri [Steven Hancock], Bath
Mai Lykkegaard Schmidt, Aarhus
Patrik Sibolt, Roskilde
Marianne Knap, Aarhus
Susanne Bekke [Faisal Mahmood], Herlev
Jenny Bertholet, Aarhus
Simon Skouboe, Aarhus
Camilla Skinnerup Byskov, Aarhus

Group 9 Proton therapy: Inter- and intra-fractional challenges
Chairs: Marta Peroni and Katia Parodi
Stine Korrman, Aarhus
Kia Busch, Aarhus
Maria Fuglsang-Jensen, Aarhus
Alina Santiago, Marburg
Emma Colvil, Aarhus
Thomas Berger, Aarhus
Toke Printz Ringbæk, Giessen

Group 10 Functional imaging: MRI

Chairs: Faisal Mahmood and Erik Morre Pedersen

Ane Iversen, Aarhus

Jesper Kallehauge, Aarhus

René Winter, Tübingen

Morten Bjoern Jensen, Aarhus

Poster abstracts

Poster discussion group 1

Poster #1

Tordis J. Dahle, Bergen, Norway

Sensitivity of the Microdosimetric Kinetic Model to variations in model parameters

Dahle TJ (1), Magro G (2), Stokkevåg CH (3), Ytre-Hauge KS (1), Mairani A (2,4). (1) Department of Physics and Technology, University of Bergen, Bergen, Norway, (2) Centro Nazionale di Adroterapia Oncologica (CNAO), Pavia, Italy, (3) Department of Oncology and Medical Physics, Haukeland University Hospital, Bergen, Norway, (4) Heidelb.

Introduction: A challenge in treatment planning for carbon ion therapy (CIRT) is the quantification of the relative biological effectiveness (RBE). Delivery of homogeneous biological dose to the target depends on the accuracy of the applied RBE model and its input parameters. Treatment planning for CIRT at NIRS in Japan is based on the Microdosimetric Kinetic Model (MKM) with parameters optimized for HSG cells. In this work we studied the sensitivity of the MKM to variations in the model parameters. Materials and methods: The MKM is based on estimations of specific energy (z) in small volumes called domains. We generated tables connecting the kinetic energy of the particles to z, using the Kiefer-Chatterjee track structure model with saturation corrections. This was implemented in the FLUKA Monte Carlo (MC) code, and the biological dose for a spread out Bragg peak (SOBP) scenario was calculated from the MC output. The linear-quadratic model parameters α and β, the nucleus radius (Rn) and the domain radius (rd) were then varied one at a time by ±{5, 25, 50}% and compared to the SOBP without offsets. The resulting SOBPs were scaled and only the shapes were compared. Result: The output from the FLUKA implementation agreed with results from the NIRS TPS. A change of 5% in the parameters resulted in relatively small variations (below 5%) from the non-perturbed SOBP. When changing the parameters by 25 or 50%, the variations were more significant, especially when varying rd and Rn, which completely altered the SOBP shape. When changing the parameters by 25 and 50%, a difference in the biological dose throughout the SOBP could be as high as 22 and 42% compared to the SOBP with no offset. Conclusions: The shape of the SOBP calculated with MKM was not significantly altered by small variations in the input parameters, but could be by larger variations. Hence, the use of accurate parameters in the MKM is important. Further work includes studying parameters for other cell-lines.

Poster #2

Steffen Nielsen, Aarhus, Denmark

Patient-specific Gene Expression Patterns Predictive of Radiation-induced Fibrosis Are Comparable After Proton Pencil Beam Scanning and Cobalt-60 Irradiation

Nielsen S 1, Bassler N 2, Alsner J 1, Swakon J 3, Andreasen CH 1, Olko P 3, Overgaard J 1, and Sørensen BS 1. 1Department of Experimental Clinical Oncology, Aarhus University Hospital, Aarhus Denmark : 2Department of Radiation Physics, Stockholm University, Sweden : 3Cyclotron Centre Bronowice, Institute of Nuclear Physics, Krakow, Poland.

Introduction: The severity of radiation-induced fibrosis (RIF) following photon radiotherapy varies significantly between patients, partly due to genetic differences. Despite growing use of scanning proton beams, only scant focus has been on patient-specific radiosensitivity in proton therapy. A predictive 9-gene test using induction of gene expression in photon-irradiated fibroblasts has previously been used to classify individual patients as either sensitive or resistant to RIF development. The aim was to evaluate whether established patient-specific gene expression patterns induced by photon radiation are preserved following proton pencil beam scanning. Methods: The study included 30 primary fibroblast cultures established from normal skin biopsies. Biopsies were from head and neck cancer patients treated with photon radiotherapy. Patients were previously classified as either radiosensitive or radioresistant. Fibroblasts were irradiated with either proton pencil beam scanning or Co-60 photons as reference irradiation. Dose was delivered in 3 fractions x 3.5 GyE (RBE 1.1). Real-time PCR was performed to establish gene expression levels. The genes used in the RIF test are CDC6, CXCL12, FAP, LMNB2, LUM, MXRA5, SOD2, SOD3, and WISP2. Preliminary results: Induction of gene expression was less substantial in irradiated fibroblasts from radioresistant patients than in radiosensitive patients for most test genes; irrespective of the radiation type. The test genes generally provided the expected separation of the two predefined groups. Only CDC6 could not be used to differentiate between the sensitive and resistant groups. Conclusions: The individual classification of head and neck cancer patients as sensitive or resistant based on in vitro gene expression patterns in primary fibroblast cultures is independent of radiation type. This is the first indication that patient specific factors for risk of radiation-induced fibrosis may be similar for photons and protons.

Poster #3

Jakob Ödén, Stockholm, Sweden

Will breathing motion and a variable relative biological effectiveness jeopardize the plan quality in proton radiotherapy of breast cancer?

Jakob Ödén (1,2), Iuliana Toma-Dasu (1,3), Kjell Eriksson (2), Anna Maria Flejmer (4) and Alexandru Dasu (5,6). (1) Department of Physics, Medical Radiation Physics, Stockholm University, Stockholm, Sweden (2) RaySearch Laboratories, Stockholm, Sweden (3) Department of Oncology and Pathology, Karolinska Institutet, Stockholm, Sweden (4) Department of Oncology and D.

Purpose: Proton radiotherapy of breast cancer has been suggested to improve target coverage and lower doses to organs at risk (OARs) compared with photon therapy. This study aims to assess the effect of breathing motion and a variable relative biological effectiveness (RBE) on proton plan robustness. Methods: Photon and robustly optimized proton plans were generated to deliver 50 Gy(RBE) in 25 fractions (RBE=1.1) to the CTV (whole left breast) for twelve patients on a free-breathing CT scan. The constant RBE of 1.1 and the variable RBE model by Wedenberg et al. (2013) were used for plan evaluation. Robustness analyses against breathing motion and setup/range uncertainties were performed for all proton plans. Results: All original plans met the clinical target goals. Applying the variable RBE resulted in a mean RBE of 1.18 for the CTVs (range 1.14–1.21) and RBE values substantially higher than 1.1 in the OARs. However, the dosimetric impact of this latter aspect was minor due to the low physical OAR doses. For all cases the predicted NTCP for the lungs was low (<1%) and similar between photons and protons. The proton plans were shown to be robust for all patients. However, in the most extreme situations, the CTV receiving 95% of the dose dropped from 99–100% to around 96% for patients with large breathing motion. When including α/β uncertainties in the robustness analysis, the variable RBE also predicted substantially higher OAR doses than the constant RBE in the worst-case scenarios. Conclusions: Breathing motion and variable RBE might impact the potential benefit of protons, but could probably be neglected in most cases with normal breathing and where the physical OAR doses are low. In certain situations though, with e.g. the heart close to the chest wall and/or large breathing motion, the variable RBE and breathing motion might lead to increased OAR doses and/or worse target coverage and should hence preferably be considered in a NTCP-based plan comparison.

Poster #4

Silke Ulrich, Heidelberg, Germany

Impact of respiratory motion on variable relative biological effectiveness in 4D dose distributions for protons

Ulrich S (1)(2), Wieser HP (1)(2), Cao W (3), Mohan R (3), Bangert M (1)(2). (1)German Cancer Research Center (DKFZ), Medical Physics in Radiation Oncology, Heidelberg, Germany (2) Heidelberg Istitute of Radiation Oncology (HIRO), Heidelberg, Germany (3) MD Anderson Cancer Center, Radiation Oncology, Houston, Texas.

Organ motion during radiation therapy with scanned protons leads to deviations between the planned and the delivered physical dose. Using a constant relative biological effectiveness (RBE) of 1.1 linearly maps these deviations into RBE-weighted dose. However, a constant value of 1.1 cannot account for potential nonlinear variations in RBE suggested by variable RBE models. Here, we study the impact of motion on recalculations of RBE-weighted dose considering McNamara's variable RBE model. 4D dose calculation including variable RBE was implemented in matRad. We used a 4D-CT of a liver cancer patient (5.4mm target motion, 2 Gy(RBE) prescribed dose), assumed a regular 5s breathing period, and considered a single lateral proton field. Four dose distributions were compared: (A) the optimized static dose distribution with constant RBE, (B) a static recalculation with variable RBE, (C) a 4D dose recalculation with constant RBE and (D) a 4D dose recalculation with variable RBE. For (C) the physical dose is accumulated with direct dose mapping; for (D) dose-weighted alphas and betas are accumulated to model synergistic irradiation effects on RBE. Dose recalculation with variable RBE leads to an increased biological dose at the end of the proton field, while 4D dose recalculation exhibits deviations everywhere depending on the interplay of beam delivery and organ motion. For the reference dose (A), we observe D95=1.98 Gy(RBE) in the GTV and a homogeneity of HI = D2/D98 = 1.04. For recalculation using variable RBE (B) with α/β = 2 (10) D95 changes to 2.103 (1.89) Gy(RBE) and HI = 1.09 (1.07). If motion is considered (C), D95 decreases to 1.79 Gy(RBE) and homogeneity drops to 1.19. If motion and variable RBE are considered (D), both effects show up in the accumulated dose distribution, resulting in D95 = 1.94 Gy(RBE) and HI = 1.23 for α/β = 2. For the studied liver case, intrafractional motion does not reduce effects of variable RBE for a single beam treatment with protons.

Poster #5

Kristian Ytre-Hauge, Bergen, Norway

Biological dose to patients receiving cranio-spinal irradiation with protons

Ytre-Hauge KS(1), Fjæra LF(1), Rørvik E(1), Thörnqvist S(1,2) and Stokkevåg CH(2). (1):Department of Physics and Technology, University of Bergen, Norway (2):Department of Oncology and Medical Physics, Haukeland University Hospital, Norway.

Introduction Proton therapy offers improved dose conformity compared to photons for patients receiving cranio-spinal irradiation (CSI). In current clinical practice, proton treatment planning is based on a constant relative biological effectiveness (RBE) of 1.1. However, proton RBE has been shown to vary with linear energy transfer (LET), tissue type and dose, properties that have been included in variable RBE models. The objective of this work was to investigate the biological doses to patients receiving CSI with protons. Materials and methods Intensity Modulated Proton Therapy (IMPT) plans for two children were generated using the Eclipse treatment planning system. The PTV included the cranio-spinal axis including vertebra bodies prescribed 23.4 Gy(RBE) and a high-dose boost to the posterior fossa up to 54 Gy(RBE). The plans were recalculated in the FLUKA Monte Carlo (MC) code, where dose and dose-averaged LET distributions were obtained. Biological doses for a range of organs at risk (OARs), including heart, lung, thyroid and esophagus, and other regions of interest were calculated using LET dose-weighting and two different RBE models (Wilkens- and McNamara model). Results The resulting biological doses were higher for all considered OARs and ROIs when using the RBE models, compared to doses from constant RBE (RBE1.1), with the highest biological doses estimated from the Wilkens model. The LET-weighting approach gave slightly higher biological doses for most OARs while the mean doses for target volumes were comparable to 1.1. Compared to RBE1.1 doses, the mean dose to the lungs increased by 5-6% with LET-weighted dose, 14-16% for the McNamara model and 25-30% for the Wilkens model. Similar trends were seen for other dose parameters including D2% and for other OARs. Conclusions Considering the biological dose, preferably using multiple RBE models, could give important insight when evaluating proton therapy plans for CSI.

Poster discussion group 2

Poster #6

W. van Elmpt, Maastricht, The Netherlands

Influence of grey level discretization on radiomic feature stability for different CT scanners, tube currents and slice thicknesses: a phantom study

van Elmpt, W., Larue, R.T.H.M., van Timmeren, J.E., de Jong, E.E.C., Feliciani, G., Leijenaar, R.T.H., Lambin, P. Department of Radiation Oncology (MAASTRO), GROW – School for Oncology and Developmental Biology, Maastricht University Medical Centre (MUMC), Maastricht, the Netherlands.

Introduction Radiomics analyses of CT images provides prognostic information that can potentially be used for personalized treatment. Optimizing grey level (GL) discretization may improve robustness of radiomics analyses. The aim of this study was to investigate the stability of radiomic features for a range of bin widths for different CT acquisitions. Materials and methods A phantom with 10 different inserts (Mackin et al. 2015) was scanned on a Siemens Biograph (scanner 1) or Sensation Open (scanner 2) with a tube current of 40 mA or 80 mA. Scans were reconstructed with 1.5 mm or 3 mm slice thickness using a B31f kernel. Image preprocessing comprised GL-discretization in 7 different bin widths ranging from 10 to 40 HU. Subsequently, 95 textural radiomic features were extracted from a 4.2 cm3 sphere in the center of each insert. Feature stability was assessed by calculating the concordance correlation coefficient (CCC) for different combinations of scanners, tube current and slice thickness. Results The total number of stable features (CCC>0.85) when comparing both scanners was hardly influenced by HU bin width for 80 mA and 1.5 mm (84; 74-89 [median; range]), 80 mA and 3 mm (84; 73-86) and 40 mA and 3 mm (68; 60-72). Also when comparing the 40mA tube current with 80mA on scanner 1, feature stability hardly depended on the bin width. However, more features were stable for 1.5 mm (86; 80-89) than for 3 mm slice thickness (65; 60-70). Less features were stable when comparing different slice thicknesses for both scanner 1 (38; 35-41) and 2 (45; 38-48) using 80 mA. Conclusions Stability of textural radiomic features is hardly dependent on GL-discretization or tube current (at 1.5 mm). Optimization of GL-discretization to potentially improve the prognostic value can be performed without compromising feature stability. However, comparing different slice thicknesses drastically reduces this stability. Other preprocessing, i.e. resampling, should therefore be investigated.

Poster #7

Jurgen Peerlings, Maastricht, The Netherlands

Repeatability of Radiomics features derived from test-retest diffusion-weighted MR images

Jurgen Peerlings (1,2), Jessica M. Winfield (3), Jennifer C. Wakefield (3), Ralph T.H. Leijenaar (1), Aniek J.G. Even (1), Ruben T.H.M. Larue (1), Felix M. Mottaghy (2,4), Nandita M. deSouza (3), Philippe Lambin (1). 1. Department of Radiation Oncology (MAASTRO), GROW- School for Oncology and Developmental Biology, Maastricht University Medical Center+, Maastricht, The Netherlands; 2. Department of Radiology and Nuclear Medicine, Maastricht University Medical Center+,

INTRODUCTION Diffusion-weighted magnetic resonance imaging (DW-MRI) is used to assess tumor cellularity by quantifying apparent diffusion coefficient (ADC) maps. By extracting quantitative tumor phenotypic features from ADC maps, Radiomics may provide complementary information to determine tissue pathology and predict treatment response. For reliable Radiomics models, stable and reproducible features need to be selected from a set of imaging biomarkers. The aim of this study is to assess variability in, and robustness of MR-based Radiomics features on test-retest images of the same lesion. METHODS Twelve patients with ovarian cancer underwent repeated 1.5 Tesla DW-MRI (1-5 day interval) as part of a prospective clinical trial. Volumes of interest were drawn over 20 adnexal masses on DW images (b=900 s/mm2) while excluding cystic and necrotic regions. On each corresponding ADC map, 138 Radiomics features were extracted describing tumor intensity (n=19), shape (n=24), and texture (n=95). A concordance correlation coefficient (CCC) of >0.85 was used to identify robust features between test and retest scans of the same lesion. RESULTS In total, 66/138 (47.8%) Radiomics signatures showed high robustness in the test-retest cohort. Most shape features (21/24, 87.5%) and 41/95 (43.1%) texture features were regarded as stable. Histogram features showed the most variability as only 4/19 (21%) were robust. Clinical interpretation of ADC maps are currently based on i.a. histogram kurtosis (CCC=0.92) and skewness (CCC=0.80). Although skewness did not reach the CCC threshold, this feature is still reasonably stable and can contain clinically important information. CONCLUSION MR-based Radiomics analyses are able to extract robust features and quantify tumor characteristics. By selecting stable features, reliable models can be created to potentially predict treatment response. Further analyses are planned to assess feature stability at multiple tumor sites and across MR-systems.

Poster #8

Sara Carvalho, Maastricht, the Netherlands

FDG-PET-Radiomics of metastatic lymph nodes and primary tumor in NSCLC – a prospective externally validated study

Carvalho S 1, Leijenaar RTH 1, Troost EGC 1, van Timmeren JE 1, Oberije C 1, van Elmpt W 1, de Geus-Oei L 2, Bussink J 3, Lambin P 1. 1 Department of Radiation Oncology (MAASTRO), Maastricht, the Netherlands; 2 Department of Radiology and Nuclear Medicine, Radboud UMC, Nijmegen, the Netherlands, 3 Department of Radiation Oncology, Radboud UMC, Nijmegen, the Netherlands.

Prognostic value of the FDG distribution has been widely studied for the primary tumor (tumor) in non-small cell lung cancer (NSCLC). Conversely, lymph node stage prior to treatment is strongly related to disease progression, capability to metastasize and poor prognosis in NSCLC. However, few studies have investigated metabolic imaging features from pre-radiotherapy 18F-fluorodeoxyglucose (FDG) positron-emission tomography (PET) of metastatic hilar/mediastinal lymph nodes (LNs). We hypothesized that these would provide with complementary prognostic information to FDG-PET descriptors to only the tumor. Two independent cohorts of 262 and 50 node-positive stage I-III NSCLC patients were used for model development and validation. Image features (i.e. Radiomics) including shape and size, first order statistics, texture, and intensity-volume histograms (IVH) (www.radiomics.org) were evaluated by univariable Cox regression on the development cohort. Prognostic modelling was conducted with a 10-fold cross-validated least absolute shrinkage and selection operator (LASSO), automatically selecting amongst FDG-PET-Radiomics descriptors from (1) tumor, (2) LNs and (3) both structures. Performance of developed models was assessed with the concordance-index. Common SUV descriptors (maximum, peak, and mean) were significantly related to overall survival when extracted from LNs, as were LN volume and tumor load (summed tumor and LNs' volumes), though this was not true for either SUV metrics or tumor's volume. Feature selection exclusively from imaging information based on FDG-PET-Radiomics, exhibited performances of (1) 0.53 – external 0.54, when derived from the tumor, (2) 0.62 – external 0.56 from LNs, and (3) 0.62 – external 0.59 from both structures, including at least one feature from each sub-category, except IVH. Combining imaging information based on FDG-PET-Radiomics features from tumors and LNs is desirable to achieve a higher prognostic discriminative power for NSCLC.

Poster #9

R.T.H.M. Larue, Maastricht, The Netherlands

Pre-treatment CT radiomics to predict 3-year overall survival in oesophageal cancer patients

Larue, R.T.H.M.(1), Klaassen, R.(2), Jochems, A.(1), Leijenaar, R.T.H.(1), Hulshof, M.C.C.M.(3), van Berge Henegouwen, M.I.(4), Sosef, M.N.(5), van Elmpt, W.(1), van Laarhoven, H.W.M.(2), Lambin, P.(1). 1Department of Radiation Oncology (MAASTRO), GROW – School for Oncology and Developmental Biology, Maastricht University Medical Centre (MUMC), Maastricht, The Netherlands. 2Department of Medical Oncology, Academic Medical Center, Amsterdam, The Netherlan.

Introduction Radiomic features retrieved from routinely acquired CT-images have been shown to provide prognostic information in several tumor sites. In this study we aimed to investigate the prognostic value of pre-treatment CT radiomic features in esophageal cancer patients. Materials and methods Two clinical datasets of independent centers were analyzed. Both datasets consisted of esophageal cancer patients treated with concurrent chemotherapy (Carbo/Taxol) and 41.4Gy radiotherapy, followed by surgery if feasible. In total 1064 shape, texture, statistics and wavelet radiomic features were calculated from the primary tumor volume. The datasets were randomly divided 50/50 in a training and validation dataset. A random forest (RF) model was trained on the training dataset to identify the 200 most important radiomic features. Using these 200 features as input, a final RF model (500 trees, maximum 5 nodes/tree) predicting 3-year overall survival was then trained and validated. Results In total 271 patients from center 1 (stage I-III, median age 64, 77% male) and 127 patients from center 2 (stage I-III, median age 65, 79% male) were eligible for analysis. The training RF model yielded an area under the curve (AUC) of 0.63 (95%CI 0.53-0.73), with 1 shape, 1 statistics and 3 (wavelet) textural features among the top-5 most important features for 3-year survival. In the validation dataset, the RF model yielded and AUC of 0.61 (95%CI 0.52-0.71). Selecting only the features that were identified as ‘stable’ in a former study (54/200 important features) resulted in a comparable performance (AUC 0.60). Conclusions A RF model predicting 3-year overall survival based on pre-treatment CT radiomic features was developed and validated in two independent datasets of esophageal cancer patients. Our results demonstrate the potential prognostic value of CT radiomic features only. Clinical variables should be considered to assess complementary prognostic information to improve the model.

Poster discussion group 3

Poster #10

Thomas Wittenborn, Aarhus C, Danmark

Preclinical Investigation of Hypoxia-induced Gene Expression in Prostate Cancer Cell Lines and Xenografts

Wittenborn T.R., Sørensen B.S., Busk M., Thomsen M.B.H., Andersen L.D., Elming P.B., Nielsen S., and Horsman M.R. Department of Experimental Clinical Oncology and Department of Molecular Medicine, Aarhus University Hospital, Aarhus, Denmark.

Introduction: Hypoxia is found in many solid tumours, and is known to reduce tumour response to radiotherapy. Identifying patients with hypoxic tumors will allow for the selection of additional treatment, either in the form of hypoxic modifiers or increased radiation dose. Our department has developed a gene profile consisting of 15 genes, which demonstrated prognostic and predictive impact for hypoxic modification in head and neck squamous cell carcinomas (HNSCC). In the current study we investigated this 15 gene profile in vitro in the PC3 and DU-145 prostate cancer cell lines, and in vivo in the PC3 xenograft model. Materials and Methods: Prostate cancer cell lines were cultured under normoxic (21% O2) or varying hypoxic conditions (0%, 0.5%, 1.0%, 2.0%, and 5.0% O2) for 24 hours, totRNA was extracted and gene expression levels measured by qPCR. PC3 cells were inoculated on the flank of female NMRI Foxn1nu/Foxn1nu mice. Two hypoxia-sensitive tracers (18F-FAZA and Pimonidazole) were administered 3-4 hours prior to tumour excision, snap-freezing, and sectioning. Autoradiography was used as a template for laser capture microdissection in order to extract hypoxic and non-hypoxic areas from the tumour sections. Dissected areas were extracted for totRNA and gene expression levels were measured by qPCR. Results: Both PC3 and DU-145 cell lines showed a hypoxia-dependent increase in gene expression for all 15 genes. The expression patterns were heterogenous, with some genes having the highest fold-upregulation when going from 21% to 5% oxygen, whereas others had it when going from 0.5% to 0% oxygen. A significantly increased gene expression for all 15 genes was observed in vivo when comparing non-hypoxic to hypoxic areas. Conclusion: A hypoxia-dependent induction of genes was observed both in vitro and in vivo. Our results suggest that the gene profile could be suitable for prostate cancers as well as HNSCC.

Poster #11

David Grosshans, Houston, USA

Radiation induces age dependent deficits in cortical synaptic plasticity

Zhang D, Duman J and Grosshans DR. The University of Texas MD Anderson Cancer Center and Baylor College of Medicine.

Introduction: Clinically, pediatric patients are relatively more vulnerable than adults to radiation-induced cognitive dysfunction. Despite the significance of radiation induced brain dysfunction, the underlying mechanisms, including reasons for age dependence, are still largely unknown. The majority of previous studies have focused on DNA damage and resultant death of neuronal precursor cells in the dentate gyrus region of the hippocampus. However, the loss of replicative cells alone may be insufficient to account for all aspects of impaired cognition following brain RT. This is particularly true for deficits in attention and executive function controlled by cortical regions. In such non-neurogenic regions, alterations in the function of mature neurons may underlie cognitive deficits. Materials and Methods: In present study, we used in vivo cortical recordings to assess radiation-induced alterations in synaptic plasticity. Juvenile and adult Sprague Dawley rats were treated with 10Gy cranial irradiation. We then assessed LTP at the CA1/subicular-prefrontal cortex (PFC) direct pathway, which is believed critical for memory and cognitive regulations, at 3 days, 2, 4 and 8 weeks post radiation. Results: At 3 days, radiation induced inhibition of LTP was observed in both adult and juvenile animals. In adult animals LTP was slowly restored and returned to near normal levels by 8 weeks. In contrast, in juvenile animals LTP remained significantly depressed over time. We also assessed the impact of memantine on LTP with or without radiation. Pretreatment, but not post-treatment, with memantine partially prevented radiation induced LTP inhibition in animals of both ages. Conclusions: The observed changes in LTP in the hippocampal-PFC connection, may contribute to the negative effects of radiation on cognition and describe potential mechanisms underlying the age difference in responses to radiation and the protective effects of memantine.

Poster #12

Jacob Lilja-Fischer, Aarhus, Denmark

Oropharyngeal cancer patient-derived xenografts: Characterization and radiosensitivity.

Lilja-Fischer JK, Ulhøi BP, Alsner J, Thomsen MS, Lassen P, Nielsen VE, Overgaard J.
Department of Experimental Clinical Oncology, Aarhus University Hospital, Aarhus, Denmark.

Introduction: Oropharyngeal squamous cell carcinoma (OPSCC) is now the most common type of head and neck cancer. HPV, tobacco smoking or a combination of the two are the major etiologic factors. Prognosis is dependent on etiology. Since OPSCC is heterogeneous in disease biology and treatment sensitivity, further personalization of treatment is needed, which is the focus of ongoing clinical trials. However, adequate pre-clinical models and biomarkers reflecting treatment sensitivity are lacking. Purpose of this study was to create a number of patient-derived xenografts (PDX) and compare the models with the original human tumors. Also, we wished to determine if the PDX model is suitable for radiotherapy research. Methods: Fresh tumor biopsies from patients with primary, untreated OPSCC were implanted subcutaneously in immunodeficient mice, and expanded upon engraftment. Xenograft tumors and human originals were compared using histology, immunohistochemistry and NGS. To characterize radiosensitivity, PDX tumors were subjected to low-dose irradiation in a growth delay assay (4 - 8 Gy, single fraction). Results: To date, tumor biopsies from 34 OPSCC patients have been xenografted resulting in xenograft tumor growth in 22 cases (65 %), from patients with HPV-positive and HPV-negative disease as well as a wide range of tobacco exposures. Most PDX tumors retained the histological appearance of squamous cell carcinoma and immunoprofile of the original tumor. Other tumors adopted a lymphoproliferative appearance. Low-dose irradiation of PDX tumors resulted in a reproducible growth delay. Conclusion: It is possible to generate PDX models that represent the clinical heterogeneity of disease. Most PDX models retain the characteristics of the original tumor. The PDX model is a promising research model, perspectives include biomarker development, testing of targeted therapies and improvement of radiotherapy.

Poster #13

Morten Busk, Aarhus, Denmark

Hypoxia PET imaging: combining information on perfusion and tracer retention to improve hypoxia-specificity

Busk M1, Munk OL2, Jakobsen S2, Horsman MR1. 1) Department of Experimental Clinical Oncology, Aarhus University Hospital (AUH), Aarhus, Denmark, 2) PET centre, AUH.

Introduction: Static PET allows mapping of tumor hypoxia, but low resolution and slow tracer retention/clearance results in poor image contrast and the risk of missing areas where hypoxic cells and necrosis are intermixed. Pharmacokinetic analysis of full dynamic scans may improve accuracy, but is clinically unappealing. A previous modeling study proposed that hypoxia-specificity can be improved by a clinically feasible blood-flow normalization procedure, that only requires a 10 min dynamic scan (perfusion/tracer wash-in), and a short late static scan, but experimental validation is warranted. Methods: Tumor-bearing rodents were injected with pimonidazole (an immunodetectable marker of hypoxic cells) and the PET hypoxia-tracer FAZA and scanned dynamically for 3h. Subsequently, the distribution of FAZA (autoradiography) and hypoxic cells was compared on sectioned tumor tissue. PET images collected 60-70 min post-injection (PETearly), which mimics the image contrast seen in patients, were compared to 3h PET (PETlate) voxel-wise. For comparison, PETearly was normalized to the Perfusion Peak Area (PPA), deduced from the first 10 min of the scan, and compared to PETlate. Results/Discussion: Post-scan tissue analysis revealed a near-perfect spatial match between FAZA signal and hypoxic cell density (pimonidazole), in a variety of tumor models. Importantly, this shows that 3h PET scans in rodents, unlike patients, provides an accurate map of hypoxia, against which earlier time-point scans and modelling can be compared. PETearly and PETlate were positively correlated but to a variable extent. Unexpectedly, no inverse correlation between PPA and PETlate was seen, and normalization of PETearly to PPA (PETearly/PPA) worsened the correlation between PETearly and PETlate, challenging the validity of a perfusion normalization approach. This may reflect that tumor blood flow and oxygen delivery capacity, and thus hypoxia, is uncoupled due to the chaotic tumor vasculature.

Poster #14

Pernille Elming, Aarhus, Denmark

Combination of Vascular Disrupting Agents and Checkpoint Inhibitors: a Method of Increasing Tumour Immunogenicity?

Elming PB, Wittenborn TR, Horsman MR. Department of Experimental Clinical Oncology, Aarhus University Hospital, Aarhus, Denmark.

Introduction: Checkpoint inhibitors are used in the clinic with success. But it only affects a small percentage of patients. Methods to increase efficacy are needed. The vascular disrupting agent Combretastatin (CA4P) induces vascular damage by targeting the tumor vasculature which leads to tumour cell death and necrosis. This may influence immune response. We are currently doing experiments with the combination of checkpoint inhibitors (CI's) and CA4P. The CI's of our interest are the anti-CTLA-4, -PD-1 and -PD-L1. Methods: CDF1 male mice were inoculated on the right rear foot with a C3H mammary carcinoma. When the tumour reached a volume of 200mm3 the mice were treated with CA4P (100mg/kg i.p.) or the CI's (all at 10 mg/kg i.p.) or the combination of CA4P with each CI. CA4P was given on days 0, 3, 7, and 10 and the CI's were given on days 1, 4, 8 and 11. Tumour size was measured daily, and the time to reach three times treatment volume (TGT3) was the endpoint. Results are listed as Mean (± SE). One-way ANOVA comparison of group means was performed, and a $P<0.05$ was considered significant Results: The TGT3 for the control group was 4.8 days (± 0.4). For the CI's anti-PD-1, anti-PD-L1 and anti-CTLA4 the TGT3 was 5.3 days (± 0.4), 4.9 days (± 0.4) and 4.80 days (± 0.2) respectively. None of these values were significantly different from controls. In the CA4P group the TGT3 was significantly increased to 6.2 days (± 0.2). When combined with the CI's this value was increased to 6.6 days (± 0.4) for anti-PD-1, 7.7 days (± 0.7) for anti-PD-L1 and 6.7 days (± 0.5) for anti-CTLA-4. These values were not significantly different from CA4P alone, although the P-value for the comparison between the CA4P and the CA4P + anti-PD-L1 group was only 0.06. Conclusion: Our data suggest a possible benefit of combining Combretastatin and checkpoint inhibitors. We will investigate the potential anti-tumour effect of combining VDA's and radiation with checkpoint inhibitors.

Poster discussion group 4

Poster #15

Timo Deist, Maastricht, The Netherlands

On the selection of classifiers for outcome prediction in radiotherapy

Deist, T.M., Dankers, F.J.W.M., Valdes, G., Solberg, T., Hsu, I.C., Lambin, P. Department of Radiation Oncology (MAASTRO clinic), GROW, School for Oncology and Developmental Biology, Maastricht University Medical Center, Maastricht, The Netherlands Department of Radiation Oncology, Radboud University Medical Center, Nijmegen, the Ne.

Introduction Classification models for predicting radiotherapy treatment outcomes receive much attention in literature. Currently, there is no consensus on the optimal classifier. General machine learning literature provides evidence in favor of some classifier families (random forest (RF), support vector machine (SVM)) in terms of classification performance. In this study we investigate how these results translate to radiotherapy datasets that differ in characteristics, e.g., size, missing data, or variable types. Materials and methods We collected 4 datasets from publications and 1 additional dataset on post-radiotherapy toxicity and survival outcomes with clinical, dosimetric, and blood biomarker variables from multiple institutions. Seven common classification algorithms (decision trees, RF, neural network, SVM, elastic net logistic regression (ENLR), k-nearest neighbor, LogitBoost) were applied on each dataset using the popular open-source R package caret. We ran a 50-repeated 5-fold cross-validation (CV). Parameter tuning was conducted in an inner 5-fold CV in the training data per algorithm using the tuning grid recommended by caret. Performance metrics (discrimination, calibration slope and intercept, accuracy, and Brier score) were computed for each outer test fold and averaged per dataset and classifier over repetitions. Results The average discriminative ability (AUC) varies on average by 0.1 over classifiers within a specific dataset. The ranking of classifiers is not stable over datasets, each classifier shifts in rank on average by 3.4 positions. However, ENLR and RF exhibit the best mean ranks of 3.1 over datasets. Conclusions There is merit in choosing the best classifier for a specific dataset because the AUC could vary up to 19% between the best and the worst classifier (10% compared to the average classifier). There is no universally superior classifier across the investigated datasets. However, ENLR or RF appear to be safe first choices.

Poster #16

Jan Alsner, Aarhus, Denmark

Associations between skin toxicity, survival, and single nucleotide polymorphisms in head and neck cancer patients receiving the EGFr-inhibitor Zalutumumab: Results from the DAHANCA 19 trial

Brøndum L, Alsner J, Sørensen BS, Overgaard J, Eriksen JGE. Department of Experimental Clinical Oncology, Aarhus University Hospital, Aarhus, Denmark; Department of Oncology, Odense University Hospital, Odense, Denmark.

Purpose To study the associations between development of moderate to severe skin rash, clinical outcome, and single nucleotide polymorphisms (SNPs) in candidate genes in head and neck cancer patients from the DAHANCA 19 trial receiving the EGFr-inhibitor Zalutumumab. Materials and methods 301 patients were included from the Zalutumumab-arm of the DAHANCA 19 study. Nine SNPs in the candidate genes EGFR, EGF, AREG, FCGR2A, FCGR3A, and CCND1 were successfully determined in 294 patients. Clinical endpoints were moderate to severe skin rash within first three weeks of treatment, loco-regional failure (LRF), disease-specific survival (DSS) and overall survival (OS). Results During the first three weeks of therapy, 86% of the patients experienced any grade of rash and 17% experienced a moderate to severe rash. Development of moderate to severe rash was not associated with LRF or DSS but was associated with improved OS, HR: 0.40 (95% CI: 0.19-0.82). The effect was similar for patients with p16-negative or p16-positive tumours (p=0.90). After adjustment for T-stage, smoking history, comorbidity, and performance status, the minor allele of SNP rs9996584 located near AREG was significantly associated with increased risk of moderate to severe rash with a per-allele odds ratio of 1.64 (1.02-2.61). SNP rs13104811 located close to rs9996584 had a borderline significant association and none of the other SNPS were significantly associated with risk of skin rash. Conclusions Moderate to severe skin rash after Zalutumumab was associated with improved overall survival, independent of HPV/p16-status. Genetic variants in AREG (member of the EGF family) may be associated with increased risk of skin rash.

Poster #17

Einar Dale, Oslo, Norway

Dose painting for reirradiation of head and neck cancer

Skjøtskift T (1), Evensen ME (1), Furre T (2), Moan JM (1), Amdal CD (1), Bogsrud TV (3), Malinen E (1,4), Dale E (1). (1) Department of Oncology, (2) Department of Medical Physics, (3) Department of Nuclear Medicine, (4) Department of Physics, University of Oslo.

Introduction: Dose painting may increase loco-regional control in head and neck cancer (HNC), potentially without added morbidity. For patients with recurrent or second primary disease, reirradiation can be very challenging due to overlap with previously irradiated volumes. Dose painting may offer a solution for these patients where focus is on delivering maximal dose to areas of high tumour burden. Here, we compare FDG-PET guided dose painting by contours (DPBC) treatment plans with conventional plans. Materials and Methods: We included 10 patients with recurrent or second primary HNC eligible for reirradiation. Our conventional reirradiation regimen is hyperfractionated radiotherapy 1.5 Gy twice daily over 4 weeks, giving a total dose of 60 Gy. For DPBC, we defined two prescription volumes (PVs) corresponding to 33% and 66 % of the highest FDG uptake in the tumor. Furthermore, the CTV prescription was a minimum dose of 60 Gy, PV33 of 65-67 Gy and PV66 of 70-73 Gy. The DPBC plan is given in the first 20 fractions and the conventional plan in the last 20 fractions. To evaluate the differences between DPBC and our standard treatment, we compared dose to organs at risk (OARs). By summing the first curative plan with the reirradiation plan using deformable registration, we also evaluated the differences in dose to small hot spots between the conventional and DPBC plans. Results: We achieved DPBC plans with adequate target coverage for all ten patients. There were no significant differences in OAR doses between the standard plans and the DPBC plans. Summation of the first curative plan with the new reirradiation plan showed that the clinically significant Dmax (dose to 2 ccm) increased from 130 Gy (113-132 Gy) to 140 Gy (115-145 Gy); median (range). Conclusions: Our three-level DPBC could be straightforwardly implemented and all patient plans met the objectives. Reirradiation of HNC with DPBC is a feasible technique not expected to cause more side-effects.

Poster #18

Simon Lønbro, Aarhus, Denmark

Immediate loss of lean body mass in locally advanced head and neck cancer during (chemo)-radiotherapy.

Lønbro, S. 1,2; Kaalund, I. 3; Hermann, P. 4; Johansen, J. 3. 1 Dept. of Experimental Clinical Oncology, Aarhus University Hospital, Aarhus, Denmark; 2 Dept. of Public Health, Section for Sport Science, Aarhus University, Denmark; 3 Dept. of Oncology, Odense University Hospital, Denmark; 4 Dept. of Endocrinology, Odense University Hospital, Denmark.

Introduction: Weight loss (WL) is common following radiotherapy in head and neck squamous cell carcinoma (HNSCC) patients and predicts quality of life and function. Investigating the temporal characteristics and constituents (lean body mass; LBM and fat mass; FM) are important to optimize treatment and appropriate interventions. Previous studies show associations between WL and changes in LBM before and after treatment. However, our primary purpose was to investigate WL during (chemo)-radiation in relation to loss of LBM and FM. Methods: 40 patients with locally advanced HNSCC stage I-IV undergoing intended curative radiotherapy (DAHANCA guidelines) were included. All completed 66-68 Gy with 5 or 6 fx. weekly, with or without concomitant chemotherapy and the hypoxic radiosensitizer nimorazole. All received weekly nutritional support. Body composition (Dual-energy X-ray absorptiometry) and weight assessments were done at baseline, at 2 week intervals during radiotherapy and 2 weeks after treatment. Results: Five patients were excluded due to disease/treatment-related reasons leaving 35 patients analyzed. Median age was 57 yrs (38-72). Primary diagnoses were pharynx and larynx cancer (85.8%), stage III-IV (74.3%). 63% received concomitant chemotherapy and 69% nimorazole. 23% received a feeding tube during treatment. Body weight declined from baseline to end of treatment (6.9%), LBM (8.8%), and FM (10%) (all $p<0.001$, ANOVA). Two weeks into treatment, LBM was reduced by 1.6% ($p=0.03$) despite no WL. Four, six and eight weeks after treatment start, WL and loss of LBM and FM were significant. Loss of LBM and FM from baseline to treatment end correlated with WL; $R2=0.81$ and $R2=0.46$, respectively ($p<0.001$, lin. regr.). Conclusion: WL correlated to equal proportions with loss of LBM and FM. Despite no initial WL, LBM was significantly reduced already two weeks into treatment. This underlines the importance of immediate intervention to counteract loss of LBM.

Poster #19

Arthur Jochems, Maastricht, Netherlands

A random forest model to predict early death in NSCLC patients receiving chemo(radio)therapy

Jochems, A.1, El-Naqa, I.2, Kessler, M.2, Mayo, C.2, Reeves, J.2, Jolly, S.2, Matuszak, M.2, Ten Haken, R.2, Faivre-Finn, C.3, Price, G.3, Holloway, L.4, Vinod, S.4, Field, M.4, Samir Barakat, M.4, Thwaites, D.4, Dekker, A.1, Lambin, P.1. 1. Department of Radiation Oncology (MAASTRO), GROW – School for Oncology and Developmental Biology, Maastricht University Medical Centre, Maastricht, The Netherlands 2. Department of Radiation Oncology (University of Michigan), 515 E Williams St., Ann A.

Introduction Early death after a treatment can be seen as a therapeutic failure. Wallington and colleagues reported that 8% of all non-small cell lung cancer (NSCLC) patients die within thirty days of systemic treatment initiation[1]. Identification of patient at risk for early mortality is crucial to avoid unnecessary harm and avoid costs. In this work, we validate the logistic regression model proposed by Wallington and colleagues in 4 independent datasets. Additionally, we develop our own model and validate it on the same datasets. The hypothesis is two-fold. First, both models can be used to predict 4-month mortality in these cohorts. Second, a radiotherapy specific model will outperform the model proposed by Wallington and colleagues in these cohorts. Material and methods Patients with NSCLC treated with concurrent chemoradiation or radiotherapy alone were included in this study. The Maastro cohort consists of 698 patients treated in routine clinical practice. The Michigan cohort consists of 121 patients. The Manchester cohort consists of 196 patients. The Liverpool cohort consists of 727 patients. A random forest (RF) model was developed by learning on the Maastro cohort. The model used Performance status, age, gender, T and N stage, total tumor volume (cc), total tumor dose (Gy) and chemo timing (none, sequential, concurrent) to make predictions. Death within 4 months of receiving first radiotherapy fraction was used as the outcome. Results Early death rates ranged from 7% to 24% within the four cohorts. The model by Wallington performed with AUC values ranging from 0.59 to 0.64 on the validation cohorts. The RF model performed with AUC values ranging from 0.62 to 0.74 on the validation cohorts. Conclusion Early mortality can be predicted by the models. These models can be embedded in decision support systems to inform patients about treatment options and thereby optimize care. References [1] Wallington et al. Lancet Oncol 2016;17:1203–1216.

Poster #20

Tinne Laurberg, Aarhus, Denmark

Intrinsic subtype classification of local recurrences and new contralateral primary tumors in patients with low risk breast cancer. Influence of age and primary surgery.

Laurberg T, Overgaard J. Dep of Experimental Clinical Oncology, Aarhus University Hospital, Aarhus, Denmark.

Introduction: To look deeper into the nature of local recurrences (LR) Material and methods: Pairs of Formalin-fixed paraffin embedded material were available from primary tumors, and 41 LR or 23 contralateral breast cancer (CC), respectively. Based on RNA-extraction Estrogen (ER), Progesterone(PR), human epidermal growth factor 2 (HER2), and Ki67 content was estimated, and Instrinsic subtype was approximated, 'RNA intrinsic subtype 4'(RIS4). Furthermore, the tumors were classified according to the researched-based PAM50-gene signature estimated by Nanostring nCounter gene expression assay. Results: Among younger (≤45 years) mastectomy patients (N=16), in 3 out of 16 cases the LR had a different RIS4 subtypes to that of the index tumor, and the proportion was similar to the younger patients with CC. Among younger patients having breast conserving therapy (BCT), 10/18 of LR were located in the scar and in 3/10 cases the LR had a different RIS4 subtype. The 8 LR with no known location to the original scar, only 1 case had a LR that differed to that of the index tumor. In the older BCT group, 6/7 LR were located in the scar and in 3/6 cases LR differed from the index tumor. An overall agreement between intrinsic subtyping based on the RIS4 classification and the PAM50 classification was observed in 75% of the tumors, most pronounced to patients characterised by HER2-negative tumors. The entire pattern and relationship between sub-classification, age and localisation of recurrence or new primary in our study was very similar when the PAM50 was applied. Conclusion: Applying intrinsic subtype classification to local recurrences and new primaries in patients with low risk breast cancer did not yield any clear distinction from the primary index tumor. Thus, the current small study did not add any further explanation to reveal the nature of the excess frequency of in-breast recurrences in younger women and the more aggressive behaviour of these.

Poster #21

Oscar Casares-Magaz, Aarhus, Denmark

The association between genitourinary toxicity and planned vs delivered bladder dose/volume metrics in radiotherapy for prostate cancer

Oscar Casares-Magaz1*, Ludvig P. Muren1, Niclas Pettersson2, Maria Thor3, Austin Hopper2, Rick Knopp2, Joseph O. Deasy3, John Einck2 and Vitali Moiseenko2. 1Dept of Medical Physics, Aarhus University Hospital, Aarhus, Denmark. 2Dept of Radiation Medicine and Applied sciences, University of California San Diego, La Jolla, USA. 3Dept of Medical Physics, Memorial Sloan Kettering Cancer Center, New York City, USA.

Introduction: Radiotherapy (RT) for prostate cancer is delivered with resource-intensive protocols involving multi-modality imaging, narrow margins, strict bladder volume control instructions and daily image-guidance. By analyzing planned vs. delivered doses in patients with and without genitourinary (GU) toxicity, this study aimed to interrogate whether radiation dose/volume metrics could be associated with the manifestation of GU toxicity after high-precision RT. Materials and Methods: Incidence of GU toxicity was low, with 7 of a total of 449 prostate cancer patients treated to 77.4-81Gy showing toxicity grade≥2. Patients were treated with IMRT, adhering to a full bladder/empty rectum protocol with daily image-guidance (on-board cone-beam CT, CBCT). A case-control analysis was performed, with each of seven patients experiencing grade≥2 GU toxicity matched with three controls free from toxicity who had similar characteristics: pre-treatment GU status, age, risk group and use of neoadjuvant therapy. A total of 13 CBCTs per patient were rigidly registered to the planning CT using the recorded treatment shifts, and bladders were manually contoured on each CBCT. Planned and delivered DVH metrics were extracted for ten bladder (sub)structures and systematically compared for planned vs. delivered for cases vs. controls. Results: Bladder volumes varied considerably during RT (CV: 15-59%). The only significant difference was observed between planned and delivered bladder volumes at the control group (meanSD: 166±73 vs. 202±80cm3). No significant differences were observed between planned and treated DVH metrics at any dose level, nor between the cases and controls. The controls had significantly lower delivered than planned high-dose metrics ($p<0.01$; V95%; V90% and V95% at posterior sector). Conclusions: Neither planned or delivered bladder dose/volume metrics was associated with the risk of developing GU toxicity after high-precision RT for prostate cancer.

Poster #22

Lotte Fog, Copenhagen, Denmark

Early pain relief and toxicity after image guided volumetric modulated radiation therapy for spinal cord compression

Fog, L S1 , Iovane, V1 , Hemer, M1 , Pappot, H1 ,Aznar, M. C2 , Sjøgren, P1, Appelt, A1,3. 1Dept. of Oncology, Rigshospitalet, University of Copenhagen, Denmark 2Nuffield Dept of Population Health, University of Oxford, Oxford, UK 3Inst of Cancer and Pathology, St James's University Hospital, Leeds, UK.

Introduction We present preliminary data from a prospective study investigating pain relief and early toxicity in SCC patients. Materials & methods 30 consecutive SCC patients treated with 10x3 Gy at our clinic were included.The patients answered the modified Brief Pain Inventory (mBPI) and Edmonton Symptom Assessment Scale (ESAS) daily on weekdays and the EORTC-QLQ-C30 questionnaire weekly for 3 weeks after radiotherapy (RT).RT was delivered as image-guided volumetric modulated arc therapy, with sparing of intestines for patients treated to abdomen and pelvis.1 pt was excluded due to a change in fractionation. Daily data on worst pain, mean pain, tiredness and "other symptoms" were compared to baseline scores using the Wilcoxon signed rank test.Increase in diarrhea and constipation compared with week 1 was recorded. Results Worst pain was significantly reduced on days 9 and 13 (3.36, n=11, p=0.01; 3.18, n=17, p=0.007) compared to baseline (5.62) as well as mean pain on days 7,9, 13 and 20 (2.52,n=22,p=0.03; 1.96,n=11, p=0.03; 1.72,n=18,p=0.01; 2.64, n=14, p=0.02) compared to baseline (3.55). Tiredness was significantly greater only on day 9 (3.07 vs 2.10, n=9, p= 0.03). 3 patients had increased diarrhea in week 2 or 3; these all had SCC at the level of Th9 or below (Th9 and L1;L1-3;Th5 and Th11). 6 patients reported increased constipation in week 2 or 3. Patients reported an average of 1.8 "other symptoms".These were oral or throat pain and difficulty in swallowing (11 pts, for all of whom the most cranially treated vertebra was Th8 or above),other bone pain (7), dizziness (2) and 12 symptoms experienced by only 1 patient. Conclusions Reduction in pain is not observed until the second week of treatment for most patients treated with RT for SCC, and not necessarily maintained after end of treatment. Patients experience multiple early toxicities – particularly oral or throat pain, difficulty in swallowing, and diarrhea, which may all be treatment related.

Poster discussion group 5

Poster #23

Ellen Marie Høye, Aarhus, Denmark

Saturation dose and quenching in proton beams in a radiochromic 3D dosimeter

Høye E M [1], Sadel M [2], Bernal-Zamorano M R [3], Muren L P [1], Petersen J B B [1], Skyt P S [1], Swakon J [4], Bassler N [5], Balling P [2]. [1] Aarhus Univ. Hospital2 Dept. of Physics and Astronomy, Aarhus Univ. 3 Center for Nuclear Technologies, Technical Univ. of Denmark 4 Inst. of Nuclear Physics, Polish Academy of Sciences, Krakow 5 Dept. of Physics, Stockholm Univ..

Track-structure theory for ions has successfully been applied to predict biological outcome as well as dosimeter response in ion beams. Similar to relative biological effectiveness, most dosimeters exhibit changes in relative efficiency (quenching) when exposed to ion beams. In track-structure theory, 1-hit dosimeters with high dose sensitivity exhaust their sensitive elements faster than less sensitive dosimeters, and are therefore expected to saturate at lower doses. We have measured the saturation dose for a 3D silicone-based radiochromic dosimeter, at a fixed sensitive element concentration, for three chemical compositions that display different sensitivity and quenching in proton beams. The long-term goal of this work was to develop a model allowing predictions of the dosimeter response, in order to facilitate its use for clinical proton therapy delivery validation. M&M Three batches of cuvette-sized dosimeters were produced with 0.26% leuco-malachite green dye and curing agent (CA) ratios of: 5%, 9% and 11%. They were irradiated with 60MeV protons with entrance doses up to 30Gy, and with a Co-60 source up to 110kGy. The optical density change was measured in a laser scanner for the proton irradiations (depth-dose profiles) and in a spectrophotometer for the Co-60-irradiations. Quenching in the Bragg peak was evaluated using the peak-to-plateau ratio (PPR). Results The linear dose response for protons was highest for 5% CA, while it was 49% lower for 9% CA and 62% lower for 11% CA. The PPR was 4.3 for the ionization chamber, while at 30Gy (entrance dose) it was 2.6 for 5% CA, 3.6 for 9% CA and 4.0 for 11% CA. The dose response in photon beams saturated at approximately 2kGy for all three CA concentrations. Bleaching was observed at 110kGy. Conclusions The CA concentration influences the quenching in proton beams, but does not affect the Co-60 saturation dose significantly. This could potentially be used to develop a linear energy transfer-sensitive detector.

Poster #24

Jeppe Brage Christensen, Roskilde, Denmark

On the potential of proton dosimetry using Cerenkov radiation in optical fibers

Christensen JB and Andersen CE. Technical University of Denmark, Center for Nuclear Technologies, Roskilde, Denmark.

Introduction Fiber-coupled dosimetry with organic scintillators is known to exhibit a nonlinear response to high-LET beams, termed ionization quenching. Although corrections can be applied using Birks' formula, such procedures are cumbersome and require prior knowledge of the beam hitting the detector. Materials and methods One possible way to circumvent the ionization quenching is to exploit Cerenkov light produced in optical fiber cables. The distribution of emitted Cerenkov photons as a function of depth correlates well with the depth-dose profile for electron beams, whereas the agreement is less clear in a proton beam. Nonetheless, excellent experimental agreements between the Cerenkov radiation and dose distributions have been reported in both electron and proton beams. This work investigates the Cerenkov profiles in electron and proton beams with a model in Geant4, which has been validated in an electron beam. Results Geant4-modelling of the creation and guidance of the Cerenkov photons in optical fibers show an excellent agreement with measurements conducted with 20 MeV electrons. The experimentally validated Monte Carlo code is subsequently used to investigate the Cerenkov photon distribution in a proton beam, where especially the angular dependence of the secondary electrons is crucial. The results indicate, that Cerenkov radiation in a proton beam may be difficult to relate to the dose-profile since the majority of the Cerenkov photons arise from scattered secondary electrons. Conclusions The Cerenkov light in optical fibers can be used to measure the depth profile of electron beams. However, the situation is more subtle in proton beams, where the orientation of the Cerenkov photons are more randomly distributed than in electron beams. Furthermore, the Cerenkov light signal in optical fibers exposed to a proton beam may be suppressed by fluorescence which challenges measurements.

Poster #25

Thomas Henry, Stockholm, Sweden

Proton grid therapy (PGT) with mm-wide beam elements: a Monte-Carlo simulation study

Henry T, Ureba A, Tsubouchi T, Valdman A, Bassler N, Siegbahn A. Department of Physics, Stockholm University, Stockholm, Sweden / Department of Oncology and Pathology, Karolinska University Hospital, Stockholm, Sweden / Department of Radiation Oncology, Osaka University, Osaka, Japan.

Purpose: Grid therapy has in the past normally been performed with photon-beam grids, incident from one direction. With this setup, a distribution of alternating high (peak) and low (valley) doses is produced in the target volume. In an ongoing research project, we are investigating the possibility to create more uniform target volume doses in grid therapy, by crossfiring grids of mm-sized proton-beam elements over the target volume. Methods: Dose distributions for circular and elongated proton-beam elements, 0.5-3 mm wide (FWHM), were simulated in a 200x200x200 mm3 water phantom for different beam energies (70-230 MeV). The Monte-Carlo (MC) simulations were performed with the MC code TOPAS. Depth-dose curves, transversal dose profiles and lateral penumbras for the different beam widths were determined. The dose distributions produced by proton-beam grids were simulated, using the single-beam data. The dose distributions produced when crossfiring the target volume with interlaced grids were thereafter evaluated. Results: The relative increase of the beam width with depth was largest for the smallest beams. The Bragg peak to entrance dose ratios were reduced when the beam-element size was decreased and when the beam energy increased. With the interlaced crossfiring setup, acceptable dose coverage of the cubic target volume was obtained. The need to select a beam-element center-to-center distance which provides a suitable trade-off between a high target- to entrance-dose ratio, target-dose uniformity and a low valley dose in the normal tissue was identified. Conclusions: A nearly homogeneous dose distribution can be obtained in the target volume by crossfiring grids of millimeter-wide proton-beam elements, while maintaining the grid structure of the dose distribution at large depths in the normal tissue, close to the target volume.

Poster #26

Gracinda Mondlane, Stockholm, Sweden

Evaluation of TCP and NTCP after radiosurgery of liver metastases with photon- or scanned proton-beams

Mondlane G1,2; Gubanski M3; Lind PA3,4; Ureba A1, Siegbahn A1. 1Department of Physics – Medical Radiation Physics, Stockholm University, Stockholm, Sweden; 2Department of Physics, Universidade Eduardo Mondlane, Maputo, Mozambique; 3Department of Oncology and Pathology, Karolinska University Hospital, Stockholm, Sweden.

Introduction: Proton-beam therapy provides the potential to reduce the irradiation of healthy tissues, compared to radiotherapy performed with photon beams. However, side effects after radiotherapy will still appear. The aim of this study was to estimate the TCP and the NTCP after photon- or proton-beam based radiosurgery of liver metastases. Materials and methods: Ten patients diagnosed with colorectal liver metastases, previously treated with photon-beam stereotactic body radiation therapy (SBRT), were retrospectively planned with intensity-modulated proton therapy (IMPT), using a two-field configuration. The TCP was assessed using the Poisson model. The NTCP was calculated using two distinct radiobiological models, the Lyman-Kutcher-Burman (LKB) model and the relative seriality model (s-model). The following OARs were considered: healthy part of the liver, skin, lungs, esophagus, spinal cord and right kidney. The dose per fraction was converted to equivalent 2-Gy per-fraction schemes using the LQ-model. A relative biological effectiveness of 1.1 was assumed for the proton-beams. The results were compared pairwise with a two-sided Wilcoxon signed-rank test with significance level of 0.05. Results: TCPs of 100 % were obtained for all patients with both the SBRT- and IMPT-plans. An NTCP of 100 % was obtained for the healthy part of the liver with both the SBRT- and IMPT-plans ($p = 0.38$), using the LKB-model. With the s-model, NTCP of 71 % (SBRT-plans) and 87 % (IMPT-plans) ($p = 1.0$) were obtained for the healthy part of the liver. For the skin, NTCP of 2 % (SBRT-plans) and 1 % (IMPT-plans) were obtained with LKB-model ($p = 0.64$). With the s-model, an NTCP value of 1 % was calculated for both the SBRT and IMPT plans ($p = 0.25$). For the remaining OARs, NTCP values of 0 % were obtained for both the LKB- and s-model ($p < 0.05$). Conclusions: Similar TCP- and NTCP-values were estimated for liver-metastases patients planned for radiosurgery with either IMPT or photon-SBRT.

Poster #27

Camilla Hanquist Stokkevåg, Bergen, Norway

Normal tissue sparing in very young children treated with proton therapy

Stokkevåg CH, Ugland M, Nordberg T, Engeseth GM, Brydøy M, Muren LP. 1 Department of Oncology and Medical Physics, Haukeland University Hospital, Bergen, Norway. 2 Department of Medical Physics, Aarhus University / Aarhus University Hospital, Aarhus, Denmark.

Purpose: Very young children are at particular risk of radiation-induced morbidity and are therefore routinely referred to proton therapy (PT), aiming at reducing doses to healthy tissues. To investigate the actual gain of referring these young patients to PT we have compared the delivered PT plans to contemporary photon-based radiotherapy (XT) available locally. Methods: Six patients aged four years or younger treated at external PT facilities were included. Four patients with ependymoma received post-operative PT (54 GyRBE) delivered by three passive modulation fields while two patients with neuroblastoma (spine and neck; 21 GyRBE) were treated with two-three posterior passive modulation fields. The original CT-scans and contours were used to re-plan the patients using state-of-art XT (IMRT/VMAT). Doses to between 15 and 30 contoured organs were analysed for each patient. Results: PT reduced the volumes that received low doses compared to the XT re-plans; e.g. the volume receiving 5 Gy or higher was 22-52% lower with PT. For most organs distant from the tumour volumes close to no dose was reported from PT. For organs closer to the tumour, the doses were more comparable and favoured either PT or XT depending on the specific treatment plan. For ependymoma, 3/4 patients received a mean dose (Dm) >5 GyRBE to one or more of the hippocampal heads; this was also seen for the re-planned XT. All patients except one received well below 30 GyRBE to the mastoids, cochleas and nasopharynx, but with lower doses from the delivered PT plans compared to the XT re-plans (XT Dm up to ten times higher). The neuroblastoma patients received lower Dm to the heart and lungs compared to XT. Conclusions: Low dose volumes were shown to be reduced with the delivered PT plans compared to XT re-plans, while for the volumes close to the tumour the doses were comparable. Depending on tumour location and the specific treatment plan, intermediate and high-dose volumes did not always favour PT.

Poster #28

Laura Toussaint, Aarhus, Denmark

Doses to brain structures associated with cognitive impairment following radiotherapy of paediatric CNS tumours with contemporary photon vs. proton techniques

Toussaint L (1), Lassen-Ramshad Y (2), Stokkevåg CH (3), Petersen JBB (1), Vestegaard A (1), Schrøder H (4), Høyer M (2), Indelicato DJ (5), Muren LP (1). 1 Department of Medical Physics, Aarhus University Hospital, Aarhus, Denmark 2 Department of Oncology, Aarhus University Hospital, Aarhus, Denmark 3 Department of Oncology and Medical Physics, Haukeland University Hospital, Bergen, Norway 4 Department of Paediatrics and Adolescent Medicine, Aarhus University Hospital, Aarhus, Denmark.

Introduction: Cognitive impairment after radiotherapy (RT) of paediatric brain tumours can be a devastating condition. Several brain structures have been associated to cognition, but their radiation dose/volume effects are unclear. Proton therapy (PT) is promising to preserve cognitive function. Planning of both photon-based RT and PT often focus on sparing critical structures such as the brainstem through beam angle selection. However the implications of such beam selections on doses to cognitive structures have not yet been investigated. The aim of this study was therefore to investigate the doses delivered to brain structures associated with cognitive impairment for photon vs PT. Materials and methods: CT and MR scans of a pediatric patient with a posterior fossa tumour were used to contour brain structures related to cognition. Volumetric modulated arc therapy (VMAT), intensity-modulated RT (IMRT) and two intensity-modulated PT (IMPT) plans (two oblique fields; two oblique plus a vertex field) were generated (prescribed dose 59.4Gy(RBE)). For each structure we compared the fraction of volume receiving low (10Gy), intermediate (40Gy) and high-doses (60Gy) based on a published model for cognitive impairment. Results: All plans had comparable target coverage. Compared to VMAT and IMRT, IMPT reduced the irradiated volumes of the investigated brain structures. IMPT avoided in particular the large low-dose volumes compared to VMAT/IMRT whereas the volumes receiving intermediate and high doses were similar for protons and photons. E.g. the volume fraction of the right hippocampus receiving at least 10Gy was 80% for IMRT, 81% for VMAT, 35% for IMPT and 44% for IMPT with a vertex field. Conclusion: Compared to photon techniques, IMPT for posterior fossa tumours can reduce the dose to brain structures critical to cognitive development. Better dose-effect models of cognitive impairment including brain subsites are needed to take full advantage of the potential of IMPT.

Poster #29

Charlotte Espensen, Copenhagen, Denmark

Ruthenium-106 brachytherapy and proton therapy for uveal melanomas: Biologically Effective Dose for tumour and organs at risk from comparative dose planning

Espensen CA (1,2), Thariat J (3), Kiilgaard JF (2), Herault J (3), Aznar MC (4), Caujolle J-P (5), Maschi C (5), Fog LS (1), Appelt AL (6,1). 1) Department of Oncology, Section of Radiotherapy, Rigshospitalet, Copenhagen, Denmark 2) Department of Ophthalmology, Rigshospitalet, Copenhagen, Denmark 3) Department of Radiation Oncology, Centre Antoine-Lacassagne, Nice, France 4) Nuffield Department.

Introduction Eye-preserving radiotherapy with proton therapy (PT) and Ruthenium-106 brachytherapy (BT) are commonly used primary treatments for uveal melanomas (UM). The two techniques have rarely been compared directly for individual patients. We present the results of a comparative dose planning study, estimating biologically effective doses (BED) to tumour, macula and optic disc (OD). Materials and methods 33 consecutive UM patients suitable for both PT and BT were selected for the study. Dual PT and BT planning were carried out for each patient, using EyePlanTM for PT and Plaque SimulatorTM for BT. PT dose planning aimed to deliver homogeneous dose (52 Gy in 4 fractions) to the entire tumour with a 2.5 mm margin. BT dose was heterogeneous, with prescribed dose (100 Gy) to tumour apex. Both planning techniques minimized doses to macula and OD. BED was calculated using well-established models; Holloway & Dale 2013 for PT and Joiner 2009 for BT, with literature-based assumptions for relevant parameters. Wilcoxon signed-rank test was used to evaluate differences in BED. Results Median tumour height was 4 mm(interquartile range: 3-5); median treatment time for BT was 69 hours(54-126). Minimum tumour BED (BED99%) and BED50% were both higher for BT, with median 128 Gy for PT compared to 172 Gy(146-180), and 128 Gy compared to 468 Gy(412-537), both with $p<0.0001$. Median differences in mean physical dose (Dmean) and BEDmean to macula between BT and PT were 49 Gy(13-173, $p<0.0001$) and 66 Gy(15-1023, $p<0.0001$), respectively. Median differences in maximum physical dose (D1%) and BED1% to OD were 22 Gy(7-41, $p<0.0001$) and 9 Gy(-161-88, $p=1$), respectively. Conclusions were sensitive to choice of model parameters, although mainly for changes in repair half times. Conclusions Ru-106 brachytherapy and proton therapy for uveal melanomas result in different BED to the tumour and differential sparing of macula, with BT delivering higher BED. BED to the optic disc was comparable.

Poster discussion group 6

Poster #30

Evelyn de Jong, Maastricht, Netherlands

Quality assessment of [18F]FDG PET scans of the NVALT12 imaging sub-study: Recommendations for future multicenter PET trials

de Jong E.E.C., van Elmpt W., Hoekstra O.S., Groen H.J.M., Smit E.F., Boellaard R., Lambin P., Dingemans A.-M.C. Radiation Oncology and Pulmonology, Maastricht, Netherlands; Nuclear Medicine, Pulmonary Diseases and Thoracic Oncology, Amsterdam, Netherlands; Pulmonary Diseases and Nuclear Medicine, Groningen, Netherlands.

Introduction Standardization protocols and guidelines for FDG-PET in multicenter trials are available, despite a large variability in image acquisition and reconstruction parameters exist. In this study, we investigated the compliance of FDG-PET scans to the guidelines of the European Association of Nuclear Medicine (EANM) for tumour imaging version 1.0. From these results, we provide recommendations for future multicenter studies using FDG-PET. Materials and Methods Patients included in a multicenter randomized phase II study, had repeated [18F]FDG PET scans for early response assessment. Relevant acquisition and reconstruction parameters were extracted from the DICOM header of the images. The FDG-PET image parameters were compared to the by the EANM recommended parameters. Results From the 223 included patients, 167 baseline scans and 118 response scans were available from 15 hospitals. Scans of 19% of the patients had an uptake time that full filled the Uniform Protocols for Imaging in Clinical Trials response assessment criteria. Scans performed on Siemens or GE scanners had less missing parameters, but a larger variability in reconstruction methods existed compared to scans performed on Philips scanners. The average quality score over all hospitals was 69%, which means that on average more than two third of the image parameters were EANM guideline compliant. Scans with a non-compliant uptake time had a larger standard deviation of SUVmean of the liver than scans with compliant uptake times. Conclusion Although a standardization protocol was agreed on, there was a large variability in imaging parameters which potentially influences analysis of multicenter imaging studies. For future multicenter studies including FDG-PET imaging, the input of local nuclear medicine experts is of utmost importance. Furthermore, a prospective central quality review during patient inclusion is needed to improve compliance with image standardization protocols as defined by EANM.

Poster #31

Marta Lazzeroni, Stockholm, Sweden

Evaluation of third treatment week as temporal window for assessing responsiveness on repeated FDG-PET scans in NSCLC patients

Lazzeroni M (1), Uhrdin J (2), Carvalho S (3), van Elmpt W (3), Lambin P (3), Dasu A (4), Toma-Dasu I (1,5). (1) Oncology-Pathology Dept., Karolinska Institutet, Stockholm, Sweden; (2) RaySearch Laboratories AB, Stockholm, Sweden; (3) Dept. of Radiation Oncology, GROW-School for Oncology and Developmental Biology, Maastricht University Medical Center, Maastricht.

Early assessment of tumour response to treatment with repeated FDG-PET imaging has potential for treatment adaptation, but it is still unclear what the optimal window for this evaluation is. Previous studies indicate that mean SUV and the effective radiosensitivity (αeff) are predictive of 2-year overall survival (OS) when imaging is performed before and during the second week of radiotherapy. This study aims to investigate if multiple PET-derived quantities during the third week are also able to predict the response. Twenty-eight non-small cell lung cancer patients were imaged with FDG-PET before the treatment and during the third week of radiotherapy. 45 Gy in 1.5 Gy fractions were delivered twice-daily followed by a dose-escalation up to 69 Gy in daily 2 Gy fractions. Mean and max SUVs in the first and second PET scan as well as their difference, together with tumour volume were determined for the primary GTV. αeff, accounting for the accumulated dose at the time of the second PET scan and variations in the FDG uptake, was also determined. Correlations were sought between different PET-derived quantities and the OS using ROC analysis. The ROC analysis indicated lack of correlation between the difference in mean and max SUVs of the first and second PET scan (AUC=0.6 and 0.5, respectively) as well as average αeff (AUC=0.5, p=0.7) and the negative fraction of αeff (AUC=0.5, p=0.8) and OS. None of the other quantities (mean, max SUV, tumour volume) was of relevance for outcome prediction purposes. The lack of correlation between the determined quantities from repeated FDG PET images and OS indicate that the third week of treatment might not be as suitable for assessing the responsiveness to treatment as the images taken during the second week, but validation on a larger dataset is warranted. Comparatively, the second week after the start of the treatment appears to be a better time window for response assessment.

Poster #32

Aniek Even, Maastricht, The Netherlands

Predicting hypoxia in non-small cell lung cancer: combining CT, FDG PET and dynamic-constrast enhanced CT parameters

A.J.G. Even(1), B. Reymen(1), Matt D. La Fontaine(2), M. Das(3), A. Jochems(1), P. Lambin(1), W. van Elmpt(1). (1)Department of Radiation Oncology (MAASTRO), GROW – School for Oncology and Developmental Biology, Maastricht University Medical Center, Maastricht, the Netherlands; (2)Department of Radiation Oncology, The Netherlands Cancer Institute, Amsterdam, the Netherlands.

Introduction Most solid tumors contain inadequately oxygenated regions. These hypoxic areas are more aggressive and treatment resistant. Hypoxia PET allows visualization of hypoxia and may enable treatment adaptation. However, hypoxia PET is not widely available, expensive and time-consuming. We aimed to predict hypoxia levels in non-small cell lung cancer (NSCLC) using more easily available imaging, FDG PET/CT and dynamic-contrast CT (DCE-CT). Materials and methods For 34 NSCLC patients, included in 2 trials, a hypoxia HX4 PET/CT, planning FDG PET/CT, and DCE-CT were acquired before radiotherapy. All scans were non-rigidly registered to the planning CT. Tumor blood flow (BF) and blood volume (BV) were calculated by kinetic analysis on DCE-CT. Within the gross tumor volume, independent clusters, i.e. supervoxels, were created based on FDG PET/CT (Achanta, 2012). For each supervoxel, tumor-to-background ratios (TBR) were calculated (median SUV / aorta SUVmean) for HX4 PET/CT and supervoxel features (median, SD, entropy) for the other modalities. A random forest (cross-validated: 10 folds, 5 repeats) was trained to predict TBR based on CT, FDG, BF and BV features. Patients were split in a training (trial NCT01024829) and independent test set (trial NCT01210378). For each patient, predicted and observed hypoxic volumes (TBR>1.2) were compared. Results 15 patients (3291 supervoxels) were used for training and 18 patients (1502 supervoxels) to validate the model. TBR root-mean-square error (RMSE) was 0.19±0.01 for training and 0.28 for testing. 17/18 tumors of the test set were correctly classified as normoxic or hypoxic (hypoxic volume>1cm3). Hypoxic volumes were 10.8±18.8cm3 based on hypoxia PET/CT and 7.4±9.9cm3 for our predictions. Conclusion We created a random forest that allows prediction of hypoxia using CT, FDG PET and DCE-CT features in NSCLC. The model correctly classifies almost all tumors and could therefore aid hypoxia based patient stratification.

Poster #33

Ingvild Støen, Oslo, Norway

Optimal threshold for PET-based autocontouring of boost volume for radiotherapy of anal carcinoma

Støen I, Rusten E, Rekstad B, Undseth C, Al-Haidari G, Hellebust TP, Guren MG, Malinen E. Oslo University Hospital / University of Oslo, Oslo, Norway.

Introduction For patients with anal carcinoma (AC), the glucose-avid tumor volume reflected in 18F- fluorodeoxyglucose PET (FDG-PET) may be an attractive boost volume (BV) for radiotherapy (RT) dose escalation in order to improve local control. The purpose was to use a thresholding procedure to identify the optimal threshold to automatically extract the BV from FDG-PET images. Materials and methods Nineteen patients with AC referred to chemoradiotherapy were prospectively included. FDG-PET/CT was done prior to RT. Three oncologists manually delineated the gross tumor volume (GTV) and the FDG-avid BV. For autocontouring within GTV, a volume BV_T based on a percentage threshold of SUVmax or SUVpeak was generated. The percentage threshold was varied systematically. The similarity between delineated and thresholded volumes was estimated by Dice similarity coefficient (DSC). Interobserver variability was included for comparison. Statistical tests were done by Wilcoxon signed rank test and Mann-Whitney U test. Results The maximal DSC was found at thresholds of 17.5% and 22.5 % for SUVmax and SUVpeak, respectively. At these thresholds, the DSC median and range was 0.62 (0.18, 0.87) and 0.67 (0.23, 0.89), respectively. The increase in DSC for peak-based compared to max-based thresholding was significant ($P<0.001$). In comparison, the inter-observer variability in manual volume delineation was 0.68 (0.30, 0.86). For peak-based thresholding, the DSCs for small (< 12 cc) lesions were significantly lower than DSCs for large (>12 cc) lesions (median DSCs were 0.57 vs 0.73; $P<0.001$). Conclusions The optimal threshold for autocontouring of the PET-based BV is 22.5 % of SUVpeak. This procedure causes a variability comparable to inter-observer variability in manual delineation. The performance of the thresholding was less optimal for small lesions, but these are not expected to be candidates for dose escalation.

Poster #34

Espen Rusten, Oslo, Norway

The prognostic value of FDG-PET uptake parameters in anal cancer

E. Rusten1,2, C. Undseth3, J.E. Holtedahl4, E. Hernes4, M. Guren3,5, E. Malinen1,2. 1Department of Physics, University of Oslo, Oslo, Norway. 2Department of Medical Physics / 3Department of Oncology/ 4Department of Radiology and Nuclear Medicine / 5K.G. Jebsen Colorectal Cancer Research Centre, Oslo University Hospital, Oslo, Norway.

Purpose: For anal cancer (AC) varying results have been reported for FluoroDeoxyGlucose Positron Emission Tomography (FDG-PET) imaging biomarkers. The current study evaluated the prognostic value of pre- and mid-radiotherapy FDG-PET uptake parameters, such as such as the maximum of the Standardized Uptake Value (SUVmax) and Metabolic Tumor Volume (MTV), combined with clinical factors. Materials and Methods: Eighty-eight patients with AC referred to chemoradiotherapy were prospectively included. Patients underwent a FDG-PET/CT scan prior to (n=88) and two weeks into (n=39) therapy. Regular follow-up for relapse was performed at 3-6 month intervals. Prognostic classifiers were constructed by dividing patients in high risk (20 %) and low risk (80 %) groups. The following parameters were evaluated: SUVmax, SUVPeak, MTV, Total Lesion Glycolysis (TLG), Gross Tumor Volume (GTV), T/N stage and gender. Also, a Z-normalized classifier SUVzpm combining MTV and SUVpeak was constructed a priori. Univariate and bivariate Cox regression was used to assess the prognostic impact of the classifiers. Results: In univariate analysis, N-stage(>2), gender(male), GTV(>177cm3), MTV(>23cm3), TLG(>266cm3) and SUVzpm were significant classifiers ($p<0.05$). TLG ($p=0.001$, HR = 5.8) and SUVzpm ($p=0.002$, HR = 5.5) showed the strongest association with outcome. In bivariate analysis, gender combined with TLG or SUVzpm gave even stronger classifiers ($p < 0.0005$). For PET two weeks into therapy, MTV was on average reduced by 50% and the SUVpeak decreased by 33%, but the prognostic values remained unchanged when including this information in the PET classifiers. Conclusions: Volumetric PET measures (MTV and TLG) were prognostic in the current cohort, while the intensity-based SUV values were not. The prognostic impact of neither TLG nor SUVzpm was improved by the mid therapy scans, though both were improved by including gender in the classifiers and together they represented the best classifiers.

Poster #35

Mette Marie Fode, Aarhus, Denmark

Functional treatment planning using 2[18F]fluoro-2-deoxy-D-galactose PET/CT for stereotactic body radiotherapy of liver metastases – a phase I study

1:Fode MM; 3,4:Bak-Fredslund K; 2:Petersen JB; 2:Worm E; 3,4:Sørensen M and 5:Høyer M. 1:Department of Oncology; 2:Department of Medical Physics; 3:Department of Nuclear Medicine & PET Centre, 4:Department of Hepatology & Gastroenterology; 5:Danish Centre for Particle Therapy. Aarhus University Hospital, Denmark.

Introduction: 2[18F]fluoro-2-deoxy-D-galactose (FDGal), a hepatocyte-specific positron emission tomography (PET) tracer was used for functional treatment planning (FTP) in stereotactic body radiotherapy (SBRT) of liver metastases with the aim to minimize the radiation dose to the sub-volumes of best functioning liver tissue. Materials and methods: Fourteen patients were referred for SBRT for liver metastases. Eight patients had previously had surgical resection, radiofrequency ablation or SBRT for liver metastases. FDGal PET/CT was performed before and one month after SBRT. The sub-volume of liver tissue with the 10% (± 10%) highest values of SUV was defined as V'~10%. V'~20% was denoted as the sub-volume of 20% (± 10%) liver tissue, etc. CTV was subtracted from the sub-volumes and the contours were transferred to the planning CT scan using deformable co-registration. These sub-volumes were used in the optimization of the intensity modulated radiotherapy (IMRT) plans. The prescribed Dmean to the CTV was 45 - 60 Gy in 3 - 6 fractions with CTV enclosed by 95% and the PTV by the 67% isodose. Results: In general the treatment was well tolerated. One patient developed grade 2 increase in fatigue, but no severe acute morbidity was observed. The mean doses (Dmean) to the sub-volumes, of the best functioning liver tissue in the FTPs were 8.6 Gy (D~10%), 8.5 Gy (D~20%), and 8.2 Gy (D~30%) and Dmean to the liver was 10.4 Gy. A linear dose-dependent reduction in FDGal uptake was observed in irradiated liver. The hepatic metabolic function was reduced by 12% for each 10 Gy increase in radiation dose. The 50% reduction in hepatic metabolic function (D50%) was observed at 22.9 Gy (CI 95%: 16.7 - 30.4 Gy) in three fractions. Conclusions: This phase I study demonstrates the feasibility for FTP in patients with liver metastases. The average reduction in Dmean to the sub-volumes of best functioning liver tissue was 1.8 Gy in V~10%, 1.9 Gy in V~20% and 2.2 Gy in V~30%.

Poster #36

Azadeh Abravan, Oslo, Norway

PET based evaluation of lung toxicity after radiotherapy- Assessment of two approaches for dose response evaluation

Abravan Azadeh1,2. Knudtsen Ingerid1,2. Eide Hanne3,4. Helland Åslaug3,4. van Luijk Peter5,6. Malinen Eirik1,2. Department of Physics, University of Oslo, Norway 2Department of Medical Physics, Oslo University Hospital, Norway 3Department of Oncology, Oslo University Hospital, Norway 4Institute for Cancer Research, Oslo University Hospital, Oslo, Norway 5 Departmen.

Introduction: Patients with lung cancer given external radiotherapy (RT) are at risk of radiation induced alternation in the lung. Mean density changes from CT (in Hounsfield units) may be used to assess such alterations. However, a combination of mean density changes from CT scans with corresponding standard deviations has been shown to be a more sensitive method. In the current work, we investigated whether such a combined approach is feasible for 18F-FDG PET data as well. Methods: 15 patients with lung cancer undergoing fractionated RT (10×3 Gy) were examined by 18F-FDG-PET/CT at three sessions and the lung was delineated in the planning CT images. The RT dose matrix was co-registered with the PET images. For each PET image series, mean (μ) and standard deviation (σ) map were calculated based on cubes in the lung (3×3×3 voxels) and were used to quantify local structure (S). The spread in μ and σ was characterized by a covariance ellipse (in pre-therapy PET series) in a sub-volume of 3×3×3 cubes. Mahalanobis distance is used to measure the distance of individual cube values to the origin of the ellipse and to further form S maps. ΔS and Δμ maps are calculated by subtracting pre-therapy maps from maps of mid- and post-therapy. Results: The structure difference maps (ΔS) identified new areas of interest in the lungs compared to the mean difference maps (Δμ). 18F-FDG dose response was analyzed up to total dose of 15 Gy by first order linear regression. The relative slopes of the regression lines were 0.036, 0.018, 0.052, and 0.061 for Δμ (mid-pre), ΔS (mid-pre), Δμ (post-pre), and ΔS (post-pre), respectively. A significant dose response was only seen for ΔS taken between post- and pre-therapy PET. Conclusion: The new method using local structures in 18F-FDG PET images visualizes new region of interest and providing a clearer 18F-FDG uptake dose response six weeks post RT and may be valuable in future studies addressing lung toxicity.

Poster #37

Tine Bisballe Nyeng, Aarhus, Denmark

Comparing functional lung volumes obtained by using 2 different methods: Do perfusion SPECT and 4D-CT ventilation maps define the same voxels in lung cancer treatment?

Nyeng TB 1, Hoffmann L 1, Farr KP 2, Khalil AA 2, Grau C 2 and Møller DS 1. 1 Department of Medical Physics, Aarhus University Hospital, 2 Department of Oncology, Aarhus University Hospital.

Introduction: Radiotherapy (RT) of lung cancer is often associated with severe radiation pneumonitis (RP). Former studies indicate that the RP incidence is associated with the dose to the functional lung (FL), either obtained from perfusion (Q) SPECT or from 4D-CT deformable registration ventilation maps. This study compares the FL volumes obtained by the two methods. Materials and methods: Ten patients receiving RT for non-small cell lung cancer (NSCLC) had a pre-treatment Q-SPECT and 4D-CT scan. The FL volume from Q-SPECT, VFL-SPECT, was defined as the voxels within the total lung volume (VLTot) with values exceeding a threshold of 40% of the maximum perfusion count. The ventilation based FL volumes were obtained from the 4D-CT scans by deformable registration of the exhale to the inhale phase. The expansion was identified as values of the Jacobian determinant of the deformation vector field (JDVF) above 1. The FL volume from the 4D-CT registration was defined as the voxels with JDVF > 15% of the maximum JDVF, resulting in volumes comparable in size to the Q-SPECT FL volumes. Overlap fractions, defined as ((VFL-SPECT∩VFL-4Dvent)/Min[VFL-SPECT,VFL-4Dvent]), were calculated between the two FL volumes. Results: FL volumes of the ten patients defined by Q-SPECT and 4D-CT ventilation maps were comparable in size, with a median[range] of 1256cm3[989-2340] and 1191cm3[1060-1858], respectively. The median overlap fraction of the FL volumes was 55%[34-65]. The median overlapping volume, i.e. the volume defined as FL by both methods, was 19%[6-24] of the VLTot. The union of the two types of FL volumes corresponded to a median 55%[34-63] of VLTot. Conclusions: The FL volumes obtained by the two methods are only partly overlapping, though both are shown to predict RP outcome. Before incorporating FL avoidance into treatment planning for NSCLC, a thorough investigation of the combination of Q-SPECT and 4D-CT ventilation map FL volumes most predictive of RP is required.

Poster discussion group 7

Poster #38

Kristina Giske, Heidelberg, Germany

In-silico patient models: beyond contour propagation in radiation therapy

Giske K(1,2), Stoll M(1,2), Teske H(1,2), Bartelheimer K(1,2), Kirchhof S(1,2), Debus J(2,3), Bendl R(1,2,4). (1) Division of Medical Physics in Radiation Oncology, German Cancer Research Center (DKFZ), Heidelberg; (2) National Center for Radiation Research in Oncology (NCRO), Heidelberg Institute for Radiation Oncology (HIRO); (3) Department of Radiation Oncolog.

Introduction: Modern radiotherapy, using photons or particles, requires precise localization of anatomical structures for assignment of various tissue properties in the patient anatomy. Integrated imaging modalities, ranging from optical surface imaging, fluoroscopy, CBCT to MRI, allow visualizing more information of patient anatomy. Image processing algorithms are getting better at measuring anatomical changes, propagating contours throughout the treatment course or merging multi-modality scans at different time points. Yet, imaging quality, artefacts, constraints in patient positioning and fixation, and limited availability of fast 3D or 4D imaging pose considerable challenges for segmentation and registration to meet the requirements for spatial accuracy. Materials and methods: Based on daily images of head and neck region (CBCTs) and pelvic region (MRI), we demonstrate the application of in-silico bio-mechanically regularized and multi-parametric patient models to master anatomical changes and lay the foundations for 4D dynamic biological process descriptions. Results: Once established, the specific patient model is used to fit data like a surface point cloud e.g. acquired by time-of-flight cameras, volumetric images like CT or CBCT and MRI scans, with the promise to sample pseudo CTs or augment organ segmentation. Statistical distributions over patient-fitted instances of a cohort allow predicting most likely anatomical changes for a new patient at the planning stage. Information from images of complimentary modalities can be merged even if imaging posture considerably deviates from the planning position like e.g. arms up and arms down. Conclusions: In-silico patient models have reached maturity regarding image based anatomical change estimation. Next steps need to be directed towards including more data from functional and follow-up images to enrich the in-silico patient with statistical properties on tumor spread tendency and treatment response.

Poster #39

Anne Holm, Aarhus, Dk

Carotid sparring intensity modulated radiotherapy for early laryngeal glottis cancer; What is clinically achievable?

Holm, A.I.S.(a), Jensen K.(b), Elstrøm, U.V.(a). (a) Medical Physics, Aarhus University Hospital, Denmark, (b) Department of Oncology, Aarhus University Hospital, Denmark.

Introduction In radiotherapy of early larynxcancer, the irradiated volume, typically includes the carotid arteries, and side effects may include endothelial injury and subsequent risk of stroke or transient ischemic attack. This study explores the feasibility of a PTV margin reduction, when the daily CBCT match is changed from a bony match to a soft tissue match. Moreover, the dosimetric advantages of a margin reduction were estimated. Materials/methods Nine patients, treated in our clinic were included in this study. All patients received 66 Gy in 33 fractions with daily CBCT bone match. The Clinical Target Volume (CTV), defined on the planning CT, was transferred to each CBCT after deformable registration of the two scans. The CTV-of-the-day was then transferred to the planning CT either via the 4D rigid bony match or a 4D rigid match on the CTV contour. Irradiated Volumes (IVs) were generated as the sum of all the rigidly transferred CTVs and the coverage for these were extracted. An acceptance criterion for IV coverage of V95%>98 % were used to evaluate the two match strategies. Treatments plans for transverse PTV margins of 3mm and 5mm were made and for comparable target coverage, near-max doses of the carotid arteries and the spinal cord have been compared. Results The ITV coverage's for a 3mm PTV margin were unacceptable in two cases using the bone match, whereas the soft tissue match yielded an acceptable IV coverage for all patients. Thus, a reduction of the PTV margin is feasible, by a change in the clinical setup strategy. Reducing the PTV margin, decreases the near-max right/left carotid doses from 53±11 Gy/56±11 Gy to 40±14 Gy/39±9 Gy (mean dose±SD). Conclusion The transverse PTV margin can be reduced without introducing a geometrical target miss by changing the setup method in the clinic. This margin reduction leads to a substantial dose reduction for the carotid arteries.

Poster #40

Lone Hoffmann, Aarhus, Denmark

Anatomical changes in advanced lung cancer patients occurring during RT can be predicted from pre-treatment characteristics.

Lone Hoffmann1, Azza A. Khalil1, Marianne M. Knap1, Markus Alber2 and Ditte Sloth Møller1. 1 Department of Oncology, Aarhus University Hospital, Aarhus, Denmark; 2 Department of Radiation Oncology, Heidelberg University Hospital, Heidelberg, Germany.

Introduction: Anatomical changes prompt adaptive radiotherapy (ART) for a large number of lung cancer patients in order to avoid target under dosage. However, this costs additional work load. We investigated the correlation between patient characteristics before RT and anatomical changes during RT in order to identify the patients eligible for ART. Material/methods: A decision support protocol for ART was used for treatment of 165 lung cancer patients. Patient setup on the primary tumour (T) was based on daily CBCTs. Deviations in T >2mm, lymph nodes (N) >5mm or changes in atelectasis (A) triggered replanning. The daily CBCTs were reviewed to score changes above trigger limit in T or N position, changes in A, or T/N shrinkage >1cm. Correlations to pre-treatment patient characteristics were found using a Fisher's exact test for comparison. Results: 53 patients (32%) were adapted due to changes in A (8%), T (6%), N (15%) or T+N (3%). A was seen at planningCT in 50 patients (30%) and in 12 patients (7%), A appeared during RT. Presence of A before RT was not significantly correlated with replanning. Changes in A during RT increased the probability of replanning (p=0.03). A within 5mm of T or N was significant (p=0.01). Patients with T0 or N0 had a low risk of replanning (p=0.01, p=0.03) while N volume >30cm3 had a high risk (p=0.02). No correlation was found for T location, T size, T/N shrinkage, or histology. The imaging rate may be decreased for patients with T0 and no A, as none of these were adapted. For patients with N0 and no A, only 11%, were replanned. On the contrary, 60% of the patients with A and N volume>30cm3 were replanned. Conclusion: Prognostic factors for replanning of lung cancer patients are changes in A during RT, A in the vicinity of T or N, more than one target and large N volume. No correlation between risk of replanning and T size nor location was found. The imaging frequency could be adjusted based on these pre-treatment characteristics.

Poster #41

Karen Zegers, Maastricht, Netherlands

3D dose evaluation in breast cancer patients to define parameters for adaptive radiotherapy

Zegers CML, Baeza JA, Elmpt W, Murrer LHP, Verhoeven K, Boersma L, Verhaegen F, Nijsten SMJJG. Department of Radiation Oncology (MAASTRO), GROW - School for Oncology and Developmental Biology, Maastricht University Medical Centre, Maastricht, The Netherlands.

I: In this study we aim to define parameters for dose guided adaptive radiotherapy (DGART) by evaluating changes in 3D dose parameters in breast cancer patients that were selected for adaptation based on image guided radiotherapy (IGRT). M: In 2016 we adapted 3% of breast cancer treatment plans (N=24), after visual assessment based on strict IGRT guidelines. Reasons for adaptation were variation in seroma (N=18), hematoma (N=1), edema (N=1), positioning (N=2) or problems using voluntary deep inspiration breath hold (N=2). 16 patients received a homogeneous dose to the breast (CTV1). 7 patients were treated with a simultaneous integrated boost (SIB) to CTV2. DVH parameters for the CTV and organs at risk were calculated (ECLIPSE AAA 10.0) on the planning CT (pCT) and by copying the original plan on the CT during treatment (reCT) or available stitched CBCT (≤1d interval to reCT; N=12). CT images were rigidly registered. The extreme scenario was evaluated, assuming all treatment fractions were given to pCT, reCT or CBCT. Reported are mean±SD (range). R: 1 patient was excluded due to an unacceptable registration. For all other plans, the mean dose difference between pCT and re-CT was -0.3% (-3.1 to 1.8%) for CTV1 and -1.4 (-4.3 to 1.0) for CTV2. The difference in V95% was for CTV1 -2.0% (-19.9 to 5.7%) and CTV2 -9.8 (-18.5 to 0%). Using a threshold of CTV >-2% mean dose difference or >-5% decrease in V95%; 6/23 plans would have required adaptation of which 5 included a SIB. The difference in mean lung dose (MLD) ranged from -0.8 to 0.6Gy. For mean heart dose (MHD) this was -0.5 to 0.3Gy. Differences between stitched CBCT and re-CT analysis were on average 0.4±0.7% (CTV1mean), 1.5±0.5% (CTV2mean), -1.3±5.1% (CTV1 V95%), 2.3±3.3% (CTV2 V95%), 0.0±0.1 Gy (MHD), 0.0±0.1 Gy (MLD) C: Not all IGRT observed changes provide a clinically significant variation in the evaluated DVH parameters. Differences are larger for the CTV receiving a SIB. These results could be used for DGART.

Poster #42

Karina Lindberg Gottlieb, Odense, Denmark

A new adaptive position verification protocol for breast cancer with simultaneous boost

Gottlieb KL 1, Lorenzen EL 1,2, Dupont J 2,3, Nielsen MH 3, Ewertz M 2,3. 1. Laboratory of Radiation Physics, Odense University Hospital, DK-5000 Odense, Denmark 2. Institute of Clinical Research, University of Southern Denmark, DK-5000 Odense, Denmark 3. Department of Oncology, Odense University Hospital, DK-5000 Odense, Denmark.

Introduction The present study proposes and evaluates an adaptive protocol for daily IGRT using CBCT of breast cancer patients with simultaneous boost. A threshold is set for the allowed difference between the whole target match and the boost specific match. If the two matches differ by less than the threshold, the boost volume and the total volume is treated in the same setup. If the two matches differ by more than the threshold, the total target volume is matched and treated and then secondly an additional CBCT is performed and matched on the boost volume which is then treated. Materials and methods In order to evaluate the match protocol, a total of 180 CBCTs were analysed retrospectively. Two matches were performed for each fraction: First, a chest wall-match was performed, where CBCT images were registered automatically to the planning CT on the thorasic wall. Secondly, a boost specific match was performed, where the surgical clips were registered manually to their position on the planning CT. Results The systematic and random errors between the thorasic wall and the clips based boost matches were calculated and the corresponding required CTV-PTV margin to account for these discrepancies was calculated. If no re-matching on the clips was performed, the required CTV-PTV margin for the boost volume was 8mm. Using a threshold of maximum allowed difference, this margin could be reduced though at the cost of required re-scanning. If e.g. a threshold of 3mm was used, the margin could be reduced from 8mm to 2,8mm and rescanning would be required in 10% of the fractions. Conclusions The presented adaptive protocol can reduce the required CTV to PTV margin for the boost region by re-scanning and re-matching the boost region only for patients where the two regions differ by more than a set threshold. The presented protocol is now used for breast cancer patients treated with simultaneous boost at our institution.

Poster #43

Annette Schouboe, Aarhus, Denmark

Full bladder approach sparing bowel in external radiotherapy for cervical cancer patients

Annette Schouboe, Eva Bruun Kjaersgaard, Nina Boje Kibsgaard Jensen, Lars Fokdal, Lars Nyvang, Marianne Sanggaard Assenholt, Jakob Christian Lindegaard, Kari Tanderup, Anne Vestergaard.. Department of Oncology, Aarhus University Hospital, Aarhus, Denmark.

Purpose/objective: Inter-fractional organ motion is a challenge in radiotherapy of locally advanced cervical cancer(LACC) and may compromise target coverage and result in a large volume of bowel being irradiated. To reduce inter-fractional organ motion, a bladder filling protocol aiming for a full bladder during radiotherapy was introduced in our department. The purpose of the study is to evaluate the correlation between bladder filling variations and bowel dose. Materials/methods: Eight consecutive patients with LACC were included in the study. A bladder filling protocol was applied with oral and written instructions, advising patients to drink 450 ml of water 15 minutes post micturition and 1 hour prior to each fraction. All patients were retrospectively re-planned with a uniform dose of 45 Gy in 25 fractions. The CTV encompassed the GTV, cervix, parametria, uterus, upper vagina and the nodal CTV. A PTV margin of 1.5cm was applied for the GTV, cervix, and uterus and 5mm for the nodal CTV and parametria. The Bladder and the bowel was delineated on all daily CBCTs (n=210). The Bowel was defined as outer extension of loops and included sigmoid. All structures were copied to the planning CT to assess bowel V30 Gy for each fraction. Bowel V30 was evaluated as a function of changes in bladder filling. Results: Large variations in bladder filling volumes were observed and found to be patient dependent. A correlation between bowel V30 and bladder volume was found. Linear regression showed that an 100 cc increase in bladder volume resulted in a mean decrease in bowel V30 of 58 cc (range: 10 – 87 cc). In only one patient, there was no clear correlation between bladder volume changes and dose to the bowel. Conclusion: Treatment with a full bladder significantly reduce bowel irradiation during radiotherapy in LACC and is considered as standard in our department.

Poster #44

Akos Gulyban, Liege, Belgium

Margin of the day with ITV concept during EBRT for locally advanced cervical cancer: Evaluation of 0, 5 and 10 mm safety margins with dose accumulation uncertainty

A. Gulyban1, M. Baiwir1, S. Nicolas1, M. Enescu2, V.P. Nguyen1, P. Berkovic1, M. Gooding2, T. Kadir2, J. Hermesse1, P.A. Coucke1, V. Baart1, F. Lakosi 1,3. 1Liege University hospital, Department of Radiation Oncology, Liege, Belgium. 2Mirada Medical Ltd., Oxford, United Kingdom. 3University of Kaposvar, Health Science Center, Kaposvar, Hungary.

Introduction: Large organ motion during external beam radiotherapy (EBRT) of locally advanced cervical cancer (LACC) is challenging. Internal target volume (ITV) approach (based on full/empty bladder planning CTs) could account for movements. However optimal margin from ITV to the planning target volume (PTV) and actually delivered dose to organs are still unknown. We aim to 1) determine dose deformation uncertainties 2) reveal movement thresholds for various margins and 3) simulate the target dose coverage with these factors. Materials and methods: Eleven patients were treated using 10 mm ITV-PTV margin with daily CBCT verification. On each image set the clinical target volume (CTV=uterus+cervix), bladder and rectum were delineated. Constraint based deformation were created between the full bladder CT and each CBCT. Dose deformation uncertainties from volume compression and residual surface matching errors were evaluated. Three plans with 10/5/0 mm margins were generated to determine 95% Hausdorff-distance (HD95) thresholds associated with acceptable CTV dose coverage (V95%>90% of prescribed dose). Delivered dose to CTV were accumulated based on the thresholds and deformation uncertainties. Results: The constraint based surface registration showed an average 7.0/6.9/9.5 mm HD95 for CTV, bladder and rectum respectively resulting in a maximum of 3.8%(4.6%), 6.9%(7.2%) and 5.7%(6.2%) dose deformation (and total) error. HD95% between daily CTV and ITV showed good correlation. 17.4 and 23.5 mm thresholds resulted in acceptable dose coverage loss of CTV with 0 and 5 mm margins. 54.1% and 25.3% of all fractions could have been delivered with a 0 and 5 mm margin leading to reduced dose to OARs. Conclusions: Constraint based deformation results in low dose deformation uncertainty, providing a reliable tool for dose accumulation in large organ motion. Using HD95 as a decision support tool, up to 80% of the fractions could be treated with smaller margin during LACC EBRT.

Poster #45

Marianne Sanggaard Assenholt, Aarhus, Denmark

Bladder filling feed back and CBCT monitoring during external beam radiotherapy with tight margins for patients with locally advanced cervical cancer.

Marianne Sanggaard Assenholt, Anne Vestergaard, Nina Boje Kibsgaard Jensen, Eva Bruun Kjærsgaard, Annette Schouboe, Lars Fokdal, Jakob Christian Lindegaard, Kari Tanderup. Department of Oncology, Aarhus University Hospital, Aarhus, Denmark.

Introduction Organ movement during external beam radiotherapy (EBRT) in locally advanced cervical cancer (LACC) constitutes a significant challenge as uterus and cervix move due to changes in organ filling. This study investigated an adaptive tight margin strategy based on bladder filling feedback and CBCT monitoring during EBRT. Materials and methods The new strategy was implemented 09-2016 and 12 locally advanced cervical cancer pts have been treated so far. VMAT was used to deliver 45Gy/25fx to a CTV including all pelvic lymph nodes combined with an ITV related to the High Risk CTV (CTVHR) including primary tumour, cervix, uterus, parametria and upper vagina. ITV was generated individually according to information from (PET)-CT with full and empty bladder and MRI with full bladder according to the Embrace II protocol. The PTV margin was 5mm. Bladder filling was regulated by voiding followed by intake of 450ml of water 1h prior to treatment. RTTs evaluated daily CBCT and scored: 1) if uterus and CTVHR was inside the PTV and 2) if rectum and bladder was small, medium or large. The patients received daily feedback to improve bladder filling in succeeding fractions. If CTVHR or uterus were outside the target during 1 or 3 fractions respectively, a new dose plan with expansion of the ITV was considered. Target location at all fractions, were reviewed by a physicist. Results RTTs were able to identify the target coverage in 278/294 fractions. The bladder filling protocol was changed in 4 pts: 2 pts had to wait longer before irradiation and 2 to drink less. Review of target location identified one fraction where CTV was marginally outside PTV while first scored to be inside. In 3 pts a new dose plan with extended ITV was generated. Conclusion Feedback on bladder filling and visualization of target coverage on CBCT is possible in the majority of patients allowing for use of tight CTV to PTV margins in LACC.

Poster discussion group 8

Poster #46

Ander Biguri, Bath, UK

Improving image quality of 4D-CBCT respiratory-correlated and motion-corrected reconstruction using iterative algorithms and GPU acceleration

Biguri A.1, Hancock S.2, Dosanjh M.2, Soleimani M.1. 1Engineering Tomography Lab (ETL), University of Bath, Bath, UK. 2CERN, Geneva, Switzerland.

Imaging has become an intrinsic part of cancer detection and treatment, especially in IGRT. A CBCT scanner is one of the most commonly used devices in IGRT, due to its compactness and low radiation dose compared to other CT modalities. CBCT has lower data quality, due to the lower intensities used to avoid a high dose to the patient. In addition, for some tumour locations respiratory motion can effectively blur and hide the exact tumour size and shape. While the FDK algorithm is the principal one used in clinical applications, it has been shown that iterative algorithms outperform FDK, especially in limited-data, high-noise cases. Iterative algorithms are used in this work to show their improved image quality compared to FDK. To remove the effect of blurring due to motion, two approaches for 4D-CBCT have been presented in the literature. One is respiratory-correlated reconstruction, where projection data are binned according to their phase and a series of pseudostatic 3D-CBCT images are reconstructed. The other method, motion-corrected 4D-CBCT, uses modified algorithms with prior knowledge of expected breathing motion to use all the projection data to reconstruct a single image in any arbitrarily chosen respiratory phase. The first method suffers from low data, the second from errors in motion knowledge. Both methods are evaluated using FDK and a series of iterative algorithms. The latter, especially when properly tuned and chosen, show a clear improvement in image quality. Additionally, motion-corrected 4D-CBCT permits the reconstruction of images in all respiratory phases with a very limited amount of data, hence allowing the reduction of the radiation dose to the patient without sacrificing the quality of the image. Iterative algorithms show a clear improvement in image quality in 4D-CBCT reconstruction. Motion-corrected 4D-CBCT has the potential to reduce radiation dose while providing the same or better information than respiratory-correlated 4D-CBCT

Poster #47

Mai Lykkegaard Schmidt, Aarhus, Denmark

Intrafraction baseline shifts between setup CBCT and treatment delivery of involved mediastinal lymph nodes of lung cancer patients

Schmidt ML, Hoffmann L, Knap MM, Rasmussen TR, Folkersen BH, Møller DS, Poulsen PR. Department of Oncology and Department of Pulmonology, Aarhus University Hospital, Aarhus, Denmark.

Introduction Internal target motion results in geometrical uncertainties in lung cancer radiotherapy. The lymph node (LN) targets in the mediastinum are difficult to visualize in cone-beam computed tomography (CBCT) scans for image-guided radiotherapy, but implanted fiducial markers enable visualization on CBCT projections and fluoroscopic kV images. In this study, we determined the intrafraction motion and baseline shifts of mediastinal LN targets between setup imaging and treatment delivery. Material&Methods Ten lung cancer patients had 2-4 fiducial markers implanted in LN targets. The patients received IMRT with daily setup CBCT for online soft tissue match on the primary tumor. At a total of 122 fractions, 5Hz fluoroscopic kV images were acquired orthogonal to the MV treatment beam during treatment delivery. Offline, the 3D trajectory of the markers was determined from their projected trajectory in the CBCT projections and in the intra-treatment kV images. Baseline shifts and changes in the respiratory motion amplitude between CBCT and treatment delivery were determined from the 3D trajectories. Results Systematic mean LN baseline shifts of 2.2mm in the cranial direction (standard deviation (SD): 1.8mm) and 1.0mm in the posterior direction (SD: 1.2mm) occurred between CBCT imaging and treatment delivery. The frequency of cranial baseline shifts exceeding 5mm was 7%. The baseline shifts resulted in systematic mean geometrical errors during treatment delivery of 2.7mm(cranial) and 1.4mm(posterior) for the LNs. In general, the largest LN motion amplitude was observed in the cranio-caudal direction both during CBCT and treatment delivery. The mean motion amplitudes during CBCT and treatment delivery agreed within 0.2mm in all three directions. Conclusions Systematic cranial and posterior intrafraction baseline shifts between CBCT and treatment delivery were observed for mediastinal LN targets in lung cancer patients. Intrafraction motion amplitudes were stable.

Poster #48

Patrik Sibolt, Roskilde, Denmark

Monte Carlo evaluation of dose-escalated lung radiotherapy in free-breathing and deep-inspiration breath-hold

Sibolt P.(1,2); Ottosson W.(2); Andersen C.E.(1); Behrens C.F.(2). (1)Center for Nuclear Technologies, Technical University of Denmark, Roskilde, Denmark (2)Radiotherapy Research Unit, Department of Oncology, Herlev and Gentofte Hospital, Herlev, Denmark.

Introduction Radiation dose escalation can potentially increase the cure rate for locally advanced non-small cell lung cancer (NSCLC) patients. Moreover for standard dose fractionation, Deep-Inspiration Breath-Hold (DIBH) is proven to reduce the dose to organs-at-risk (OARs) compared to free-breathing (FB). DIBH may then facilitate even more dose escalation and increased cure rate. However, commercially available dose calculation algorithms have known issues to accurately calculate dose in the thorax region. This could have larger implications for dose-escalated lung treatment plans, why quantification of this issue using Monte Carlo (MC) calculations should be considered. This study focuses on evaluating dose-escalated lung radiotherapy by MC calculations, in DIBH and FB. Material & Methods Dose escalated RapidArc treatment plans were calculated using the AAA dose calculation algorithm (Varian Medical Systems) on 16 NSCLC patients, which were dual-CT scanned in DIBH and FB. Dose was heterogeneously escalated to a mean dose of maximum 95 Gy to the gross tumor volume (excluding lymph nodes), with a minimum dose corresponding to standard fractionation and without any restriction on maximum dose. Treatment plans were re-calculated using the EGSnrc MC codes BEAMnrc and DOSXYZnrc, preserving the number of monitor units. MC and AAA calculated dose distributions were finally compared and evaluated. Results Both AAA and MC calculated treatment plans reveal that DIBH has the potential to decrease the dose to the OARs, compared to FB. MC simulations furthermore revealed deviations in the dose to the target as calculated by AAA. Conclusions The current study show a benefit in using DIBH compared to FB for dose-escalated lung radiotherapy. This could manifest in either reduced dose to OARs or further dose escalation while maintaining the dose to OARs. Furthermore, MC revealed that issues with AAA calculated dose coverages could have an impact on the achievable escalation dose.

Poster #49

Marianne Knap, Aarhus, Denmark

Difference in target volume using three different methods to include respiratory uncertainty in advanced lung cancer

Knap MM1, Hoffmann L2, Nyeng TB2, Kandi M1, Holt MI1, Khalil AA1, Hansen J2 and Møller DS2. 1 Department of Oncology, Aarhus University Hospital, 2 Department of Medical Physics, Aarhus University Hospital.

Introduction: Different strategies to account for respiratory (resp) uncertainties are used in radiotherapy(RT) of advanced lung cancer producing different treatment volumes and the choice of strategy is debatable. Materials/methods: For 15 lung cancer patients with 4D-CT scans, lymph node (N) and tumour (T) GTVs were delineated on the midventilation phase (mv). Based on a deformable propagation from the mv-phase to the remaining phases, the center-of-mass respiratory amplitude (A) was found for GTVmv-T and GTVmv-N. Accumulating the GTV-volumes on all phases and manually correcting the accumulated contours yields GTV's including resp (iGTV). For both GTVmv and iGTV, a 5 mm expansion produced CTVmv and iCTV. Three different PTV margins were calculated by the standard margin formula (IJROBP, 1121,47,2000) taking into account all uncertainties due to planning and delivery of RT. Only the method used to incorporate resp uncertainty differed. Three PTVs were created. iPTV: resp is included in iCTV and not in PTV margin. PTVmv: resp is included as an A/3 random uncertainty in the CTV-PTV margin. PTVitv: resp is included as an A/2 systematic uncertainty in the CTV-PTV margin as described in IJROBP 70, 4, 2008. Results: The median[range] PTVmv was 5%[-1%,12%] smaller than iPTV. In only one case iPTV was marginally smaller than PTVmv. Both PTVmv and iPTV were smaller than PTVitv. Including resp as a patient specific uncertainty in the delineation process (iPTV) yields in median 10%[-11%,26%] smaller volumes than as a systematic error in the margin calculation (PTVitv). In three cases, visual inspection reveals target deformations that are included in iPTV, but not included in the 3D margin expansion for PTVmv and PTVitv. Conclusion: Small volume differences are seen between PTVmv and iPTV. In some cases, deformation in target are not taken into account by the PTVmv. PTVitv should not be used since it produces large volumes without including all target deformations.

Poster #50

Susanne Bekke, Herlev, Denmark

Non-interchangeability of respiratory gating areas using surface scanning in deep inspiration breath-hold radiotherapy

Bekke, S.N. (1,2), Kügele M. (3,4), Behrens C.F. (1), Helt-Hansen J. (2), Ceberg S. (3,4), Mahmood F (1). (1) Radiotherapy Research Unit, Herlev and Gentofte Hospital, DK. (2) Nutech, DTU, Risø Campus, DK. (3) Dept. of Medical Radiation Physics, Lund University, SE. (4) Dept. of Haematology, Oncology and Radiation Physics, Skåne University Hospital, SE.

Introduction: Deep inspiration breath-hold (DIBH) is used for heart and lung sparing in radiotherapy of breast cancer patients. The patient's breathing motion can be assessed on different anatomical structures; for example, centrally at corpus mammae or bony structures such as the xiphoid process. In this study the agreement between respiratory motion signals acquired using two gating areas was studied. The aim was to investigate the feasibility of changing gating area during the course of treatment. The inter-fraction variation of the respiratory motion signal baseline was also studied together with its dependence on patient body index (comparable to body mass index). Material and Methods: The study included 276 patients with left-sided breast cancer. Optical surface scanning (C-RAD Positioning AB, Uppsala, Sweden) was used to measure a primary respiratory motion signal at the xiphoid process or the right breast, and an additional secondary signal at the left breast. The correlation between the primary and secondary respiratory motion signal was evaluated using Pearson's linear correlation coefficient. Results: The correlation between the two respiratory motion signals from the xiphoid process or the right breast, and the left breast was 0.16 for all patients. Eleven out of 194 patients had a strong correlation (> 0.5). The standard deviation of the respiratory motion signal baseline across the treatment course increased significantly with patient body index. Conclusion: The study showed a weak correlation between the two respiratory motion signals acquired at different gating areas, which implies that the gating area in general should not be moved from the xiphoid process or right breast to the target breast. Obese patients with high body index showed higher inter-fraction variation of the gating signal baseline, indicating that these patients are more difficult to position prior to treatment.

Poster #51

Jenny Bertholet, Aarhus, Denmark

Validation of a fully automatic real-time liver motion monitoring method on a conventional linac

Bertholet J. 1, Hansen R.1, Worm E.S. 1, Toftegaard J. 1, Wan H. 2, Parikh P.J.2, Høyer M.1, Poulsen P.R.1. 1 Department of Oncology, Aarhus University Hospital, Denmark. 2 Department of Radiation Oncology, Washington University School of Medicine, St-Louis, USA.

Introduction Intrafraction motion is a challenge for accurate liver radiotherapy delivery. Real-time adaptation may mitigate the detrimental effects of motion, but it requires reliable target motion monitoring. We developed and validated a framework for fully automatic monitoring of thoracic and abdominal tumors on a conventional linac by combining external monitoring with sparse kV imaging of implanted markers. Materials and Methods A fully automatic real-time motion monitoring framework was developed: A pre-treatment CBCT is first acquired with simultaneous recording of the motion EXT(t) of an external block on the abdomen. The markers are auto-segmented in every CBCT projection. Their 3D motion is estimated from the observed 2D motion and used to establish an external correlation model (ECM) of the 3D internal marker motion INT(t) as a function of EXT(t). During treatment, INT(t) is estimated from EXT(t) at 20Hz, while MV-scatter-free kV images are acquired every 3s during beam pauses and used for marker segmentation. The ECM is continuously updated with the latest estimated 3D marker position. The method was validated using Calypso-recorded internal motion and simultaneous camera-recorded external motion of 10 liver SBRT patients. The validation included both experiments with a programmable motion stage and simulations hereof for the first patient as well as simulations for the remaining patients. The real-time estimated 3D motion with and without ECM updates were compared to the known tumor motion. Results The simulations agreed with the experimental 3D root-mean-square error (rmse) within 0.4mm. For all patients, the mean 3D rmse was 1.8mm with ECM updates and 2.3mm without ECM updates. Conclusions A fully automatic motion monitoring method was developed and validated using Calypso recorded liver tumor motion. It can be used on a conventional linac without additional time or hardware even for non-coplanar fields where the kV imaging system cannot be deployed.

Poster #52

Simon Skouboe, Aarhus, Denmark

Real-time gamma evaluations of motion induced dose errors as QA of liver SBRT tumour tracking

Skouboe S. (1) , Poulsen P.R. (1, 2), Hansen R. (3), Worm E. (3), Ravkilde T. (3). (1) Department of Oncology, Aarhus University Hospital, (2) Department of Clinical Medicine, Aarhus University, (3) Department of Medical Physics, Aarhus University Hospital.

Introduction Organ motion during radiotherapy can seriously deteriorate the intended dose distribution. MLC tracking may mitigate the effects of motion but defies the use of standard pre-treatment plan QA. Here we present a method for continuous online evaluation of the tracking dose delivery. Methods Experiments were performed on a TrueBeam linear accelerator with target motion being recorded by a Calypso transponder system. A HexaMotion motion stage carrying a Delta4 dosimeter reproduced the motion traces previously measured for five liver SBRT patients. The clinically applied VMAT SBRT treatment plans of each patient were delivered to the moving dosimeter with MLC tracking, without tracking (simulating the actual delivery) and to a static phantom for reference (planned delivery). Dose distributions were measured at 72 Hz. Accelerator parameters were streamed at 21 Hz to prototype software that continuously reconstructed the dose in real time by a simplified non-voxel based 4D pencil beam convolution algorithm. On a separate thread, the 3%/3mm gamma errors were calculated continuously throughout beam delivery to quantify the motion-induced deviation from the planned static dose. After experiments, these gamma errors were compared with gamma calculations based on the measured dose rather than the real-time reconstructed dose. Results The motion induced gamma errors were well reconstructed both spatially and temporally. In 95% of the time both actual and planned doses were reconstructed within 100 ms. The median time for dose reconstruction was 65 ms (about 15 Hz). 95% of gamma evaluations were performed within 1.5 s (median: 1.2 s). Over all experiments the root-mean-square difference between reconstructed and measured time-resolved gamma failure rates was 2.9%. Conclusions Motion induced dose errors were accurately and continuously reported by gamma evaluations. Such monitoring may improve patient safety by treatment intervention in case of gross treatment errors.

Poster #53

Camilla Skinnerup Byskov, Aarhus, Denmark

Intra- vs. inter-fractional target motion in radiotherapy of rectal cancer evaluated with repeat volumetric imaging

Byskov CS1, Nyvang L1, Spindler KLG2, Pedersen EM3, Kronborg CJS2, Harbøll A2, Schouboe A2, Vestergaard A1, Muren LP1. 1 Dept. of Medical Physics, Aarhus University Hospital, Aarhus, Denmark; 2 Dept. of Oncology, Aarhus University Hospital, Aarhus, Denmark; 3 Dept. of Radiology, Aarhus University Hospital, Aarhus, Denmark.

Introduction: Development of adaptive radiotherapy (ART) strategies for rectal cancer requires characterisation of both the inter- and intra-fractional components of target motion, as well as potential tumour regression. Cone-beam CT (CBCT) scans are used for online image-guidance/adaptation but may have limited soft-tissue contrast. The aim of this study was therefore to establish a method to analyse intra- vs. inter-fractional motion of the rectum and to compare motion patterns assessed by CBCTs vs. magnetic resonance imaging (MRI). Materials and methods: Two patients treated with RT for rectal adenocarcinoma according to an institutional protocol (R-ART) underwent daily pre-treatment and weekly post-treatment CBCTs as well as weekly repeat MRI (cine, T2W, voxel size: 0.78x0.78x4.4 mm, scan time: 41 s). Following rectum delineations, 2D maps of the distance between contour points and the centroid of each slice were created by virtually unfolding all contour slices. The intra-fractional difference was measured for nine pairs of pre- and post-CBCTs (median 6 min apart) and for seven pairs of MR scans (median 9.5 min apart). This was compared to nine pairs of inter-fractional motion measurements between the planning CT and weekly pre-treatment CBCTs. Results: For the pre- and post-CBCT scans, 96 % (median; range: 48–98 %) of the rectum surface map points were within ± 3 mm. In the corresponding MRI scans, 91 % (median; range: 85–99 %) of the surface points were within ± 3 mm. A few outliers had < 94 % of the points within ± 3 mm; these were seen for one patient. Larger inter-fractional changes were observed, where only 56 % (median; range 11–91 %) of the surface map points were within ± 3 mm. Conclusion: We have established a method to analyse 2D patterns of intra- vs inter-fractional target motion for rectal cancer. Initial results indicate that the intra-fractional motion in off-line MRI and online CBCTs is similar and much smaller than the inter-fractional motion.

Poster discussion group 9

Poster #54

Stine Korreman, Aarhus, Denmark

Minimum prescription concept for dose painting with protons increases robustness towards geometrical uncertainties

Korreman, S. Dept of Oncology, Aarhus University Hospital, Aarhus Denmark.

Purpose Dose painting proton therapy with heterogeneous dose-escalation is vulnerable to geometrical errors, which deteriorate benefits of dose-escalation substantially. This study investigates use of a minimum prescription concept to increase plan robustness. Material/Methods Dose-escalation was prescribed based on hypoxia-PET scan for H&N cancer patients, with high degree of heterogeneity. Minimum dose was 60Gy, and dose-escalation was based on a linear correspondence model, with maximum dose up to ~90Gy. Dose painting IMPT plans were optimized using the Eclipse TPS and a contour-based dose-escalation scheme. Two planning strategies were tested: (1) Robust optimization with minimum and maximum dose constraints on all subvolumes (exact-map), and (2) Minimum constraints on all subvolumes but with only one overall maximum constraint (V82Gy<4cc) without robustness (minimum-map). Geometrical errors were simulated by isocenter displacements up to 2mm. Quality index metrics were compared for the two strategies. Results For the minimum-map approach, minimum dose was met in all voxels. With robust exact-map optimization, substantial volumes received less than prescribed dose. The volume receiving high doses was larger for the minimum-map than for the exact-map approach, but the overall maximum dose constraint was met. With geometrical errors, the voxel doses were decreased in the exact-map robust approach, while for the minimum-map approach the V82Gy<4cc increased by up to a doubling. Conclusion Using a minimum dose prescription concept for dose painting with only one overall maximum constraint, gives plans that are at least as robust as voxel-by-voxel exact dose prescription using a robust optimization algorithm, with higher adherence to minimum voxel doses. Geometrical errors introduced a small overdosage for the minimum-map approach.

Poster #55

Kia Busch, Aarhus, Denmark

On-line dose-guided proton therapy to account for inter-fractional motion: a proof of concept

Busch K, Muren LP, Pedersen J, Andersen AG, Petersen JBB. Department of Medical Physics, Aarhus University Hospital/Aarhus University, Aarhus, Denmark.

Introduction: Protons are sensitive to inter-fractional motion and density variations due to their finite range. We propose the concept of online dose-guided proton therapy (DGPT) to find the optimal re-positioning of a patient using online dose re-calculations of all relevant isocenter shifts. The aim of this study was to investigate the use of DGPT to account for inter-fractional target motion during treatment of prostate cancer (PC). Materials and methods: A patient model was created using the CT of a patient with locally advanced PC, with the CT numbers for soft tissues and bones overwritten to water and the average of bone, respectively. An intensity-modulated proton therapy (IMPT) plan was created (Eclipse, Varian Medical Systems) using two lateral opposed beams. The prostate planning target volume (PTV) was moved 3, 5, 10 and 15 mm in both anterior and posterior direction, afterwards the fields isocenter was moved according to this 'geometrical' shift and re-calculated. DGPT was explored by calculating a multiple number of plans with the isocenter shifted an additional 3-15mm away from the geometrical shift along the three main axes. The resulting DGPT plans were evaluated on the PTV using the volume receiving 95% of the prescribed dose (V95%). Results: For all eight target positions one (or more) of the DGPT plans (with isocenter different from the geometrical shift) improved the target coverage. V95% for the targets increased by up to 15% (median 4%). The largest increase (V95% increased from 81% to 96%) occurred for the 15mm posterior shifted target when the plan was shifted an additional 10mm anterior. When the targets were shifted either anteriorly or 5 and 10mm posteriorly, improved coverage was obtained when shifting the plan posterior from the geometrical shift (V95% increased with 4-5% and 2-3%, respectively). Conclusion: This study has shown the potential of online DGPT to secure dose coverage when targets are subject to inter-fractional motion.

Poster #56

Maria Fuglsang Jensen, Aarhus, Denmark

Optimizing delivery speed of lung cancer treatments using single and multi field intensity-modulated proton therapy

Fuglsang Jensen, M. (1,2), Hoffmann, L (2), Petersen, J.B.B (2), Møller, D.S. (2), Alber, M.L. (3). (1) Danish Centre for Particle Therapy, Aarhus University Hospital, Aarhus, Denmark. (2) Department of Oncology, Aarhus University Hospital, Aarhus, Denmark. (3) Department of Radiation Oncology, Heidelberg University Hospital, Heidelberg, Germany.

Introduction: For proton therapy of lung cancer, robust delivery can be ensured by gating and rescanning techniques. This, however, increases the treatment time which translates into a higher risk of intra fractional changes. Treatment times can be reduced by limiting the number of energy layers but this can also challenge the target coverage and plan robustness. We investigate to what extend the number of layers can be reduced in single field optimization (SFO) and multi field optimization (MFO) plans. Materials and methods: We implemented three layer reducing strategies in the treatment planning system Hyperion; predefined constant energy steps, predefined exponential energy steps and an adaptive strategy, where the spot weights are exposed to a group sparsity penalty in combination with layer exclusion during optimization. For these three strategies, SFO and MFO plans with three treatment fields were created for 10 lung cases on the mid ventilation phase to simulate gating. A minimum dose to the target was ensured for each degree of layer reduction, causing the plan quality to be reflected in the maximum target dose and the outcome of a robustness evaluation, where the dose was shifted 2 mm or 4 mm in 6 directions. Results: The three strategies resulted in very similar robustness and target coverage as a function of removed layers; D02 increased unacceptably for the SFO plans after 50% layer removal (as compared to the dense 2 MeV stepped plan) while all MFO plans were clinically acceptable (highest removed percentage of 70%). The robustness did not depend much on the number of layers and the difference D98-meanD98(2mm) was ~1 Gy for SFO plans and ~3 Gy for MFO plans. Conclusion: The number of energy layers can be reduced by at least a factor of 2 more for MFO plans compared to SFO plans without compromising the plan quality. This time reduction could potentially make a difference, when the entire plan is rescanned several times during one treatment session.

Poster #57

Alina Santiago, Marburg, Germany

Beam-specific planning target volumes for scanned particle therapy of lung tumors under tumor fixation conditions

Santiago A.(1,2), Ringbæk T.P.(1,3), Bassler N.(4), Grzanka L.(5,6), Iancu G.(2), Fritz P.(7), Zink K.(2,3), Engenhart-Cabillic R.(1,2) and Wittig A.(1). 1:Dept of Radiotherapy and Radiation Oncology, Philipps-University, Marburg, DE 2:Dept of Radiotherapy and Radiation Oncology, University Medical Center, Gießen and Marburg, DE 3:Technische Hochschule Mittelhessen (THM), Gießen-Friedberg, DE 4:Medical Rad.

Different concepts for target margin design for scanned ion beam therapy, so-called beam-specific planning target volumes (bsPTV), have been developed in recent years. By assuming irradiation under tumor fixation, range changes upstream the target caused by respiratory motion do not need to be considered. We will apply and compare three different margin concepts: an isotropic CTV-to-PTV expansion, and bsPTVs including setup errors and range uncertainties both in water equivalent length units as well as adapted to local lung tissue densities. Single-field uniform dose proton plans were created with Varian Eclipse for all margin concepts for 12 early-stage NSCLC patients originally treated with photon SBRT under high-frequency jet ventilation applied to achieve tumor fixation. Plans were dosimetrically evaluated in terms of target coverage, homogeneity, conformity, and dose to OAR. Photon SBRT plans, as applied originally on the patient cohort, were compared to the particle beam plans. Additionally, carbon ion plans were produced in TRiP98 for selected patients for a simple robustness study. Our self-developed software could, based on WEPL calculations, generate VOXELPLAN bsPTVs readable by TRiP98, and using PyTRiP they were converted into DICOM structure files for import in commercial treatment planning systems. The median (range) volumes for the isotropic margins for the whole patient cohort is 24.3 (7.2-71.5) ml. In comparison, geometric expansions resulted on average in 130% larger volumes for all cases except for one superficial tumor. Margins adapted to the local densities resulted in 155% larger volumes than the isotropic expansion, due to the low lung tissue density. Preliminary analysis of selected proton plans shows in all cases adequate target coverage, with the PTV or bsPTV receiving a V95% of at least 97%. Dose to surrounding normal tissue such as the ipsilateral lung and ribs is increased for the novel bsPTV designs.

Poster #58

Emma Colvill, Aarhus, Denmark

Validation of fast motion-including dose reconstruction for proton scanning therapy in the liver

Colvill E, Petersen J, Høyer M, Worm E, Hansen R, Poulsen P. Aarhus University Hospital.

Introduction: In this study, we validate a method of fast dose reconstruction, which uses real 3D target motion and utilizes a commercial treatment planning system (TPS) to calculate the delivered dose for liver scanning proton therapy treatments. Materials and methods: The 4DCTs of 9 liver patients treated with photon SBRT were used for this study; for each, proton plans on inhale and exhale phases were created using three-field single-field-optimization with ~6 mm spot spacing and mean IGTV coverage of 56.25Gy/3Fx. A dose reconstruction plan was created for all inhale and exhale plans with all odd layers shifted to the opposite phase. Motion was incorporated into the dicom plans by shifting each proton spot to its position as seen in tumor's eye view. Depth motion and SSD variations were modeled by modifying the beam energy. The dose reconstruction plans were imported into the TPS and calculated on the original CT phase. Ground truth doses were created by splitting the original plans into sub-plans with odd and even layers, calculating one sub-plan in the original CT phase and the other in the opposite phase, and then summing the two dose maps. The errors associated with the differences in anatomy were assessed by comparing the D5 and D95 for the GTV and the root-mean-square (RMS) dose errors for dose points >70% and >90% of the dose reconstruction and ground truth plans. Results: The mean and range (n=18) of the fast dose reconstruction errors due to anatomical differences for the GTV D5, D95 and RMS errors >70% dose and >90% dose were 0.5(-1.0 – 11.4), -0.7(-10.7-8.2), 3.3(1.4-9) and 2.8(0.8-10.4) respectively. Conclusion: Validation of a method of fast dose reconstruction to assess the dosimetric impact of tumor motion on scanning proton therapy for liver SBRT treatments was performed. The results show that the dose reconstruction can utilize a single phase of a 4DCT with only small dose calculation errors due to anatomical differences.

Poster #59

Thomas Berger, Aarhus, Denmark

Dosimetric impact of air cavities and weight loss with intensity modulated proton therapy in locally advanced cervical cancer patients.

Berger1 T., Petersen1 J. B. B., Lindegaard1 J. C., Fokdal1 L., Tanderup1 K. 1: Aarhus University Hospital, Aarhus, Denmark.

Purpose:To evaluate the dosimetric impact of bowel gas cavities and body outline variations occurring during a complete course of RT in locally advanced cervical cancer (LACC) patients. M&M:Seven pelvic LACC patients were studied. Two had 2 positive lymph nodes [LN]. The elective LN target and primary tumour including ITV margin (ITV45) was planned according to the Embrace II protocol with 45Gy/25fx using four beams (30, 90, 270, 330°), and positive LN targets (ITVNx) with 55Gy in a simultaneous integrated boost. On planning CT (pCT), all air pockets were virtually filled with mean bowel/faeces Hounsfield Unit (HU). On all CBCTs air cavities and body outlines were delineated. CBCT contours were transferred to the pCT after a bony match. Two times 25 modified CT scans were generated to represent daily cavities and body outline, respectively, of each fraction by 1) overwriting with air HU the bowel gas and 2) adding/removing fat HU to reflect the actual body outline. In another modified 25 CT scans, air pockets and body outlines were combined. On each of these 75 images the dose was recalculated. Dosimetric impact was evaluated via accumulated D98 and D99.9 of target and accumulated V43 for bladder, bowel and rectum Results:With air cavities added, the median and range of accumulated ITV45 D98 and D99.9 were 99.6%[98.3-99.9%] and 99.3%[97.5-99.8] of planned dose, respectively. Considering body outline variations, the median and range of ITV45 D98 and D99.9 were 99.1%[97,9-99.8%]and 98.3%[96.1-99.6%],respectively. When air pockets and body outlines were combined, the median and range of ITV45 D98 and D99.9 were 98.7%[97.7-99.6%] and 97.9%[95.8-99.2%], respectively. In the latter scenario, minimum and maximum deviations of V43 for bladder, bowel and rectum were 94% and 104.4%. Worst accumulated ITVNx D98 was degraded by 1.8% Conclusion:For the 7 patients studied, CBCT air cavities and body outline variations had limited dosimetric impact on the dose to targets and OARs.

Poster #60

Toke Printz Ringbæk, Gießen, Germany

Evaluation of new 2D ripple filters in scanned proton therapy.

Ringbæk, T. P.(1,2), Weber, U.(3), Santiago, A.(2,4), Simeonov, Y.(1), Fritz, P.(5), Wittig, A.(2,4), Iancu, G.(4), Grzanka, L.(6,7), Bassler, N.(8), Engenhart-Cabillic, R.(2,4) and Zink, K.(1,4). 1)University of Applied Sciences, Gießen-Friedberg, DE. 2)Radiotherapy and Oncology, Philipps University, Marburg, DE. 3)Department of Biophysics, GSI, Darmstadt, DE. 4)Radiotherapy and Oncology, University Hospital, Gießen-Marburg, DE. 5)Radiotherapy Dep.

We have shown previously that ripple filters (RiFis) of an improved 6 mm thick design with two-dimensional pins can be used in scanned carbon ion therapy for widening the Bragg peak (BP) to reduce the accelerator energy shifts needed to homogeneously cover the target volume and thus reduce the irradiation time. This design could potentially be used in proton therapy too, widening the BP to an extent, which would be beneficial in treatment planning. RiFis are normally not used with protons due to larger scattering and straggling effects. Measured proton Bragg curves confirm the functionality of the new RiFi design. Base data for treatment planning in the form of depth-dose distributions and lateral profiles were generated with the Monte Carlo code SHIELD-HIT12A with and without the RiFi and imported in the treatment planning systems TRiP98 and proton Eclipse. Proton plans on simulated spherical targets in water were done in TRiP98 for a systematic analysis of the RiFi performance and for comparisons with carbon ion plans for the same respective energy step sizes. For a dosimetric evaluation of the RiFis on clinical cases, proton plans for 12 NSCLC lung tumours fixated under high-frequency jet-ventilation were calculated in Eclipse. Slightly worse dose conformity and homogeneity were found with RiFis compared to without the RiFi but satisfactory dosimetric results within the planning objective could be obtained for all cases. A general increase in conformity and homogeneity was found as a function of target size and isocenter depth. This effect is found to be more pronounced for protons than for carbon ions. For small superficial targets requiring low beam energies, the RiFi might result in an unacceptable large lateral beam broadening, which could be lowered by opting for a combined RiFi and range shifter setup. Experimental and simulated data as well as planning studies illustrate that 2D RiFis could be used in proton therapy to lower the irradiation time.

Poster discussion group 10

Poster #61

Ane Iversen, Aarhus, Denmark

Functional imaging of cancer metabolism using hyperpolarized 13C magnetic resonance spectroscopy to monitor the effect of vascular disrupting agents

Iversen AB 1, Busk M 1, Bertelsen LB 2, Laustsen C 2, Munk OL 3, Nielsen T 4, Wittenborn TR 1, Bussink J 5, Lok J 5, Stødkilde-Jørgensen H 2 and Horsman MR 1. 1 Department of Experimental Clinical Oncology, 2 MR Research Centre, 3 PET Centre and 4 CFIN, Aarhus University Hospital, Aarhus, Denmark; 5 Department of Radiation Oncology, Radboud University Medical Center, Nijmegen, The Netherlands.

Introduction: Targeting tumor vasculature with vascular disrupting agents (VDAs) results in substantial cell death that precede tumor shrinkage. Here we investigate the potential of hyperpolarized magnetic resonance spectroscopy (HPMRS) as a functional imaging technique to monitor early metabolic changes associated with VDA treatment. Materials and methods: CDF1 mice bearing C3H mammary carcinomas were treated with the VDAs combretastatin-A4-phosphate (CA4P) or the analogue OXi4503. VDAs were injected intraperitoneally 3 (CA4P) or 6 (OXi4503) hours prior to HPMRS. Similarly treated mice were positron emission tomography (PET) scanned following administration of the glucose analogue fluordeoxyglucose (FDG). The metabolic imaging parameters were compared to tumor regrowth delay effects and histological assessment of necrosis 24-hours after treatment. VDA-induced effects on tumor perfusion were also assessed using dynamic contrast-agent enhanced magnetic resonance imaging (DCE-MRI) and histological analysis of Hoechst-33342 perfused areas. Results: VDAs induced dose dependent effects on tumor growth inhibition and necrosis development, with OXi4503 having a greater effect. VDAs impaired tumor perfusion (DCE-MRI and Hoechst 33342) and reduced FDG uptake. HPMRS assessment revealed that the [1-13C]pyruvate-to-[1-13C]lactate conversion remained unaltered, whereas [1-13C]lactate-to-[13C]bicarbonate (originating from respiratory CO2) ratios increased significantly following treatment. Conclusion: DCE-MRI and FDG-PET revealed loss of vessel functionality, impaired glucose delivery and reduced metabolic activity prior to cell death. The [1-13C]lactate-to-[13C]bicarbonate ratios increased significantly during treatment, indicating a shift towards anaerobic metabolism driven by the onset of hypoxia. HPMRS is promising for early detection of metabolic stress inflicted by VDA’s, which cannot easily be inferred based on blood flow measurements.

Poster #62

Jesper Kallehauge, Aarhus, Denmark

Comparison of common approaches for DCE-MRI analysis in cervical cancer

Jesper Folsted Kallehauge1, Petra van Houdt2, Uulke van der Heide2, Kari Tanderup1. 1 Department of Medical Physics, Aarhus University Hospital, Aarhus, Denmark; 2 Radiotherapy Department, National Cancer Institute, Amsterdam, The Netherlands.

A major source of uncertainty connected to kinetic modeling of DCE-MRI data is the correct estimation of an arterial input function. Certain methods do however, not require use of a population/patient specific arterial input function (AIF), but trade away this error-prone estimation by giving up on a more rigorous quantification. An example of a well known method that requires an AIF is the Tofts' model (TM) while the Brix model (BM) avoids the use of an AIF. Both models have successfully been used in the outcome prediction of cervical cancer. Here we aim to compare extracted parameters from the TM and the BM where these models are supported by the data. DCE-MRI data from 25 patients with advanced cervical cancer were scanned using a high temporal (Δt=2.1s) 3D spoiled gradient echo technique using two different 1.5 T scanners (Philips Ingenia). Pearsons correlation coefficients were estimated between parameters from the TM and BM for pooled for entire patient population. The correlations were determined both inside and outside the regions where the BM was optimal as assessed by the corrected Akaike information criterium On average the BM was found to be optimal in 15.2% (median; range 2.0-30.3) of tumor voxels. Within the region where the BM was optimal we found the correlation between the extravascular-extracellular volume fraction (ve) from the TM and the BM amplitude parameter (AB) to be: 0.72 and between the forward transport rate constant (Ktrans) from the TM and the product between AB and the efflux rate constant (kep) from the BM to be: 0.74. Outside the BM optimal region the correlation were between ve and AB 0.81 and between Ktrans and ABkep 0.68. The assumptions of the AIFs behind both models are strikingly different however these results show that the models describe the data very similarly. This may suggest that the use of a model that does not require estimation of an AIF may be suffucient even though the correlations are not perfect.

Poster #63

René Winter, Tübingen, Germany

Simultaneous PET/MRI in radiotherapy treatment position: Diffusion-weighted imaging in head and neck cancer

Winter R1, Schmidt H2, Leibfarth S1, Zwirner K3, Welz S3, Schwenzer N2, la Fougère C4, Nikolaou K2, Gatidis S2, Zips D3, Thorwarth D1. 1 Biomedical Physics, Radiation Oncology, University Hospital Tübingen, Tübingen, Germany 2 Diagnostic and Interventional Radiology, University Hospital Tübingen, Tübingen, Germany 3 Radiation Oncology, University Hospital Tübingen, Tübingen, Germany.

Combined PET/MRI has high potential to improve radiotherapy (RT). However, its integration requires accurate co-registration with the RT planning CT. Therefore, patient examination in RT-specific position is essential. PET/MRI examinations in RT position require immobilization tools to be combined with the MRI hardware. A dedicated hardware solution has recently been proposed for head and neck cancer (HNC) [1]. In this study we report on its clinical performance with focus on geometric fidelity of diffusion-weighted MRI (DWI). 11 HNC patients were examined with combined PET/MRI (Siemens mMR) including T2w-MRI and echo-planar imaging (EPI)-based DWI prior to RT. For each patient, two scans were performed - using a RT-specific and a standard diagnostic setup. Geometric and quantitative accuracy of DWI was assessed for different anatomical regions. Distortion correction for DWI was realized based on repeated data collection with reversed phase encoding directions (RPED). ROI-based similarity measures included Dice similarity index (DSI), relative volume difference (RVD) and average symmetric surface distance (ASSD). Relative to T2w-MRI, DSI (mean±std) of distortion corrected/uncorrected DWI was 0.84±0.04/0.53±0.18 and 0.79±0.16/0.53±0.17, RVD was -2.6±13.1/-14.9±12.1% and -3.4±15.7/-13.3±20.8% and ASSD was 0.4±0.2/1.3±0.5 mm and 0.5±0.4/1.4±0.8 mm for the RT and the diagnostic setup, respectively. The magnitude of distortion was similar for both setups. Distortion correction based on RPED yielded significant improvement in geometric accuracy. The relative difference of ADC values in corrected maps was 0.71±9.80% (p=n.s.). PET/MRI examination of HNC patients in RT position using dedicated positioning aids is clinically feasible. Distortions in DWI can effectively be reduced by RPED. Thus, the presented imaging solution enables precise integration of simultaneous PET and DWI into RT planning for future personalized RT strategies. [1] DH Paulus et al., Med Phys 2014

Poster #64

Morten Bjoern Jensen, Aarhus, Denmark

Diffusion Tensor Imaging driven growth modelling for target definition in gliomas

Jensen M. B., Lukacova S., Kallehauge J. F., Guldberg T. L., Harbøll A. Department of Oncology Medical Physics, Aarhus University Hospital, Aarhus, Denmark.

Purpose/Objective: The Clinical Target Volume (CTV) for gliomas is routinely based on contrast enhanced T1w (+Gd) and T2 FLAIR MRI. The growth of gliomas favors spread along the fiber tracts with reduced infiltration in grey matter. We investigated the feasibility of diffusion tensors (DTI) driven growth model for target definition in gliomas.
Material/methods: Eight glioma patients were scanned using the standard T1w, T2 FLAIR, T1w+Gd and DTI on a Philips Ingenia 1.5T and the White Matter (WM), Grey Matter (GM) and Cerebral Spinal Fluid (CSF) were segmented. The gross tumor was used for the Fisher-Kolmogorov growth model assuming a uniform proliferation rate and a difference in white and grey matter diffusion of a factor 10. For the tensor directionality, an anisotropy weighting parameter of zero (γ0) and twenty (γ20) were used. The volumes for the standard CTV and the DTI derived CTV were assumed equal. Hausdorff distance, Dice similarity coefficient (DSC) and surface area were used for volumetric comparison. Results: The results show significant differences between all three compared metrics using the one-tailed parried Student's t-test with a significance level of 0.05. Thus the Dice was significant less than one; the Hausdorff distance was significantly greater than zero and the surface area was greater than the area of the standard CTV margin for both scenarios of γ0 and γ20. Conclusion DTI driven growth models resulted in significantly more irregular volumes. For dose delivery, a highly modulated technique such as protons may be advantageous.

Poster #65

Erik Pedersen, Aarhus, Denmark

Real-time magnetic resonance imaging of the simultaneous motion of lung tumors and metastatic mediastinal lymph nodes

Poulsen PR (1), Knap MM (1), Brix L (2), Sørensen TS (1), Schmidt ML (1), Hoffmann L (1), Pedersen EM (3). (1) Department of Oncology, (2) MR Research Centre, (3) Department of Radiology, Aarhus University Hospital, Aarhus, Denmark.

Introduction: Radiotherapy (RT) of lung cancer often includes both a primary lung tumor and metastatic mediastinal lymph nodes (LN) that move differently from each other. Treatment uncertainties and margins may be reduced by in-room magnetic resonance imaging (MRI) of both targets. This study investigates MRI tracking of the simultaneous tumor and LN motion. Methods: Ten patients with a solitary lung tumor and metastatic mediastinal LNs were treated with chemo-RT. After 0-7 days of radiotherapy, several 1-minute 2D real-time MRI series were recorded at 3.5-5.3Hz at a dedicated imaging session, including the following: (1) A single MRI plane aligned parallel with the superior-inferior (SI) axis and passing through both targets. (2) Two alternating parallel MRI planes (sagittal or coronal) passing through one target each. (3) Three alternating planes with two parallel planes passing through one target each (as in (2) above) and one plane passing through both targets (as in (1) above). The simultaneous tumor and LN motion was extracted by template-based segmentation and compared between the three imaging strategies. Results: For two patients, the tumor or LN could not be identified reliably by MRI due to shrinkage during chemotherapy. For the remaining patients, the extracted SI motion was similar for the three imaging strategies except for occasional irregular motion. The mean motion range was larger for LNs (6.4mm) than tumors (3.8mm) for this patient group, where several tumors were attached to the chest wall. Conclusions: Feasibility of MRI for simultaneous real-time tracking of multiple radiotherapy targets in the lung and mediastinum was demonstrated. The number of alternating 2D MRI planes involves a trade-off between more motion directions being resolved and longer waiting time between the updates of a given image plane. Loss of MRI visibility due to target shrinkage following pre-RT chemotherapy might be a concern for direct target tracking by in-room MRI.

Poster #66

Anders Traberg Hansen, Aarhus, Denmark

Isotoxic treatment planning strategies for stereotactic liver irradiation: The price of dose uniformity

Hansen AT 1, Poulsen PR 1,2, Høyer M 3 and Worm ES 1. 1 Department of Oncology, 2 Institute of Clinical Medicine, 3 The Danish Centre for Particle Therapy, Aarhus University Hospital, Aarhus, Denmark.

Introduction To find the optimal dose prescription strategy for liver SBRT, this study investigated the trade-offs between achievable target dose and dose to the healthy liver for a range of uniform and non-uniform PTV dose level prescription strategies. Methods Ten patients received three-fraction liver SBRT with intrafraction motion monitoring during their treatment. Later, four VMAT treatment plans were made for each patient. All plans had a mean GTV dose of 18.8Gy/fraction, while the PTV was covered by 50%, 67%, 80%, and 95% of this dose, respectively. The PTV margin was 5mm (LR, AP) and 10mm (CC). The 50%, 80%, and 95% plans were then renormalized to be isotoxic with the standard 67% plan according to an NTCP model for radiation induced liver disease. The D98 and mean CTV dose of the four iso-toxic plans were calculated both without and with the observed intrafraction motion, using a validated method for motion-including dose reconstruction. Results Under isotoxic conditions, the average [range] mean CTV dose decreased gradually from 21.2 [20.5—22.7]Gy to 15.5[15.0—16.6] Gy and the D98 decreased from 20.4 [19.7-21.7] Gy to 15.0 [14.5-15.5] Gy, as the prescription level to the PTV rim was increased from 50% to 95%. With inclusion of target motion the mean dose decreased to 19.7 [15.7-22.5]Gy and 15.1 [13.5-16.4]Gy and the D98 decreased to 16.8[11.4-20.9]Gy and 13.7 [8.4-15.4]Gy for the 50% and 95% PTV dose prescriptions, respectively. Conclusions Requirements of a uniform PTV dose prescription come at the price of excess normal tissue dose. A non-uniform PTV dose prescription allows increased CTV mean doses at the cost of robustness towards intrafraction motion. The increase in planned CTV dose by non-uniform prescription clearly outbalances the dose deterioration caused by intrafraction motion.

Poster #67

Jasmin M. Mahdavi, Herlev, Denmark

Critical dose reduction effect of unwanted air gaps under bolus in volumetric modulated arc therapy

Mahdavi JM, Petersen TH, Sjölin M, Behrens CF, Mahmood F. Radiotherapy Research Unit, Department of Oncology, Herlev and Gentofte Hospital, University of Copenhagen, Herlev, Denmark.

Introduction In radiotherapy bolus is used to increase patient surface dose. In this study the dosimetric effect of air gaps between bolus and patient surface in volumetric modulated arc therapy (VMAT) treatments is investigated. The practical aim is to improve the assessment of surface dose when air gaps are observed in patient setup imaging during the course of treatment. Methods and Materials VMAT treatment plans were generated in Eclipse (v. 10.0, Varian Medical Systems, Inc.) with 6 MV photons based on a CT scan of the anthropomorphic Alderson ART-300A phantom: four plans with full arc and four plans with double half arc. The plans were made with 3 and 5 mm bolus linked to the treatment field, respectively. Planning target volumes (PTV) at the neck (PTV-neck) and at the forehead (PTV-forehead) were investigated. Air gaps of 0, 5, 10 and 15 mm, respectively, were moulded into immobilization masks. The treatment plans were delivered with a Varian 2300 iX Clinac and dose measurements performed using GafChromic EBT3 film. Results Decrease in surface dose was observed with increasing air gap independent of PTV location, arc technique, and bolus thickness. At air gaps of 0 (no gap), 5, 10, and 15 mm, respectively, the measured dose for all PTV forehead plans and all PTV neck plans showed dose levels in the interval 98-110%, 84-105%, 80-96%, and 72-89% of the calculated surface dose at no air gap. Conclusions This study shows that the dose delivered to the patient surface may be critically reduced at air gaps of 5 mm and above. Our results may be used for improved estimation of the dosimetric impact during patient setup and at off line verification of setup images, when unintended air gaps under the bolus are observed.

Poster #68

Helena Sandström, Stockholm, Sweden

Multi-institutional study of the variability in target delineation for six targets commonly treated with radiosurgery

Sandström H (1,2), Jokura H (3), Chung C (4), Toma-Dasu I (1,2). 1 Oncology-Pathology Dept., Karolinska Institutet, Sweden, 2 Dept. of Physics, Stockholm University, Sweden, 3 Suzuki Memorial Gamma House, Furukawa Seiryo Hospital, Osaki, Japan, 4 University of Texas MD Anderson Cancer Center, USA.

One of the key factors of success in stereotactic radiosurgery typically delivered in a single large fraction of radiation is the accurate delineation of the target. In spite of the high importance of contouring the volume to be irradiated, very few studies have been performed to assess the variability in target delineation between different centres in order to determine the need for guidelines for contouring in radiosurgery. The aim of the present study was therefore to quantify the variability in target delineation for six targets regarded as common in stereotactic radiosurgery, one cavernous sinus meningioma, one pituitary adenoma, one vestibular schwannoma and three cases of metastases under the hypothesis that common targets would show a low disagreement in contouring variability in comparison to complex targets that were previously investigated. Twelve Gamma Knife centres participated in the study by contouring the target and organs at risks according to the local clinical practice and performing one treatment plan for each case of the cavernous sinus meningioma, pituitary adenoma, vestibular schwannoma and the three metastases. The analysis of target delineation variability was based on agreement volumes derived from overlapping structures following a previously developed method. The 50% agreement volume (AV50), the common and the encompassing volumes as well as the Agreement Volume Index (AVI) were determined. The results showed that the lowest AVI (0.16) was found for one of the analysed metastases (range of delineated volumes 1.27-3.33 cm3 and AV50=2.94 cm3). The AVI for the other two metastases were 0.62 and 0.37, respectively. The corresponding AVIs for the cavernous sinus meningioma, pituitary adenoma and vestibular schwannoma were 0.22, 0.37 and 0.50. This study showed that the variability in the contouring was much higher than expected and therefore further work in standardizing the contouring practice in radiosurgery is warranted.

Poster #69

Christian Rønn Hansen, Odense, Denmark

Automatic treatment planning facilitates fast adaptive re-planning for oesophageal cancer treatments

Hansen CR1,2, Nielsen M1, Hazell I1, Bertelsen A1, Bjerregaard JK2,3, Zukauskaite R2,3, Holtved E3, Brink C1,2. 1. Laboratory of Radiation Physics, Odense University Hospital, Odense, Denmark 2. Institute of Clinical Research, University of Southern Denmark, Odense, Denmark 3. Department of Oncology, Odense University Hospital, Odense, Denmark.

Introduction The quality of radiotherapy (RT) planning has improved substantially in the last decade. However, changes in patient and tumour anatomy during RT potentially reduce these benefits. Adaptive RT (ART) handles this by plan adjustment when anatomical changes occur during RT. This is resource demanding and time consuming thus in order for ART to be feasible in the clinical setting automation is needed. The purpose of this study was to analyse the plan quality and efficacy of automatically (AU) generated VMAT plans for inoperable oesophagus cancer patients. Methods Thirty-two consecutive inoperable patients with oesophageal cancer originally treated with manually (MA) generated VMAT plans were retrospectively re-planned using the Autoplanning function in Pinnacle version 9.14. All plans were optimized according to local clinical practice with 60 Gy to primary target and 50 Gy to the elective target. The planning techniques were blinded before clinical evaluation by three specialised oncologists. To supplement the clinical evaluation the optimization time for the AU plan was recorded along with DVH parameters for all plans. All statistical analyses were performed with a paired Wilcoxon-signed rank test. Results Upon clinical evaluation the AU plan was preferred for 24/32 patients and the MA plan preferred for 3/32 patients. In terms of DVH parameters similar target coverage was obtained between the two planning methods. The mean dose for the spinal cord increased using AU (MA = 16.4Gy, AU = 18.2Gy, p = 0.003) whereas the mean lunge dose decreased (MA = 10.0Gy, AU = 8.1Gy, p = <0.001). The AU plans were more modulated as seen by the increase in mean MUs (MA = 301MU, AU =338MU, p = 0.001). The median optimization time for AU plans was 117 min. Conclusions The AU plans were in general preferred and showed a lower mean dose to the lungs. The automation of the planning process may allow for ART plans to be generated quickly and with high quality using AU.

Poster #70

Chris Monten, Ghent, Belgium

Prone breast irradiation: Can we improve precision and accuracy of tumor bed delineation?

Monten C., Veldeman L., Vandecasteele K., Oltéanu L., De Gersem W., Vercauteren T., Mulliez T., Van Den Broecke R., De Neve W., Y. Lievens. Department of radiation oncology, Ghent University Hospital, Ghent, Belgium.

Introduction: Due to changes in position and anatomy, prone breast irradiation challenges correct tumor bed delineation, necessary for boost or external beam partial breast irradiation. A geometrical delineation protocol (GDP) was tested to improve accuracy and precision for prone breast irradiation after breast conserving surgery with full thickness closure. Materials and methods: In 12 patients, tumor bed delineation was performed by 4 radiation oncologists in accordance with a GDP, based on preoperative CT and surgical placement of an easily distinguishable indicator-clip during tumorectomy. A 20mm symmetric expansion of the center between preoperative tumor and indicator-clip, minus the minimal resection margin, resulted in a CTV-GDP. This method was compared with standard delineation (CTV-standard), which is based on delineation guidelines using clips, seroma and tissue distortion. To assess accuracy, overlap of delineated volumes with preoperative GTV and distance between indicator-clip and GTV were calculated. Delineated volumes were compared with preoperative tumor location for sensitivity, miss rate and undue toxicity. Precision was measured through an interobserver exercise. Minimal distance of CTV's to heart and lungs was calculated. Results: Overlap coefficient (0.88 vs. 0.48, p=0.002), sensitivity (0.72 vs. 0.33, p=0.003) and miss rate (0.28 vs. 0.67, p=0.003) were in favor of GDP. Delineation precision improved with GDP (CI-pairs 0.59 versus 0.38, p=0.004). Mean distance between indicator-clip and preoperative GTV was 7mm. Volumes were larger for CTV-GDP than for CTV-standard (29.0 vs. 16.9, p=0.02), but located significantly closer to lungs and heart. Conclusion: A GDP, based on preoperative imaging and introduction of an indicator-clip improved accuracy and precision and facilitated avoidance of undue toxicity in the context of prone breast irradiation, where the use of standard delineation guidelines is hampered by anatomical distortion.

Poster #71

Cecile Wolfs, Maastricht, The Netherlands

Dosimetric consequences of simulated anatomical changes in lung cancer patients

Wolfs, C.J.A.; Brás, M.G.; Gil Conde, M.; Schyns, L.E.J.R.; Nijsten, S.M.J.J.G.; Podesta, M.; Verhaegen, F. Department of Radiation Oncology (MAASTRO), GROW – School for Oncology and Developmental Biology, Maastricht University Medical Centre+, Maastricht, The Netherlands.

Introduction Anatomical changes during the course of radiotherapy treatment can affect the dose to the target volume and to organs-at-risk (OARs). The severity of dose deviations due to simulated anatomical changes was investigated to determine when clinically relevant changes occur and whether they can be detected using electronic portal imaging device (EPID) dosimetry methods. Materials and methods For 6 lung cancer patients, tumor shift, tumor regression and pleural effusion were simulated to varying extents by modifying the patients' planning CT. 2D time-integrated and 2D time-resolved portal dose images, as well as 3D time-integrated doses were calculated for each modified CT. These were compared to the portal and 3D doses of the original CT using DVH and gamma analysis with several gamma criteria. Relative deviations in D95% of the GTV and Dmean, Dmax, D0.03cc and D2% of the spinal cord, heart, PRV mediastinum and lungs minus GTV were calculated. A deviation was considered significant if it exceeded 4%. Gamma analysis results were expressed as gamma fail rate (i.e. the fraction of pixels/voxels exceeding $|\gamma|\geq 1$). Results Simulated anatomical changes in lung cancer patients induce significant deviations in dose to the GTV, but not in the dose to OARs. Absolute deviations in dose to OARs could give more insight, as a small deviation may already cause an OAR to exceed its dose constraint. Correlations between D95% of the GTV and gamma fail rate were present for individual patients, but not for all patients as a group. The optimal combination of EPID dosimetry method and gamma criteria to detect significant deviations depended on the type of anatomical change. Conclusion Errors detected by EPID dosimetry methods can be used to predict patient dose errors, and as such inform clinical decision models for adaptive radiotherapy. However, these models should be contextualized to anatomical site and type of change, as no single method can detect all anatomical changes.

Poster #72

Yvonka van Wijk, Maastricht, the Netherlands

Development of a virtual spacer for a multifactorial decision support system for prostate cancer radiotherapy: Comparison of dose, toxicity and cost-effectiveness

van Wijk, Y; Vanneste, B.G; Walsh, S; van der Meer, S; Ramaekers, B.L.T.; van Elmpt, W; Pinkawa, M; Lambin, P. Department of Radiation Oncology (MAASTRO clinic), GROW - School for Oncology and Developmental Biology, Maastricht University Medical Center, Maastricht, The Netherlands; Department of Clinical Epidemiology and Medical Technology Assessment (KEMTA) Maast.

Introduction: Previous studies have shown that the implantable rectum spacer (IRS) can reduce gastrointestinal toxicity during external beam radiotherapy on patients with prostate cancer, but is not necessary for all patients. To tailor the decision of an IRS implementation to individual patients, virtual IRS (V-IRS) was constructed to help identify the patients for whom it is cost-effective to implant an IRS. See animation for more details: http://j.tinyurl.com/rectumspacer. Methods: The V-IRS was tested on 16 patients: 8 with a rectal balloon implant (RBI) and 8 with a hydrogel spacer. A V-IRS was developed using 7 computed tomography (CT) scans of patients with a RBI. To examine the V-IRS, CT scans before and after the implantation of an IRS were used and compared on dose, toxicity and cost-effectiveness level. IMRT plans were performed based on CT scans before the IRS, after IRS and with the V-IRS, prescribing 70 Gray (Gy) to the planning target volume. Toxicity was accessed using externally validated normal tissue complication probability (NTCP) models, and the Cost-effectiveness was analyzed using a published Markov model. Results: The rectum volume receiving 75 Gy was reduced by both the IRS and the V-IRS with on average 4.2% and 4.3% respectively. The largest NTCP reduction resulting from the IRS and the V-IRS was 4.0% and 3.9% respectively. The RBI was cost-effective for 1 out of 8 patients (12,5 %), and the hydrogel was effective for 2 out of 8 patients (25 %), and close to effective for a third patient. The classification accuracy of the model, regarding cost-effectiveness, was 100%. Conclusion: The V-IRS approach in combination with a toxicity prediction model and a cost-effectiveness analyses is a promising basis for a multifactorial decision support system regarding the implantation of either a hydrogel spacer or a rectum balloon implant. This method would enable oncologists to optimize individualized treatment decisions.

Poster #73

Iosif Papoutsis, Oslo, Norway

From dose prescription to dose delivery - can dose painting by numbers be accurately delivered?

Papoutsis I, Arnesen MR, Sande EPS, Sagstuen E, Knudtsen IS, Malinen E. University of Oslo / Oslo University Hospital, Oslo, Norway.

Introduction Dose painting by numbers (DPBN) is a radiotherapy (RT) technique where tumor doses are prescribed voxel-by-voxel according to intensity values in 3D biological image series. The approach may require an extreme degree of dose modulation over the tumor, and it is thus important to verify whether prescribed doses can be safely delivered to a realistic geometry. Materials and methods Using an in-house procedure, full voxelwise DPBN was planned on a Varian TrueBeam linear accelerator for a patient with lung cancer. [18F]FDG-PET/CT was taken prior to RT. A linear RT dose prescription based on PET intensity was employed. One plan with relatively low tumor dose modulation (Plan_L; 40 % modulation) and one with higher degree of modulation (Plan_H; 50 %) were generated. Plans were transferred to a CT scan of an anthropomorphic thorax phantom based on the patient. DPBN was then delivered to the phantom, holding alanine dosimeters in well-defined positions, at the given accelerator. Plan_L was also delivered to an intentionally misaligned phantom (Plan_E; 9 mm error). Delivered tumor doses were measured by EPR dosimetry. Quality factors (QFs) were used to evaluate the DPBN planning and delivery. Results The mean prescribed, planned and delivered fraction dose was (3.59, 3.56, 3.50) Gy and (3.49, 3.47, 3.44) Gy for Plan_L and Plan_H, respectively. The mean absolute point dose difference between prescription and delivery was typically 0.1 Gy. For Plan_E, the mean delivered tumor dose dropped with 8% compared to Plan_L. QFs for prescription->plan, plan->delivery, prescription->delivery were (2.0, 2.3, 3.1), (1.7, 1.9, 2.8) and (2.0, 7.7, 7.8) for Plan_L, Plan_H and Plan_E, respectively. Conclusions DPBN can be delivered with rather high accuracy to a static, patient-based lung phantom. The step from plan to delivery seems to be associated with the greatest dose degradation. Geometric errors cause considerable degradation of the DPBN profile in the tumor.

Poster #74

Paulo Magalhaes Martins, Heidelberg, Germany

Fast full-body reconstruction for a functional human RPC-PET imaging system using list-mode simulated data and its applicability to radiation oncology and radiology

Magalhaes Martins P., Crespo P., Couceiro M., Ferreira, N. C., Ferreira Marques, R., Seco J., Fonte P. Department of Medical Physics in Radiooncology, German Cancer Research Center - DKFZ, Heidelberg, Germany; Institute of Biophysics and Biomedical Engineering - IBEB, Lisbon, Portugal; Laboratory of Instrumentation and Experimental Particle Physics - LIP.

Background: Single-bed whole-body positron emission tomography based on resistive plate chamber detectors (RPC-PET) has been proposed for human studies, as a complementary resource to scintillator-based PET scanners. The purpose of this work is mainly about providing a reconstruction solution to such whole-body single-bed data collection on an event-by-event basis. We demonstrate a fully three-dimensional time-of-flight (TOF)-based reconstruction algorithm that is capable of processing the highly inclined lines of response acquired from a system with a very large axial field of view, such as those used in RPC-PET. Such algorithm must be sufficiently fast that it will not compromise the clinical workflow of an RPC-PET system. Material and methods: We present simulation results from a voxelized version of the anthropomorphic NURBS-based cardiac-torso (NCAT) phantom, with oncological lesions introduced into critical regions within the human body. The list-mode data was reconstructed with a TOF-weighted maximum-likelihood expectation maximization (MLEM). To accelerate the reconstruction time of the algorithm, a multi-threaded approach supported by graphical processing units (GPUs) was developed. Additionally, a TOF-assisted data division method is suggested that allows the data from nine body regions to be reconstructed independently and much more rapidly. Results and Conclusions: The application of a TOF-based scatter rejection method reduces the overall body scatter from 57.1% to 32.9%. The results also show that a 300-ps FWHM RPC-PET scanner allows for the production of a reconstructed image in 3.5 minutes following a 7-minute acquisition upon the injection of 2 mCi of activity (146 M coincidence events). We present for the first time a full realistic reconstruction of a whole body, long axial coverage, RPC-PET scanner. We demonstrate clinically relevant reconstruction times comparable (or lower) to the patient acquisition times on both multi-threaded CPU and GPU.

Poster #75

Jose A Baeza Ortega, Maastricht, The Netherlands

Validation and uncertainty analysis of a pretreatment prediction model for EPID dosimetry

Baeza J.A., Wolfs C.J.A., Nijsten S.M.J.J.G., Verhaegen F. Department of Radiation Oncology (MAASTRO), GROW - School for Oncology and Developmental Biology, Maastricht University Medical Centre, Maastricht, The Netherlands.

Introduction: Independent verification of complex treatment delivery using the electronic portal imaging device (EPID) has been pursued to detect and prevent errors in radiation therapy. This work presents the validation and uncertainty analysis of a model that predicts 2D portal dose images at the EPID level, without a patient or phantom in the beam. Materials and Methods: The prediction model is based on an exponential point dose model with separable primary and secondary components, which uses an input fluence matrix calculated by taking into account the different linac head components. The model includes a scatter kernel, off axis ratio map, transmission values and penumbra kernels for jaws and MLC leaves, and tongue and groove (TG) and dosimetric leaf gap (DLG) width factors. These parameters were derived through a model fitting procedure fed with point dose and profile measurements of fields with a range of complexity. A measured head scatter factor correction was included as well. The model was validated against the Eclipse TPS (Varian Medical Systems) for complex clinical scenarios (including VMAT). To estimate the uncertainty of the model, a sensitivity analysis was performed by varying fitted parameter values and determining the effect on the model output for several fields. For the most sensitive parameters, the uncertainty of the fit was evaluated. Results: The validation of the prediction model against the TPS showed a good agreement, with more than 99% of pixels passing a (3%,3mm) global gamma analysis in both static and dynamic plans. Preliminary results of the uncertainty analysis show that for jaw-defined fields, the scatter kernel parameters are most sensitive. With MLC-defined fields, the TG and DLG factors become more pronounced. Conclusion: A model for predicting accurate 2D portal dose images in complex RT scenarios is validated and clinically used as a benchmark for EPID pretreatment measurements.

Poster #76

Ebbe Lorenzen, Odense, Denmark

Automatic treatment planning of FFF VMAT for breast cancer: fast planning and fast treatment

Lorenzen E.L., Gottlieb K.L., Veldhuizen E.V., Jensen H.R.,Hansen C.R. Laboratory of Radiation Physics, Odense University Hospital, Odense, Denmark.

Introduction Forward planned tangential radiotherapy is the standard technique used in many centres for breast cancer radiotherapy. Helical techniques such as VMAT can be used to increase conformity but are less robust to anatomical changes and the treatment planning can be time-consuming. In the present study, we evaluate FFF VMAT using automated planning by comparison with manually planned tangential radiotherapy. Materials and methods Twenty patients, ten right-sided and ten left-sided, were selected by including all patients receiving partial breast radiotherapy in a three month period. All patients were treated with forward planned tangential fields. For each patient, an additional plan was generated, using two small (30-40 degrees) 6 MV FFF VMAT fields with tangential like beam angels. Dose planning was done in Pinnacle 9.10 and Autoplan was used for generation of the VMAT plans. Results VMAT plans were generated fast with a median time of 10.5 min (range: 9 min – 12 min). The doses to organs at risk were similar from both plans except for the dose to the ipsilateral lung being significantly lower from the VMAT plans. The dose to ipsilateral lung was lower for all dose levels in the VMAT plans even though the coverage of the PTV was better. The mean delivery time of all VMAT fields were 14,5 s (range: 10 s -22 s). As a result, all VMAT plans could be delivered within two breath holds. In comparison the median number of breath holds required for the forward planned treatment was 4 (range: 2 – 7). Conclusions Autoplan in Pinnacle allowed fast planning of FFF VMAT plans for breast cancer radiotherapy. Compared to forward planned tangential radiotherapy the VMAT plans were better at both sparring of the ipsilateral lung and in covering the PTV. The VMAT plans could be delivered quickly, and as a result patients treated in breath hold could be treated with half the number of breath holds.

Poster #77

Esben Svitzer Yates, AArhus, Denmark

Total Body Irradiation – patient in vivo dosimetry.

Yates ES1, Hansen J1, Rose HK2, Safwat AA. 1 Department of Medical Physics, Aarhus University Hospital, 2 Department of Oncology, Aarhus University Hospital.

Introduction: Hematopoietic stem cell transplantation (HSCT) is a potentially curative treatment in certain hematological diseases, such as acute leukaemias, transformed lymphomas and Hodgkins disease. Conditioning can be either myelablative chemotherapy or a combination of chemotherapy and total body irradiation (TBI). The role of TBI in conjunction with chemotherapeutic agents is to destroy malignant or genetically disordered cells and to immunosuppress the patient prior to HSCT. A new TBI technique with 2 open opposite fields, several segments with MLC compensation and SSD 400 cm was introduced in our department. Materials and methods: Between October 2015 and February 2017, 15 patients (eight females and seven males) were treated with TBI 12.5 Gy/7 fractions. The average age was 48,6 years (ranging from 18-68). Five of them had an allogenic transplantation, ten of them had an autologous. The thermo luminescent dosimeters (TLD) was used as the standard detector for patient in vivo dosimetry. In vivo dosimetry was carried out by pasting TLD dosimeters at multiple sites throughout the patient body to measure the dose received. All TLD dosimeters was placed behind build up plates. The entrance dose was measured on the first fraction. Results: The patient doses were measured on head, hips, knees and between knees varied between 96% to 109% of the prescribed dose. The minimum lung dose was 79% of the prescribed dose. The reason for the low lung dose was because of a maximum mean lung dose should be less than 11 Gy, and the total body dose is between 11,25 Gy and 15 Gy of the prescribed dose. There was also a coherence between the patients thickness and measured entrance dose. Conclusion: The practice of using TLD dosimeters for in vivo dosimetry was a good option for TBI dosimetry, however it is very time consuming. It is still necessary to find a calculation method to compare in vivo dosimetry with calculated patient central axe dose for TBI planning.

Poster #78

Marie Louise Milo, Aarhus, Denmark

Pectus excavatum and adjuvant radiotherapy for early breast cancer: is the heart an issue?

Milo MLH(1), Spejlborg H(2), Thorsen LBJ(1), Offersen BV(1). (1)Department of Oncology, Aarhus University Hospital, Denmark, (2) Department of Medical Physics, Aarhus University Hospital, Denmark.

Introduction. Pectus excavatum (PE) is a chest wall deformity representing a challenge for adjuvant radiotherapy (RT) in patients with early-stage breast cancer. This study aimed to evaluate the suitability of 3-dimensional conformal radiotherapy (3D-CRT) for treatment planning in this patient group. Materials and methods. During 2013-2017, 18 consecutive early breast cancer patients with PE were referred for adjuvant RT. All target delineation was based on the ESTRO consensus for target delineation (thus CTVn_IMN included IC3). For each patient, an initial 3D-CRT dose plan based on standard field arrangements was made. The plan ensured optimal dose to targets, accepted a lung dose up to maximum constraint and did not spare the heart. Subsequently, a dose plan was made by modifying the initial plan to respect normal tissue constraints, while maintaining an acceptable (but lower) target coverage, and this plan was approved for treatment. The two plans were compared with focus on dose to heart. All therapies were based on 40 Gy/15fr. Results. Dose coverage to the breast/chest wall was identical for the two plans with a minimum V95 of 95%. The median V90 to CTVn_IMN for left-sided breast cancer was 98.9% (range, 92.5% to 99.3%) for the initial plan compared with 87.8% (64.7% to 94.9%) for the approved plan. Median Mean heart dose (MHD) for left-sided breast cancer with nodal irradiation was 3.1 Gy (2.7 Gy to 3.8 Gy) for the initial plan and 1.4 Gy (1.3 Gy to 2.2 Gy) for the approved plan. Conclusion. It was possible to achieve an acceptable coverage to CTVp_breast/chest wall and lymph nodes including IMN with the use of 3D-CRT when accepting a dose up to maximum constraint for ipsilateral lung. The compromise was on PTV, thus indicating less robustness of the approved plan. MHD was higher in the initial plan than the approved plan, but compared with MHD reported in women without PE it was relatively low.

Poster #79

Manjit Dosanjh, Geneva, Switzerland

Collaborative strategies for meeting global needs for affordable, high quality radiation therapy (RT) treatment

Dosanjh M, Pistenmaa D A, Coleman C N. CERN, Geneva, Switzerland; International Cancer Expert Corps, Washington, DC, USA.

BACKGROUND: Annual global cancer incidence will increase from 15 million in 2015 to 25 million in 2035, two-thirds will occur in low- and middle-income countries (LMICs). Recent estimates from IAEA and Global Task Force for Radiation for Cancer Control for UICC are a shortage of at least 5000 RT units globally, a lack of trained technical and support personnel and lack of physical infrastructure. METHODS: Meeting the need for affordable equipment, high quality expertise and sustainable infrastructure for high quality cancer care in LMICs is a core mission of ICEC (iceccancer.org). A brainstorming with leading experts from key international bodies, research institutes, universities, hospitals and RT companies to discuss needs, goals and possible solutions by ICEC & CERN. A major challenge is designing a linear accelerator system that works well in LMICs.
RESULTS: Following the workshop, an oversight committee and 3 task forces were established: (cerncourier.com/cws/article/cern/67710). 1.Technology task force: stimulate innovation in RT technologies and systems. Near-term - develop optimal design requirements for novel, high quality, lower cost treatment solutions; long-term - identify shortfalls in existing critical subsystems and stimulate development of next generation solutions. 2.Education, training and mentoring: identify requirements for current as well as future novel treatment systems. 3.Global connectivity: improve global connectivity of cancer control efforts and develop strategies for securing financial support for the task forces. FUTURE: Aim is to make treatment available for cancer patients in LMICs and underserved regions in the next 5–10 years with geometric expansion thereafter to meet the projected need of improving access to RT worldwide as an integral part of cancer control. This requires broad multi-sector collaboration and sustainable investment.

Poster #80

Virginia Greco, Geneva, Switzerland

ENLIGHT (European Network for Light Ion Hadron Therapy): a network to foster collaboration and train experts in hadrotherapy

Dosanjh M., Greco V. CERN.

1. Introduction ENLIGHT was launched in 2002 to build an international multidisciplinary platform where participants could collaborate, share knowledge, innovate and train the future generation. It continues to play a key role in the development, communication and education of highly professionals in this cutting edge technological field. 2. Materials and methods ENLIGHT has created a pan-European platform coordinating and catalysing efforts in hadrontherapy, bringing together diverse communities. Since networking and information sharing is key to enhancing progress, ENLIGHT organises an annual meeting highlighting the latest developments open to all the community. It also aims to offer to young researchers a high-level multidisciplinary training that will make them the experts of tomorrow and specialized training for advanced researchers to keep up with the progress in field. ENLIGHT also reaches out to community through the HIGHLIGHTS magazine, news publications and website enlight.web.cern.ch. 3. Results ENLIGHT is now 15 years old and can count on a strong support from over 600 members in over 100 institutes from more than 20 countries. Thanks to its effort, experts and researchers working on different areas of this field have established a fruitful collaboration and many researchers have been trained. Efforts are underway to have the ENLIGHT education and training programme included in the CERN & Society Foundation, which would allow it to become a self-sustaining section. 4. Conclusions ENLIGHT has played and continues playing a key role in the development and dissemination of hadrontherapy, as well as in the education of future experts. Maintaining ENLIGHT and nurturing its potential would allow the community to expand geographically, increase its activities and educate future and current professionals of the field.

Poster #81

Maja Bendtsen Sharma, Aarhus, Denmark

Simultaneous integrated prophylactic cranial irradiation in sino-nasal cancer

Sharma MB(a), Jensen K(a), Lenler-Eriksen S (b), Friis P (c), Holm AIS(d). (a) Department of Oncology, Aarhus University Hospital, Aarhus, Denmark. (b) Department of Pathology, Aarhus University Hospital, Aarhus, Denmark. (c) Department of otorhinolaryngology, Head and Neck Surgery, Aarhus University Hospital, Aarhus, Denmark.

Sinonasal cancer has a poor prognosis, particularly small cell carcinoma or high-grade neuroendocrine tumours (NET). These types of cancer tend to spread to the brain, and prophylactic cranial irradiation (PCI) is recommended. However, adding PCI after radiation therapy is complicated, as some areas of the brain will already have received radiation dose during the primary radiation therapy. Thus, integrated PCI may be an advantage. We present two cases with sinonasal cancer treated with radiotherapy and integrated PCI. Case 1: Male, 56 years of age. Diagnosed with T4aN2cM0 small cell NET originating in the left maxillary sinus. The patient received curative intended radiation therapy. Clinical tumor volume (CTV) was defined as gross tumor volume + 5 mm, and treated to 66 Gy in 33 fractions. Additional 5 mm plus the entire remaining left maxillary sinus received 60 Gy. In the last 14 fractions, the entire brain was treated to a total dose of 25.2 Gy. The patient experienced transient, but serious encephalitis symptoms. 10 months after initiation of radiation therapy, the patient had a local and distant recurrence, and he succumbed to the disease 6 months later. Case 2: Male, 55 years of age. Diagnosed with T4bN0M0 poorly differentiated non-small cell NET originating in the right nasal cavity. He was treated with operation and radiotherapy. CTV was treated to 60 Gy in 30 fractions and encompassed preoperative tumor extension plus 5 mm margin. Remaining involved sinuses and nasal cavity was treated to 54 Gy. The patient received integrated PCI similar to patient 1. No apparent side effects were observed. The patient was without sign of recurrence at the latest follow up 24 months after initiation of radiotherapy. Conclusion: Because of the superior conformity and homogeneity, integrated PCI could be beneficial for selected head and neck cancer patients with a high risk of intracerebral metastases and low dose radiation to the brain during primary treatment.

Poster #82

Jolanta Hansen, Aarhus, Denmark

Risk of developing radiation induced secondary malignancies in the thyroid glands after radiotherapy for a pediatric brain tumour.

Jolanta Hansen, Yasmin Lassen-Ramshad, Klaus Seiersen. Oncology Department, Aarhus University Hospital, Aarhus, Denmark.

Introduction: The thyroid gland is an organ of high sensitivity for radiation carcinogenesis in childhood. It has been reported that the thyroid doses as low as 100 mGy can lead to thyroid cancer introduction, and thyroid carcinoma may be a complication of radiotherapy, even when the tissue is located outside the treatment field. We investigated the risk of secondary cancer for the thyroid gland after radiation treatment of a childhood brain tumour. Material and Methods: A four year old boy with an infratentorial ependymoma was treated postoperatively in the tumour bed with photon IMRT radiotherapy, with 54 Gy/30. Cone-beam-CT-scan (CBCT) was used for each fraction. The delivered thyroid dose was measured with thermo luminescent dosimeters (TLD). A similar IMRT and a rotational VMAT plan was calculated on a 5-year-old anthropometric female phantom. Radiation doses given by the two plans in the thyroid were measured with TLD. The risk of secondary cancer was estimated in accordance to the BEIR VII rapport. Results: The total doses of the original treatment, for the thyroid gland was 4745 mGy, and for the phantom study 2196 mGy for the IMRT plan and 329 mGy for the VMAT plan. The estimated risk of secondary cancer to the thyroid by using the original treatment was 3.61 %. In the phantom study, the risk with IMRT in the thyroid was 1.67% (male)/ 9.20% (female). With VMAT the risk in the thyroid was 0.25% (male)/ 1.38% (female). CBCT added only 0.01% to the risk. Conclusion: For the original treatment, the estimated risk of secondary cancer was the highest in the thyroid gland, if calculated for females. For the phantom study, the risk was lower for VMAT than IMRT. CBCT had almost no contribution to the risk of secondary cancer. Studies are necessary to facilitate the estimation of the risk of secondary cancer in evaluation of pediatric radiotherapy treatment plans.

List of participants *(per June 6, 2017)*

Bonny Abal
Master's student
Faculty of Mathematics and Natural Sciences
University of Bergen
Bergen, Norway
bonny.abal@student.uib.no

Azadeh Abravan
PhD candidate
Physics
UiO
Oslo, Norway
azadeh.abravan@gmail.com

Nigel Allinson
Professor
Computer Science
University of Lincoln
Lincoln, United Kingdom
nallinson@lincoln.ac.uk

Jan Alsner
Professor, MSO
Department of Experimental Clinical Oncology
Aarhus University Hospital
Aarhus, Denmark
jan@oncology.au.dk

Ureba Ana
PostDoc
Karolinska University Hospital
Solna, Sweden
ana.ureba@ki.se

Margit Holst Andersen
Nurse and RTT
Dept. Of Oncology
Aarhus University Hospital
Aarhus, Denmark
margande@rm.dk

Flemming Littrup Andersen
Computer Scientist/Physicist
Dept. Clinical Phsiology, Nuclear Medicine & PET
Rigshospitalet
Copenhagen, Denmark
fling@rh.dk

Lena Andreasson Haddad
Manager Editor
Acta Oncologica
Solna, Sweden
lena.andreasson-haddad@actaoncologica.se

Christina Ankjærgaard
Researcher
DTU Nutech
Roskilde, Denmark
cank@dtu.dk

Lomax Antony John
Head of Medical Physics
Paul Scherrer Institute
Villigen, Switzerland
tony.lomax@psi.ch

Nina B. K. Jensen
MD, PhD-student
Dept. Of Oncology
Aarhus University Hospital
Aarhus, Denmark
nina.boje@rm.dk

Jose Antonio Baeza Ortega
Project physicist
Physics Innovation
MAASTRO clinic
Maastricht, The Netherlands
jose.baeza@maastro.nl

Emanuel Bahn
Postdoctoral Researcher
Abteilung für Radioonkologie und Strahlentherapie
Universitätsklinikum Heidelberg
Heidelberg, Germany
em.bahn@gmail.com

Niels Bassler
Assoc. Prof.
Stockholm University
Stockholm, Sweden
niels.bassler@gmail.com

Lise Bentzen
MD PhD
Dept. Of Oncology
Aarhus University Hospital
Aarhus, Denmark
lise@oncology.au.dk

Thomas Berger
PhD Student
Oncology
Aarhus University Hospital
Aarhus, Denmark
tomber@rm.dk

Patrick Berkovic
Radiation Oncologist
Radiation Oncology
Liège University Hospital
Liège, Belgium
p.berkovic@gmail.com

Jenny Bertholet
PhD student
Department of Oncology
Aarhus University Hospital
Aarhus, Denmark
jennbe@rm.dk

Aleksandra Biegun
Assistant professor
KVI-Center for Advanced Radiation Technology
University of Groningen
Groningen, The Netherlands
a.k.biegun@rug.nl

Rik Bijman
Researcher
Erasmus MC
Rotterdam, The Netherlands
r.bijman@erasmusmc.nl

Simon Boeke
Physician
Department of Radiation Oncology
University Hospital Tübingen
Tübingen, Germany
simon.boeke@med.uni-tuebingen.de

Marianne Brydøy
Oncologist
Haukeland University Hospital
Bergen, Norway
marianne.brydoy@helse-bergen.no

Kia Busch
Research Assistant
Department of Medical Physics
Aarhus University Hospital
Aarhus, Denmark
kiabus@rm.dk

Morten Busk
Associate professor
Experimental Clinical Oncology
Aarhus University Hospital
Aarhus, Denmark
morten@oncology.dk

Alessandro Cancelli
Medical resident
Dept. Of Oncology
Aarhus University Hospital
Aarhus, Denmark
alessandro_cancelli88@virgilio.it

Oscar Casares Magaz
Ph.D. Student
Dept. Of Oncology
Aarhus University Hospital
Aarhus, Denmark
oscar.casares@oncology.au.dk

Jeppe Brage Christensen
PhD Student
Center for Nuclear Technologies
DTU
Roskilde, Denmark
jepb@dtu.dk

Emma Colvill
Post doctoral researcher
Oncology
Aarhus University Hospital
Aarhus, Denmark
emmcol@rm.dk

Paulo Crespo
Assistant Professor
University of Coimbra
Coimbra, Portugal
crespo@lip.pt

Olav Dahl
Professor
University of Bergen
Bergen, Norway
olav.dahl@helse-bergen.no

Tordis Johnsen Dahle
PhD Candidate
Department of Physics and Technology
University of Bergen
Bergen, Norway
tordis.dahle@uib.no

Einar Dale
Senior consultant
Department of Oncology
Oslo University Hospital
Oslo, Norway
eindal@ous-hf.no

Evelyn de Jong
PhD student
Radiation Oncology (MAASTRO), GROW-School for Oncology and Developmental Biology
Maastricht University Medical Center
Maastricht, Netherlands
evelyn.dejong@maastro.nl

Dirk De Ruysscher
RTO
Maastro Clinic
Maastricht, The Netherlands
dirk.deruysscher@maastro.nl

Timo Deist
PhD student
Radiotherapy
MAASTRO\Maastricht University
Maastricht, The Netherlands
timo.deist@maastro.nl

Peter Dendooven
Associate Professor
KVI-Center for Advanced Radiation Technology
University of Groningen
Groeningen, The Netherlands
dendooven@kvi.nl

Greet D'Olieslager
Medical Physicist
Institute Verbeeten
Tilburg, The Netherlands
dolieslager.g@bvi.nl

Manjit DOSANJH
Senior Advisor for Medical Applications
AT-DO
CERN
Geneva, Switzerland
Manjit.Dosanjh@cern.ch

Pernille Elming
PhD student
Dept. of Experimental Clinical Oncology
Aarhus University Hospital
Aarhus, Denmark
pernille.elming@oncology.au.dk

Grete May Engeseth
RTT/dosimetrist
Haukeland University Hospital
Bergen, Norway
grete.may.engeseth@helse-bergen.no

Charlotte Espensen
PhD-fellow
Department of Oncology, Section of Radiotherapy
Rigshospitalet
Copenhagen, Denmark
charlotte.alfast.espensen@regionh.dk

Aniek Even
PhD student
Department of Radiation Oncology (MAASTRO)
GROW – School for Oncology and Developmental Biology, Maastricht University Medical Centre
Maastricht, The Netherlands
aniek.even@maastro.nl

Morten Egeberg Evensen
Dosimetrist
Oslo University Hospital
Oslo, Norway
the.quin@gmail.com

Marianne Falk
Hospitalsfysiker
Danish Centre for Particle Therapy
Aarhus University Hospital
Aarhus, Denmark
marianne.falk@rm.dk

Katherina Farr
MD, PhD
Department of Oncology
Aarhus University Hospital
Aarhus, Denmark
katherina@oncology.au.dk

Malene Fischer
Overlæge
Rigshospitalet
Copenhagen, Denmark
malene.fischer@regionh.dk

Lars Fredrik Fjæra
PhD Candidate
University of Bergen
Bergen, Norway
lars.fjera@uib.no

Mette Marie Fode
MD
Department of Oncology
Aarhus University Hospital
Aarhus, Denmark
mettfode@rm.dk

Lotte Fog
Medical physicist
Dept. of Oncology
Rigshospitalet
Copenhagen, Denmark
lotte.fog@regionh.dk

Maria Fuglsang Jensen
Medical physicist
Danish Centre for Particle Therapy
Aarhus University Hospital
Aarhus, Denmark
marfugje@rm.dk

Torbjørn Furre
Medical physicist
Radium hospital
Oslo university hospital
Oslo, Norway
torbjorn.furre@gmail.com

Martina Fuss
Postdoc
Biophysics Department
GSI Helmholtzzentrum für Schwerionenforschung
Darmstadt, Germany
m.fuss@gsi.de

Kristina Giske
Research group leader
Division of Medical Physics in Radiation Oncology
German Cancer Research Center
Heidelberg, Germany
k.giske@dkfz.de

Karina Lindberg Gottlieb
Physicist
Onkologisk afdeling
Radiofysisk Laboratorium
Odense, Denmark
karina.lindberg@rsyd.dk

Cai Grau
Professor
Dept. Of Oncology
Aarhus University Hospital
Aarhus, Denmark
caigrau@dadlnet.dk

Vincent Grégoire
Professor
Cliniques Universitaires Saint-Luc
Brussels, Belgium
vincent.gregoire@uclouvain.be

David Grosshans
Associate Professor
Radiation Oncology
The University of Texas MD Anderson Cancer Center
Houston, USA
dgrossha@mdanderson.org

Leszek Grzanka
Postdoc
Division of Applications of Physics
Institute of Nuclear Physics PAN
Krakow, Poland
leszek.grzanka@gmail.com

Akos Gulyban
Medical Physicist
Department of Radiation Oncology
University Hospital of Liege
Liege, Belgium
akos.gulyban@gmail.com

Lene Haldbo-Classen
M.D and ph.d student
Dept. Of Oncology
Aarhus University Hospital
Aarhus, Denmark
Lenhaldb@rm.dk

Steven Hancock
Applied Physicist
CERN
Geneva, Switzerland
steven.hancock@cern.ch

Anders Traberg Hansen
Hospital physicist
Oncology
Aarhus University Hospital
Aarhus, Denmark
andehans@rm.dk

David Hansen
Researcher
Oncology
Aarhus University Hospital
Aarhus, Denmark
daviha@rm.dk

Christian Rønn Hansen
Medical Physicist
Oncology
Aarhus University Hospital
Aarhus, Denmark
dypper@gmail.com

Adam Espe Hansen
PET/MRI physicist
Oncology
Aarhus University Hospital
Aarhus, Denmark
adam.espe.hansen@regionh.dk

Ate Haraldsen
Medical Doctor
Nuklearmedicine Department & PET Center
Aarhus Universityhospital
Aarhus, Denmark
karhar@rm.dk

Karin Haustermans
Radiation Oncology Department
Radiation Oncology Department
University Hopitals Leuven
Leuven, Belgium
liesbeth.jonckers@uzleuven.be

Jan Heggdal
Medical Physicist
Haukeland University Hospital
Bergen, Norway
Jan.Heggdal@helse-bergen.no

Thomas Henry
PhD Student
Department of Physics
Stockholm University
Stockholm, Sweden
thomas.henry@fysik.su.se

Lone Hoffmann
Medical Physicist
Oncology
Aarhus University Hospital
Aarhus, Denmark
Lone.hoffmann@aarhus.rm.dk

Sandra Hol
Radiation technologist
Institute Verbeeten
hol.s@bvi.nl

Katrine Holgersen
Student
Dept. Of Oncology
Aarhus University Hospital
Aarhus, Denmark
ksholgersen@gmail.com

Anne Holm
Medical Physicist
Medical Physics
Aarhus University Hospital
Aarhus, Denmark
annivaho@rm.dk

Mischa Hoogeman
Head of Physics
Erasmus MC Cancer Institute
Rotterdam, The Netherlands
m.hoogeman@erasmusmc.nl

Michael Horsman
Professor
Department of Experimental Clinical Oncology
Aarhus University Hospital
Aarhus, Denmark
mike@oncology.au.dk

Christian Hvid
MD, phd student
Department of Oncology
Aarhus University Hospital
Aarhus, Denmark
chrhvi@rm.dk

Ellen Marie Høye
PhD student
Department of Medical Physics
Aarhus University Hospital
Aarhus, Denmark
elhoey@rm.dk

Morten Høyer
Professor, medical director
Danish Centre for Particle Therapy
Aarhus University Hospital
Aarhus, Denmark
hoyer@aarhus.rm.dk

Ane Iversen
MD, PhD
Department of Experimental Clinical Oncology
Aarhus University Hospital
Aarhus, Denmark
ane.bundsbaek.iversen@oncology.au.dk

Michael Jackson
Radiation Oncologist
Prince of Wales Hospital
Randwick, Australia
michael.jackson2@health.nsw.gov.au

Kirsten Legård Jakobsen
Physicist
Herlev Hospital
Herlev, Denmark
Kirsten.Legaard.jakobsen@RegionH.Dk

Morten Jensen
Medical Physicist
Department of Oncology Medical Physics
Aarhus University Hospital
Aarhus, Denmark
mobjje@rm.dk

Kenneth Jensen
MD
Department of Oncology Medical Physics
Aarhus University Hospital
Aarhus, Denmark
kennjens@rm.dk

Nina Jeppesen
Researcher
University of Oslo
Oslo, Norway
nina@fys.uio.no

Arthur Jochems
Postdoctoral researcher
Radiotherapy
Maastricht University (Maastro clinic)
Maastricht, Netherlands
a.jochems@maastrichtuniversity.nl

Jørgen Johansen
Chief Physician
Dept. Of Oncology
Odense University Hospital
Odense, Denmark
jorgen.johansen@rsyd.dk

Bleddyn Jones
Professor
University of Oxford
Oxford, England
Bleddyn.Jones@oncology.ox.ac.uk

Morten Jørgensen
Overlæge
Rigshospitalet
Copenhagen, Denmark
morten.joergensen@regionh.dk

Jesper Kallehauge
Medical Physicist
Department of Medical Physics
Aarhus University Hospital
Aarhus, Denmark
jespkall@rm.dk

Maria Kandi
Clinical Oncologist
Oncology department
Aarhus University Hospital
Aarhus, Denmark
marikand@rm.dk

Leonhard Karsch
Physicist
OncoRay
TU Dresden
Dresden, Germany
Leonhard.Karsch@oncoray.de

Azza Khalil
Consultant
Dept. Of Oncology
Aarhus University Hospital
Aarhus, Denmark
azzakhal@rm.dk

Kathrin Kirchheiner
Clinical psychologist, Research
Medical University of Vienna
Vienna, Austria
kathrin.kirchheiner@meduniwien.ac.at

Eva Bruun Kjærsgaard
RTT/ Nurse
Dept. Of Oncology
Aarhus University Hospital
Aarhus, Denmark
evakjaer@rm.dk

Marianne Knap
Dr
Department of Oncolgy
Aarhus University Hospital
Aarhus, Denmark
mariknap@rm.dk

Antje-Christin Knopf
Associate Professor
University Medical Center
Groningen
The Netherlands
a.c.knopf@umcg.nl

Ingerid Skjei Knudtsen Knudtsen
Postdoctoral fellow
Oslo University Hospital
Oslo, Norway
bingbingeling@hotmail.com

Lydia Koi
PostDoc
Dept. of Rad. Oncology and OncoRay – Natl. Center f. Rad. Research in Oncology
Institut for Radiotherapy
Dresden, Germany
Lydia:koi@ukdd.de

Stine Korreman
Associate professor
Department of Oncology
Aarhus University Hospital
Aarhus, Denmark
stine.korreman@oncology.au.dk

Mechthild Krause
Director, Dept. of Radiation Oncology and OncoRay
Dept. of Radiation Oncology and OncoRay
University Hospital Dresden
Dresden, Germany
mechthild.krause@uniklinikum-dresden.de

Anne Kristensen
RN & RTT
Danish Centre for Particle Therapy
Aarhus University Hospital
Aarhus, Denmark
annkrs@rm.dk

Camilla Kronborg
Afdelingslæge
Dept. Of Oncology
Aarhus University Hospital
Aarhus, Denmark
camkro@rm.dk

Anna Kuisma
Medical Doctor
Oncology and Radiotherapy
Turku University Hospital
Turku, Finland
ankahi@utu.fi

Ferenc Lakosi
Radiation Oncologist
Institute of Imaging and Radiation Oncology
Kaposvar University
Kaposvar, Hungary
lakosiferenc@yahoo.com

Philippe Lambin
Prof. of Radiation Oncology
Maastricht University
Maastricht, The Netherlands
philippe.lambin@maastro.nl

Andrea Lancia
Resident Physician
Department of Diagnostic Imaging, Molecular Imaging, Interventional Radiology and Radiotherapy
Tor Vergata University Hospital
Rome, Italy
andrea.lancia@alice.it

Mette Lange
Medical secretary
Dept. Of Oncology
Aarhus University Hospital
Aarhus, Denmark
metejens@rm.dk

Ruben Larue
PhD student
Department of Radiotherapy (Maastro Clinic)
Maastricht University Medical Center
Maastricht, The Netherlands
ruben.larue@maastro.nl

Tinne Laurberg
MD
Dep. of Experimental Clinical Oncology
Aarhus University Hospital
Aarhus, Denmark
tinnelaurberg@gmail.com

Louise Laursen
Academic coordinator
Dept. of Oncology
Aarhus University Hospital
Aarhus, Denmark
louise@oncology.au.dk

Marta Lazzeroni
Post Doc
Oncology-Pathology
Karolinska Institutet
Stockholm, Sweden
marta.lazzeroni@ki.se

Stefan Leger
PhD Student
OncoRay - National Center for Radiation Research in Oncology
Faculty of Medicine and University Hospital C. G. arus, TU Dresden, HZDR Dresden
Dresden, Germany
Stefan.Leger@oncoray.de

Ralph Leijenaar
PhD candidate
Department of Radiation Oncology
MAASTRO clinic
Maastricht, The Netherlands
ralph.leijenaar@maastro.nl

Yolande Lievens
Chair Radiation Oncology
UZ Gent
Gent, Belgium
yolande.lievens@uzgent.be

Jacob Lilja-Fischer
PhD student
Experimental Clinical Oncology
Aarhus University Hospital
Aarhus, Denmark
jacob@oncology.au.dk

Emely Lindblom
PhD student
Medical Radiation Physics
Department of Physics
Stockholm, Sweden
emely.lindblom@ki.se

Jacob Christian Lindegaard
Consultant
Department of Oncology
Aarhus University Hospital
Aarhus, Denmark
jacolind@rm.dk

Christina Maria Lutz
PhD student
Dept. of Oncology
Aarhus University Hospital
Aarhus, Denmark
chrilutz@rm.dk

Armin Lühr
Postdoctorial fellow
OncoRay - National Center for Radiation Research in Oncology
Helmholtz-Zentrum Dresden Rossendorf
Dresden, Germany
armin.luehr@oncoray.de

Simon Lønbro
Post.Doc.
Dept. of Experimental Clinical Oncology
Aarhus University Hospital
Aarhus, Denmark
loenbro@oncology.au.dk

Faisal Mahmood
Physicist, senior researcher
Oncology
Herlev and Gentofte Hospital
Herlev, Denmark
fama@regionh.dk

Eirik Malinen
Professor
University of Oslo
Oslo, Norway
eirik.malinen@fys.uio.no

Anfinn Mehus
Chief physicist
Department of Onkology and medical physics
Helse Bergen
Bergen, Norway
anfinn.mehus@helse-bergen.no

Marie Louise Milo
Doctor
Oncology
Aarhus University Hospital
Aarhus, Denmark
maeols@rm.dk

Radhe Mohan
Professor
MD Anderson Cancer Center
University of Texas
Houston, USA
rmohan@mdanderson.org

Gracinda Mondlane
PhD Student
Department of Physics, Medical Radiation Physics
Stockholm University
Stockholm, Sweden
gracinda.mondlane@fysik.su.se

Chris Monten
Research fellow
Radiation oncology
Ghent University Hospital
Ghent, Belgium
chrisje.monten@gmail.com

Anni Morsing
Overlæge
Rigshopsitalet
Copenhagen, Denmark
anni.morsing@regionh.dk

Dorte Oksbjerre Mortensen
Head Nurse RTT
Danish Centre for Particle Therapy
Aarhus University Hospital
Aarhus, Denmark
dortmort@rm.dk

Lise Saksø Mortensen
Medical doctor, phd
Dept. of Oncology
Aarhus University Hospital
Aarhus, Denmark
lisesaksoe@gmail.com

Ludvig Paul Muren
Professor
Dept. of Oncology
Aarhus University Hospital
Aarhus, Denmark
ludvmure@rm.dk

Johannes Müller
Phd Student
OncoRay – National Center for Radiation Research in Oncology
Faculty of Medicine and University Hospital Carl Gustav Carus, Technische Universität Dresden, Germany, Helmholtz-Zentrum Dresden – Rossendorf, Institute of Radiooncology, Dresden, Germany
Dresden, Germany
johannes.mueller@uniklinikum-dresden.de

Ditte Sloth Møller
Medical Physicist
Department of Medical Physics
Aarhus University Hospital
Aarhus, Denmark
dittmoel@rm.dk

Marta Nesteruk
PhD student
University Hospital Zurich
Zurich, Switzerland
marta.nesteruk@usz.ch

Nina Niebuhr
PhD Student
Medical Physics is Radiation Oncology
German Cancer Research Center (DKFZ)
Heidelberg, Germany
n.niebuhr@dkfz-heidelberg.de

Steffen Nielsen
PhD student
Department of Oncology/DTU Compute
Herlev Hospital / Technical University of Denmark
Herlev/Lyngby, Denmark
steffen.nielsen@oncology.au.dk

Morten Nielsen
Physicist
Department of Oncology/DTU Compute
Herlev Hospital / Technical University of Denmark
Herlev/Lyngby, Denmark
morten.nielsen@rsyd.dk

Jane Nielsen
Physicist
Department of Oncology/DTU Compute
Herlev Hospital / Technical University of Denmark
Herlev/Lyngby, Denmark
jan@rn.dk

Jonathan Scharff Nielsen
PhD candidate
Department of Oncology/DTU Compute
Herlev Hospital / Technical University of Denmark
Herlev/Lyngby, Denmark
josni@dtu.dk

Ole Noerrevang
Head Physicist
Danish Centre for Particle Therapy
Aarhus University Hospital
Aarhus, Denmark
olenoerr@rm.dk

Marianne Nordsmark
Overlæge
Dept. of Oncology
Aarhus University Hospital
Aarhus, Denmark
Marnor@rm.dk

Kinga Nowicka-Matus
1. Reservelæge
Onokologisk Afdeling
Aalborg University Hospital
Aalborg, Denmark
k.nowicka-matus@rn.dk

Tine Bisballe Nyeng
Medical Physicist
Department of Oncology, Medical Physics
Aarhus University Hospital
Aarhus, Denmark
tinenyen@rm.dk

Birgitte Offersen
MD
Dept. of Oncology
Aarhus University Hospital
Aarhus, Denmark
birgoffe@rm.dk

Lise Marie Olsen
Hospitalsfysiker
Aalborg University Hospital
Aalborg, Denmark
limao@rn.dk

Wiviann Ottosson
Medical Physicist, Ph.D.
Department of Oncology
Herlev Hospital
Herlev, Denmark
wivott01@heh.regionh.dk

Jens Overgaard
Professor
Dept. of Experimental Clinical Oncology
Aarhus University Hospital
Aarhus, Denmark
jens@oncology.au.dk

Ikechi Ozoemelam
PhD student
KVI-CART
University of Groningen
Groningen, Netherlands
i.s.ozoemelam@rug.nl

Harald Paganetti
Professor; Director of Physics Research
Massachusetts General Hospital
Boston, USA
hpaganetti@mgh.harvard.edu

Iosif Papoutsis
Student
Department of Physics
University of Oslo
Oslo, Norway
iopapout@physics.auth.gr

Katia Parodi
Professor, Department Head
Ludwig-Maximilians-Universität
München, Germany
katia.parodi@lmu.de

Erik Morre Pedersen
Consultant, Assoc Prof.
Department of Medical Physics
Aarhus University Hospital
Aarhus C, Denmark
erikpede@rm.dk

Jesper Pedersen
Ph.D. student
Department of Medical Physics
Aarhus University Hospital
Aarhus C, Denmark
jespe3@rm.dk

Jurgen Peerlings
Phd candidate
Department of Radiation Oncology (MAASTRO),
GROW - School for Oncology and Developmental Biology
Maastricht University Medical Center+
Maastricht, The Netherlands
jurgen.peerlings@maastro.nl

Marta Peroni
Imaging Physicist
Proton Therapy Center
Paul Scherrer Institut
Villigen PSI, Switzerland
marta.peroni@psi.ch

Stine Elleberg Petersen
M.D.
Dept. of Oncology
Aarhus University Hospital
Aarhus, Denmark
stinpete@rm.dk

Jørgen BB Petersen
Medical Physicist
Dept. of Medical Physics
Aarhus University Hospital
Aarhus, Denmark
joerpete@rm.dk

Stefan Pieck
Scientific Coordinator / Admin. Director
OncoRay
University Hospital Dresden
Dresden, Germany
Stefan.Pieck@oncoray.de

Richard Poetter
Emeritus Professor
University of Vienna
Vienna, Austria
richard.poetter@akhwien.at

Per Poulsen
Associate Professor
Department of Oncology
Aarhus University Hospital
Aarhus, Denmark
per.poulsen@rm.dk

Yolanda Prezado
Scientist
IMNC
CNRS
Orsay, France
prezado@imnc.in2p3.fr

Toke Printz Ringbaek
Research assistant
Technische Hochschule Mittelhessen
Giessen, Germany
tokeprintz@gmail.com

Gregers B.D. Rasmussen
PhD-student
Dept. of Oncology Section of Radiotherapy
Rigshopitalet
Copenhagen, Denmark
gras0038@regionh.dk

Bernt Rekstad
Physicist
Oslo University Hospital
Oslo, Norway
berntlr@gmail.com

Christian Richter
Research group leader
OncoRay - National Center for Radiation Research in Oncology
Dresden, Germany
christian.richter@oncoray.de

Gert Roschinski
Medical Physicist
MVZ Radiologie
Kiel, Germany
roschinski@pruenergang.de

Espen Rusten
PhD
Department of Physics
University of Oslo
Oslo, Norway
espen.rusten@gmail.com

Eivind Rørvik
PhD Student
Department of Physics and Technology
University of Bergen
Bergen, Norway
eivind.rorvik@uib.no

Mette Saksø
MD., Ph.D Student
Dept. of Experimental Clinical Oncology
Aarhus University Hospital
Aarhus, Denmark
mette.saksoe@oncology.au.dk

Helena Sandström
PhD student
Department of Physics
Medical Radiation Physics
Stockholm, Sweden
helena.sandstrom@ki.se

Sebastian Sanduleanu
PhD Student
Radiotherapy
MAASTRO
Maastricht, The Netherlands
sebastian.sanduleanu@maastro.nl

Marianne Sanggaard Assenholt
Physicist
Dept. Of Oncology
Aarhus University Hospital
Aarhus, Denmark
mariasse@rm.dk

Alina Santiago
Medical physicist
Universitätsklinikum Gießen und Marburg
Marburg, Germany
santiago@staff.uni-marburg.de

Line M H Schack
PhD student
Department of Experimental Clinical Oncology
Aarhus University Hospital
Aarhus, Denmark
schack@oncology.au.dk

Mai Schmidt
Medical Physicist
Department of Oncology
Aarhus University Hospital
Aarhus, Denmark
maiscmid@rm.dk

Annette Schouboe
RTT
Department of Oncology
Aarhus University Hospital
Aarhus, Denmark
annescho@rm.dk

Dennis Schaart
Associate Professor
Delft University of Technology
Delft, The Netherlands
d.r.schaart@tudelft.nl

Monica Serban
Medical Physicist
MGill University Health Centre
Montreal, Canada
monica.serban@mcgill.ca

Maja Bendtsen Sharma
Clinical assistant
Dept. Of Oncology
Aarhus University Hospital
Aarhus, Denmark
majasharma@oncology.au.dk

Patrik Sibolt
PhD student
Center for Nuclear Technologies
Technical University of Denmark
Roskilde, Denmark
pasi@dtu.dk

Albert Siegbahn
Senior University Lecturer
Stockholm University
Karolinska Insitutet
Stockholm, Sweden
albert.siegbahn@fysik.su.se

Vilde Eide Skingen
Student
Department of Physics
University of Oslo
Oslo, Norway
vilde_eskingen@hotmail.com

Camilla Skinnerup Byskov
Postdoc
Medical Physics
Aarhus University Hospital
Aarhus, Denmark
cambys@rm.dk

Torleiv Skjøtskift
Physician
Oslo University Hospital
Oslo, Norway
torleivtorleivtorleiv@hotmail.com

Simon Skouboe
Ph.D. Student
Department of Oncology
Aarhus University Hospital
Aarhus, Denmark
simsko@rm.dk

Jan-Jakob Sonke
Groupleader
The Netherlands Cancer Institute
Amsterdam, The Netherlands
j.sonke@nki.nl

Sofia Spampinato
Research Assistant
Dept. Of Oncology
Aarhus University Hospital
Aarhus, Denmark
sofspa@rm.dk

Camilla Stokkevåg
Postdoc researcher
Department of Oncology and Medical Physics
Haukeland University Hospital
Bergen, Norway
camilla.hanquist.stokkevag@helse-bergen.no

Kirsty Stuart
Radiation Oncologist
Crown Princess Mary Cancer Centre
Westmead Hospital
Sydney, Australia
Kirsty.Stuart@health.nsw.gov.au

Ingvild Støen
Student
Department of Medical Physics
Oslo University Hospital
Oslo, Norway
ingvild.stoen@hotmail.com

Christian Søndergaard
Medical Physicist
Danish Centre for Particle Therapy
Aarhus University Hospital
Aarhus, Denmark
chrissnd@rm.dk

Brita Singers Sørensen
Associate Professor
Dept. Of Oncology
Aarhus University Hospital
Aarhus, Denmark
bsin@oncology.au.dk

Kari Tanderup
Professor
Dept. Of Oncology
Aarhus University Hospital
Aarhus, Denmark
karitand@rm.dk

Mette Skovhus Thomsen
Head of Medical Physics
Dept. Of Oncology
Aarhus University Hospital
Aarhus, Denmark
mettthom@rm.dk

Laura Toussaint
Research Assistant
Department of Medical Physics
Aarhus University Hospital
Aarhus, Denmark
lautou@rm.dk

Vicki Taasti
PhD position
Dept. of Medical Physics
Aarhus University Hospital
Aarhus, Denmark
victaa@rm.dk

Maren Ugland
Medical Physicist
Haukeland University Hospital
Bergen, Norway
maren.ugland@helse-bergen.no

Silke Ulrich
Scientist
Medical Physics in Radiation Oncology
German Cancer Research Center (DKFZ)
Heidelberg, Germany
s.ulrich@dkfz.de

Niels Ulsø
Retired Medical Physicist
Aarhus University Hospital
Aarhus, Denmark
niels.ulsq@gmail.com

Vincenzo Valentini
Professor and Chairman
Gemelli ART
Università Cattolica S.Cuore
Rome, Italy
vincenzo.valentini@policlinicogemelli.it

Janna van Timmeren
PhD Student
Department of Radiation Oncology (MAASTRO)
GROW – School for Oncology and Developmental Biology, Maastricht University Medical Centre (MUMC)
Maastricht, the Netherlands
janita.vantimmeren@maastro.nl

Yvonka van Wijk
PhD candidate
Radiation Oncology
Maastricht University Medical Center
Maastricht, the Netherlands
yvonka.vanwijk@maastro.nl

Anne Vestergaard
Medical Physicist
Danish Centre for Particle Therapy
Aarhus University Hospital
Aarhus, Denmark
annveste@rm.dk

Bhadrasain Vikram
Chief
National Cancer Institute
Rockville, USA
vikramb@mail.nih.gov

Britta Weber
MD, PhD
Danish Centre for Particle Therapy
Aarhus University Hospital
Aarhus, Denmark
britwebe@rm.dk

Joachim Widder
Professor and Head
Medical University of Vienna
Vienna, Austria
joachim.widder@muv.ac.at

René Winter
PhD Student, Scientific staff
Radiation Oncology
Section for Biomedical Physics
University Hospital Tübingen
Tübingen, Germany
rene.winter@med.uni-tuebingen.de

Thomas Wittenborn
Postdoc
Department of Experimental Clinical Oncology
Aarhus University Hospital
Aarhus C, Danmark
wittenborn@oncology.au.dk

Cecile Wolfs
PhD Student
Department of Radiation Oncology (MAASTRO)
GROW – School for Oncology and Developmental Biology, Maastricht University Medical Centre+
Maastricht, The Netherlands
cecile.wolfs@maastro.nl

Esben Worm
Medical physicist
Dept. of Oncology
Aarhus University Hospital
Aarhus, Denmark
esbeworm@rm.dk

Esben Svitzer Yates
Physicist
Dept. of Oncology
Aarhus University Hospital
Aarhus, Denmark
esbeyate@rm.dk

Kristian Ytre-Hauge
Researcher
Department of Physics and Technology
University of Bergen
Bergen, Norway
kristian.ytre-hauge@uib.no

Daniel Zips
Chair, Professor Radiation Oncology
Department of Radiation Oncology
University of Tübingen
Tübingen, Germany
daniel.zips@med.uni-tuebingen.de

Ruta Zukauskaite
MD
oncololgy
Odense University Hospital
Odense, Denmark
ruta.zukauskaite@rsyd.dk

Jakob Ödén
PhD student
Medical Radiation Physics
Stockholm University
Stockholm, Sweden
jakob.oden@fysik.su.se